

UNIVERSITÀ
DEGLI STUDI
DI PADOVA

Università degli Studi di Padova
Dipartimento di Scienze Chimiche

Scuola di Dottorato di Ricerca in Scienza e Ingegneria dei Materiali
XXIV ciclo

**Micro/Meso-Structured Reactors for Chemical Synthesis:
Applications in Materials Science and Medicinal Chemistry**

Direttore della Scuola: Ch.mo Prof. Gaetano Granozzi

Supervisore: Ch.mo Prof. Michele Maggini

Dottorando: Emiliano Rossi

2009 - 2011

INDEX

Abstract.....	1
Riassunto	3
Preface	5

Part I

CONTINUOUS FLOW TECHNOLOGIES FOR INDUSTRIAL APPLICATIONS

Chapter 1: Introduction to Continuous Flow Technologies

1.1 Key Concepts of Small Scale Flow Technologies	11
1.1.1 Physical Aspects.....	12
1.1.1.1 Inertial and viscous forces: the Reynolds number.....	14
1.1.1.2 Convection and diffusion forces: the Péclet number.....	15
1.1.1.3 Surface and viscous forces: the capillary number.....	16
1.1.2 Engineering Aspects	17
1.1.2.1 Construction materials and technologies.....	17
1.1.2.2 Reactor sealing, interfaces and connections.....	20
1.1.2.3 Fluid movimentation.....	20
1.2 Micro/Meso Continuous Flow Processing as a Process Intensification Tool.....	21
1.2.1 Process Efficiency.....	22
1.2.2 Process Safety.....	22
1.2.3 Novel Process Windows.....	24
1.2.4 Process Monitoring.....	25
1.2.5 Productivity and Scale-Up.....	26
1.2.6 Energy and Material Savings.....	26
1.2.7 Plant Issues.....	27
1.3 Perspectives on Industrial Applications.....	27
1.3.1 Application Field.....	28
1.3.2 Economic Impact of Continuous Flow Process.....	29
References.....	31

Chapter 2: Applications of Continuous Flow Technologies

2.1 Homogeneous Chemistry.....	33
2.2 Heterogeneous Chemistry.....	34
2.2.1 Liquid-Liquid Reactions.....	34
2.2.2 Solid-Liquid Reactions.....	35
2.2.3 Gas-Liquid and Gas-Solid-Liquid Reactions.....	36
2.3 Multistep Synthesis.....	37
2.3.1 In-Line Purification and Process Automation.....	38
2.4 Photochemical Reactions.....	39
2.5 Preparation of Materials: Polymer and Nanoparticles.....	41
2.6 Industrial Applications.....	42
2.6.1 On-Site Production of Raw Materials.....	43
2.6.2 Equipment Flexibility.....	45
References.....	47

Chapter 3: Overview on Continuous Flow Equipment

3.1 Reactors Types.....	49
3.1.1 Tubular Type Reactors	49
3.1.2 Modular Type Reactors	52
3.2 Fluids Delivery and Connections	56
References.....	58

Chapter 4: A Case Study: continuous flow diazomethane generation

4.1 Diazomethane in chemistry	59
4.2 Results and Discussion.....	61
4.3 Conclusions.....	65
4.4 Experimental Section.....	65
4.1.1 Batch Reactions	66
4.1.2 Flow Experiments	66
References.....	68

Part II
CONTINUOUS FLOW SYNTHESIS OF
ONCOLOGICAL DRUGS

Chapter 5: Basic Principles on Cancer and Chemotherapy

5.1 Cancer.....	73
5.1.1 Biological Bases of Cancer.....	73
5.1.2 Cancer Incidence, Causes and Progression.....	75
5.1.2.1 Cancer Causes.....	76
5.1.2.2 Tumor Progression.....	76
5.2 Cancer Therapy.....	77
5.2.1 Cancer Chemotherapy.....	78
5.2.1.1 Treatment and Response Criteria.....	78
5.2.1.2 Functional Classes of Antineoplastic Agents.....	79
5.2.1.3 Development of Resistance in Cancer Cells.....	80
5.3 Tyrosine Kinases Inhibitors: a New Class of Selective Drugs.....	80
5.3.1 Production Confinement of Oncological Drugs	83
References.....	85

Chapter 6: Flow Synthesis of Pyrimidinamine Structures

6.1 Classical Approaches towards Imatinib Synthesis.....	87
6.1.1 Classical Batch-Wise Synthesis of Imatinib.....	87
6.1.2 Flow Approaches to Imatinib Synthesis.....	89
6.2 Continuous Flow Approach to Pyrimidinamines.....	91
6.2.1 Synthesis of 3-(dimethylamino)-1-(pyridin-3-yl)prop-2-en-1-one (36).....	92
6.2.2 Synthesis of (5-amino-2-methylphenyl)-4-(3-pyridinyl)-2-pyrimidinamine (41).....	94
6.2.3 Synthesis of Substituted Pyrimidinamine Structures.....	96
6.3 Conclusions.....	99
6.4 Experimental Section.....	99
6.4.1 Batch-wise Synthetic Procedures.....	100
6.4.2 Continuous Flow Syntheses.....	105
References.....	107

Chapter 7: Flow Synthesis of 4-anilino-quinazoline Structures

7.1 Classical Approaches towards Quinazoline Synthesis.....	109
7.1.1 Classical Synthetic Route for 4-anilino-quinazoline Moieties	110
7.2 Continuous Flow Approaches to 4-anilino-quinazolines.....	112
7.2.1 Synthesis of N'-(2-cyanophenyl)-N,N-dimethylformamidine (74).....	112
7.2.2 Synthesis of 4-(3'-chloro-4'-methoxyanilino)-quinazoline (76).....	116
7.2.3 Synthesis of a Library of 4-anilino-quinazolines	117
7.3 Conclusions.....	122
7.4 Experimental Section.....	123
7.4.1 Batch-wise Synthetic Procedures.....	123
References.....	127

Part III**CONTINUOUS FLOW TECHNOLOGIES FOR
INDUSTRIAL APPLICATIONS****Chapter 8: Continuous-Flow Synthesis of a Methanofullerene Derivative**

8.1 Introduction to Carbon Allotropes: Fullerene.....	131
8.1.1 Historical Background.....	131
8.1.2 Fullerene Structure, Properties and Uses.....	132
8.2 Organic Photovoltaics.....	134
8.2.1 OPV Functioning and Architecture.....	134
8.2.2 The Active Fullerene Component.....	136
8.3 Results and Discussion.....	138
8.3.1 Flow Synthesis of PCBtB.....	138
8.3.2 PCBtB as Component of BHJ Solar Cells.....	141
8.3.2.1 Solar Cells Assembly and Characterization.....	141
8.2.2.2 Morphology	144
8.4 Conclusions.....	146
8.5 Experimental Section.....	147
8.5.1 Characterization of Compounds.....	147
8.3.1 Synthesis of PCBtB (88) in Flow.....	148
8.3.1 Device Fabrication and Measurements.....	148
8.3.1 Thin-film characterization.....	149

References.....	150
Chapter 9: Flow Processing of Carbon Nanotubes	
9.1 Fundamentals of Carbon Nanotubes.....	153
9.1.1 Nanotubes Structure and Production	153
9.1.2 Nanotubes Properties and Applications	155
9.1.2 Enhancing Nanotubes Processability	155
9.2 Results and Discussion.....	156
9.2.1 Characterization of Functionalized CNTs.....	158
9.3 Conclusions.....	160
9.4 Experimental Section.....	160
References.....	164
Chapter 10: Flow Functionalisation of Porphyrin Derivatives	
10.1 Porphyrins and their Properties.....	165
10.1.1 Structure, Properties and Occurrence	165
10.1.2 Synthesis and Reactivity	166
10.1.3 Goals	168
10.2 Results and Discussion	168
10.3 Conclusions.....	172
10.4 Experimental Section.....	173
References.....	175
Concluding Remarks	177
List of Publications.....	179
Communications to Conferences and Seminars.....	180
Acknowledgments.....	181

Abstract

The research afforded during the present PhD project deals with the application of microfluidic technology for designing new synthetic methods. Compounds with potential applications in medicinal chemistry and material science were considered, with a focus on process suitability for large scale productions.

In this optic, development and scaling up of a continuous flow process for safe handling of diazomethane to large scale was afforded. Such study was carried out during a period of three months spent at Corning European Technology Center (CETC) of Avon, France, and the results obtained were been recently published.

Flow approaches were developed towards the synthesis, in more efficient and safer way respect to batch-wise methods, of heterocyclic compounds to be used as oncological drugs. A library of molecular structures characterized by pyrimidinamine and 4-anilino-quinazoline scaffolds was prepared, using multi-step continuous processes. This work was carried out in collaboration with a local pharmaceutical company, Fabbrica Italiana Sintetici (FIS) Spa, in the frame of FSE program.

Employment of continuous reactors was also studied for the synthesis of functionalized molecular nanostructures. In particular, fullerenes, carbon nanotubes and porphyrins derivatives were prepared, with a definite improvement over traditional synthetic methods in terms of efficiency. Compounds studied have potential useful applications as materials for photovoltaic, molecular electronics and sensoristics. Such work resulted in various publications and in an Italian patent request.

Riassunto

La tematica di ricerca affrontata nel corso del presente progetto di Dottorato è stata l'applicazione di tecnologie microfluidiche per lo sviluppo di nuove metodologie sintetiche. In particolare, sono state studiate molecole con potenziali impieghi in chimica farmaceutica e in scienze dei materiali, con particolare enfasi sulla possibilità di applicare i processi individuati alla produzione industriale.

In tale ottica è stato sviluppato, e successivamente adattato per produzioni su larga scala, un processo in flusso continuo per la produzione e l'impiego del diazometano in condizioni di sicurezza. Tale studio è stato svolto durante un periodo di tre mesi presso il Corning European Technology Center (CETC) di Avon, Francia, e i risultati ottenuti sono stati recentemente pubblicati.

L'impiego di reattori a flusso è stato inoltre studiato nella sintesi molecole eterocicliche, che possano essere impiegate come farmaci oncologici. Una libreria di composti, contenenti funzionalità strutturali di tipo pirimidinamminico e 4-anilino-chinazolinico, sono stati preparati mediante sintesi *multi-step* in flusso continuo, in modo più efficiente e sicuro rispetto alle metodologie tradizionali. Tale ricerca è stata portata avanti in collaborazione con un partner industriale, Fabbrica Italiana Sintetici (FIS) Spa, nell'ambito del progetto FSE.

Sono stati infine sviluppati processi a flusso continuo per la funzionalizzazione chimica di nanostrutture molecolari, derivate da fullereni, nanotubi di carbonio e porfirine. L'impiego di reattori in continuo in tale campo ha permesso notevoli incrementi di efficienza sintetica rispetto alle metodiche discontinue. I composti preparati hanno inoltre potenziali applicazioni nel campo dei materiali innovativi, in particolare per il fotovoltaico, l'elettronica molecolare e la sensoristica. Tali studi sono stati pubblicati in vari articoli su riviste scientifiche e hanno portato inoltre al deposito di una domanda di brevetto Italiano.

Preface

Since the very beginning of organic chemistry our ability to chemically modify organic matter has continuously improved, together with our understanding of the fundamental rules of chemical reactivity. However, despite this great technological and scientific advance, a nineteenth century chemist will probably feel himself very comfortably in one of our chemical labs, as the main equipment available to perform organic reactions has been substantially unchanged in the last two hundred years. This is true also for chemical industry, where technological improvement substantially brought to a mere increment in reactors dimension, as the engineering competences on pipelines and stirring systems evolved. Being conscious of this, chemists in the last decades have focused on development of new technological breakthroughs, mainly in the fields of environmental friendly processes and new process windows. From such interest new technologies have emerged, as microwave heating or reaction in supercritical conditions. Among these emerging new technologies for chemical synthesis, flow chemistry has attracted much attention in the last years.

Flow chemistry is a term widely used to describe the performance of reactions in a continuous manner. Continuous processing is not a brand new concept: a hundred years ago chemical industry already took advantage of easier automation, improved safety, enhanced process reliability and reproducibility that are typical of flow processes. Today bulk chemicals manufacturing, in particular oil refinery and petrochemical industry, are largely based on continuous processing. However, laboratory scale chemistry still relies almost completely on the classical discontinuous batch approach, eventually enhanced through special techniques such as microwave heating or combinatorial chemistry. In the last decades, a relatively new concept linked to flow chemistry has imposed, that led the way to diffusion of continuous processing even at the small scale, represented by micro reaction technology. This means performing reactions in a continuous way within well-defined reaction channels, where typical dimensions range from 10 to 1000 μm and volumes, at a research level, span the microliter to milliliter range. At this length scale, physics teaches us that laminar flow dominates, due to high viscous forces and surface effects, that overcomes gravity effects, so mass transfer occurs by diffusion only, whereas

heat transfer rates fall in the milliseconds range. Substantial improvements arise from pairing of continuous processing with miniaturization: smaller chemical reactors allow for improved mixing and heat transfer control, that affects reaction efficiency; numbering up, increase in product output by operating many identical devices in a parallel way, made possible an easier scale-up and the realization of smaller footprint chemical plants. For such reasons, continuous microfluidic is a research field of continuously growing interest, as stated by the huge number of publications, especially in industry oriented journals. As a consequence, microfluidic technology has grown as well, giving rise to complexity evolutions in the equipment available to the flow chemists both in development lab and in production plant: the devices of the very beginning, made of glass or silicon etched microchannels, with their very high technological content have been replaced largely by less expensive, more flexible devices especially made in polymeric materials and through soft-lithographic techniques, or to even more easier set-ups made by pairing of Teflon tubing and HPLC-style fittings and equipment. Meanwhile, the availability on the market of sophisticated, all-in-one benchtop instruments for continuous processing of large amount of materials in even harsh conditions of high temperature and pressure has similarly grown, and even a small research lab will now be able to mimic, with such instruments, the productive scale of a kilo-lab plant. Such wide availability of equipment allows for a larger accessibility to reaction conditions, and this has increased the range of applicability of microfluidic processing, as now the technology is probably near to allow easier handling of solids and suspensions even at a bench scale, that was once the holy grail of microflow processing.

Despite the large interest in academia, a widespread application of microfluidic technologies in their natural environment, chemical production, is unfortunately still far to come. This is probably due to some sort of resistance that still exists in the industry, especially regarding the perception of a continuous plant as lacking of flexibility respect to a classical batch reactor, that can easily be employed for a wide range of different reactions or work-ups procedures, whereas a continuous system is somewhat optimized for a specific task and could not easily be converted to alternative productions. Moreover, continuous processing needs for a somewhat wider range of supporting apparatus, that mainly means fluid movimentation and control systems, respect to discontinuous, as well as both upstream and downstream batch-wise processing of raw materials, thus suggesting the

requirements for high plant investments. For these reasons, only a few examples of full continuous production processes can be found in industry today, whereas the main role of continuous systems still remains the replacement of a single difficult reaction steps in a specific cascade. Nevertheless, it is estimated that nowadays acquisition cost of a batchwise plant is somewhat higher with respect to a continuous one, and this factor will hopefully drive the more innovation-driven chemical companies towards widespread employment of continuous apparatus, and some example in such sense are very encouraging.

The research carried out during the present PhD project gave a contribution to the development of such an innovative technology: the work done was focused on the employment of many different microfluidic equipments, as a proof of the flexibility and maturity reached by continuous technology, for designing synthesis with applicative targets in the fields of medicinal chemistry and materials science, and with a particular view over industrial applications of the approaches developed.

The present PhD thesis will be structured in the following way: in the first, introductory, part of the work I will briefly introduce some key concepts related to continuous flow processing and its industrial implementation together with some relevant applicative examples. As a proof of concept, a case study regarding applications of flow reactors for development of scalable synthesis involving hazardous intermediates will be presented. The second part will be dedicated to the main aim of the doctoral research project that was the development of flow approaches towards the synthesis, in a safer and more reliable way compared to batch procedures, of heterocyclic compounds to be used as oncological drugs. This work was carried out in collaboration with a local pharmaceutical company, Fabbrica Italiana Sintetici (FIS) Spa, in the frame of the FSE program. Complementary projects involved continuous processing in the synthesis of functionalized nanostructures, such as fullerenes, nanotubes and porphyrins, for material science applications will then be reported in part III.

Papers published during this PhD thesis have been adopted as part of the text where relevant for results exposed. On the contrary, results not yet published have been reported in details.

Part I

**CONTINUOUS FLOW TECHNOLOGIES FOR
INDUSTRIAL APPLICATIONS**

Chapter 1: Introduction to Continuous Flow Technologies

1.1 Key Concepts of Small Scale Flow Technologies

A systematic classification and definition of small scale flow technologies is still on course: this is due both to the relatively youngness of the technology, less than two decades, and to the fact that flow methods represent a very multidisciplinary field attracting interest of chemists, physicists, engineers and, to less extent, biologists. Moreover, a wide range of techniques and devices can be classified within small scale continuous flow technologies, with some differences based on the applicative target of reactors, meaning lab scale studies or production.

In this work, I will distinguish between micro and meso (also called milli or mini) reactors: devices with typical channels width comprised between 10 and 500 μm will be classified as microreactors, whereas systems with dimensions up to some millimeters will fall underneath the definition of mesoreactors.¹

Microreactors are characterized by small channel dimensions and device volumes. They possess excellent intrinsic properties of mass and heat transfer due to small sizes. Microreactors are well suited for lab scale optimization of flow processes, as well as kinetic or thermodynamic characterizations, thanks to the low material input and waste output. On the other hand, microreactors are not suited to large scale production, because of their limited productive potential due to low volumes and high pressure drops; they are also very sensitive to blockage if solid particles are employed. Mesoreactors are far more appealing for industrial applications: typical channel widths up to some millimeters result in robust, high throughput, low pressure drop devices. Of course, the drawback of increased dimensions is less efficient mixing and heat transmission, even if such inconvenience can be partially overcome adopting mixing enhancement elements.²

Schematic comparison between micro and meso sized reactors is reported in Table 1.1.

	Advantages	Disadvantages
Micro-sized reactors (10 - 500 μm channel width)	Low material input Low waste output Excellent heat and mass transfer properties	Low throughput Tendency to channels blockage High pressure drop
Meso-sized reactors (500 μm – some mm channel width)	High throughput Low pressure drop Possibility to handle solids	Poorer heat and mass transfer properties

Table 1.1: micro vs meso sized continuous flow reactors.

1.1.1 Physical Aspects

A detailed physical description of fluid behavior at the small scale is not the target of the present work, as its main focus remains in the applicative synthetic chemistry field. However, some key concepts will be cleared, and references for a more formal treatment of the problem will be given.

First of all, one key point should be cleared out: is there any sense in considering physics at the micro-scale? In other words, is such physics really different from the classical macroscopic systems we are used to? As chemists, we were trained to consider true classical mechanics laws until the molecular level, that means a nanometer range length, where a qualitative change from classical to quantum regime happens. If we consider a classical fluid, namely water or an organic solvent, of given volume and we plot for example fluid instantaneous density against the volume sampled, we will probably obtain a curve similar to that reported in Figure 1.1.³

At the very small scale, discrete molecular nature of the fluid will cause heavy fluctuation of values measured, as a direct consequence of the Heisenberg Uncertainty Principle; at the opposite end, for large volumes the density value will be affected by inhomogeneities in the medium or temperature changes. The linear part of the curve will represent the volume of fluid that contains enough molecules to exhibit a non discrete behavior, but sufficiently small to be considered homogeneous. This is the typical fluid element that is taken into

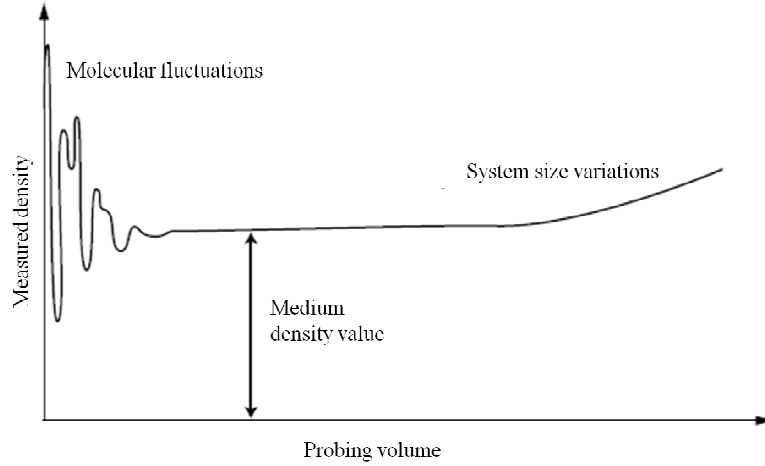


Figure 1.1: hypothetical curve describing instantaneously measured density of particles in an element of fluid respect to element volume.³

account when a classical mechanics treatment of hydrodynamic is made and for classical fluids such an element will have a volume of a few nanometers, thus far smaller than the scales at which microfluidic works. If we are not interested in nanofluidic, where impressive new properties of fluid, rather not completely explored, are exerted, but which practical applications remain far beyond our purposes, physics at the microscale should be treated exactly in a similar manner to massive fluids. Despite this, the following treatment will show how when system dimension is reduced the equilibrium of forces exerted on the fluid elements change dramatically, moving the focus from the macroscale dominant gravitational forces to more uncommon contributions, like viscosity, capillarity and surface interactions.

If classical mechanics has to be used, by considering a small element of fluid that behaves as a continuum not-discrete medium, and imposing force balance between fluid stresses on the surfaces and body forces applied on the bulk of the fluid, Navier-Stokes equation could be derived:

$$\rho \left(\frac{\partial \mathbf{u}}{\partial t} + \mathbf{u} \cdot \nabla \mathbf{u} \right) = -\nabla p + \eta \nabla^2 \mathbf{u} + \mathbf{f} \quad (1)$$

where \mathbf{u} is the flow velocity, ρ is the fluid density, p is the pressure, η is the constant dynamic viscosity and \mathbf{f} represents the sum of body forces acting on the fluid element. This is the general form of Navier-Stokes equation that represents the velocity field of an incompressible Newtonian fluid. The term on the left exploits inertial acceleration, whereas the term on the right is the sum of force components acting on the fluid, the so called stress tensor $\bar{\sigma}$. From this latter term, it clearly appears that fluid motion depends on many contrasting forces. For such a reason, when describing hydrodynamics at the small scale, recurs to dimensionless numbers is common, as they express in straightforward way the balancing between opposite force contributions.⁴

1.1.1.1 Inertial and viscous forces: the Reynolds number

One of the most cited dimensionless numbers while treating microfluids is surely the Reynolds number (Re), that express the balance between inertial and viscous forces:

$$\frac{f_i}{f_v} = \frac{\rho U_0 L_0}{\eta} = Re \quad (2)$$

where U_0 is the flow rate and L_0 is typical channel width. For a microchannel with a few hundred of microns width, at typical flow rates, Reynolds number values ranged between 10^{-6} and 10^2 . Empirically, these low values of Re affirm that viscous forces overwhelm inertial contributions. As a consequence, the nonlinear contribution to flow motion that causes turbulent, non predictive motion in bulk fluids disappears, and a simplified version of Navier-Stokes formula, called Stokes equation, could be used:

$$\rho \frac{\partial \mathbf{u}}{\partial t} = -\nabla p + \eta \nabla^2 \mathbf{u} + \mathbf{f} \quad (3)$$

In this case, the flow regime inside a microchannel could be predicted to be exclusively laminar. Purely laminar flows may be desirable or not, depending on the application:

highly linear flow behaviors are useful when a precise modelization is needed, whereas in more applicative systems a pure laminar regime could result in intolerably high mixing times, as we will see.

1.1.1.2 Convection and diffusion forces: the Péclet number

In massive, turbulent motion systems usually mixing of two fluid streams is determined by chaotic stretch and fold movements of various fluid sections, which results in a strong improvement of mass transfer gradients and fastened mixing. In purely laminar systems mass transfer depends on diffusion only, thus mixing rate is determined by physical properties of the medium and by molecules mean diffusion path. The relative importance of convection respect to diffusion in mixing phenomena is usually expressed by another dimensionless number, known as Péclet number (Pe):

$$\frac{Z}{w} \sim \frac{U_0 w}{D} = Pe \quad (4)$$

where D is the diffusion coefficient of a molecular specie and Z is the channel length required for complete mixing. As a consequence, Pe is considered to be linearly correlated with the channel length needed for complete molecular diffusion. If very simple mixer geometries are considered, as for example T or Y junctions, mixing efficiency decreases rapidly by growing of channel width: as an example, even a small protein flowing with a fluid through a $100 \mu\text{m}$ channel at $100 \mu\text{m/s}$ will require a $Pe \sim 250$ (2.5 cm) for complete mixing. As a consequence, reactors designed for high throughput synthetic applications, especially meso-sized systems, often need suitable mixing improvers in order to enhance mass transfer performances. Mixing devices relies basically on two principles: (i) reduction of the mean diffusion path and (ii) introduction of chaotic advection. In the first case, mixer geometries are studied to separate fluid streams in many smaller interpenetrating lamellae, thus facilitating molecular diffusion. Classical examples of such systems are flow focusing devices and multilamination devices. Chaotic advection relies instead in introduction, in purely linear Stokes flows, of secondary, chaotic streamlines that are still however inertia independent. Flow acquires by consequence a nearly turbulent regime that

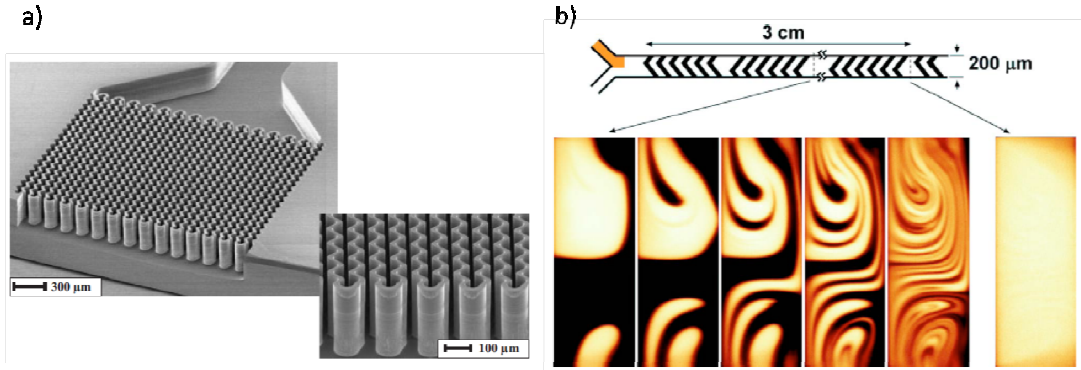


Figure 1.2: a) SEM image of a silicon made interdigital micromixing element.⁵ b) Continuous-flow staggered herringbone mixer: geometrical patterning of channel walls induces chaotic advection mixing.⁴

greatly increases mixing rate while maintaining the predictive character of linear Stokes flow.⁵ Mixing elements based on such assumptions are usually obtained by geometrical patterning of channel walls. Examples of both element types are displayed in Figure 1.2.

1.1.1.3 Surface and viscous forces: the capillary number

Thus far, we have considered only fully miscible fluids, in which dissolved molecules can freely diffuse between parallel streams with the only limitation of diffusion capability. When instead immiscible fluids are considered, a new force contribution arises from surface tension (γ). This latter introduces a competing stress against viscous forces, tending to reduce interfacial areas. The balance between the two force components is expressed through another dimensionless number named capillary number (Ca):

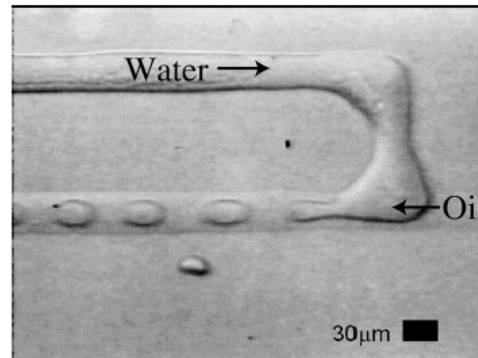


Figure 1.3: example of highly monodispersed droplets generated in a two phase streams microreactor.⁴

$$Ca = \frac{\eta U_0}{\gamma} \quad (5)$$

The net effect of balanced forces is the formation of droplets inside microchannels. By imposing the equilibrium between capillary and viscous stresses, droplet radius (R) could be readily calculated as follows:

$$R \sim \frac{\gamma}{\eta U_0} h = \frac{h}{Ca} \quad (6)$$

where h is the channel height. The ability to predict droplet size, together with the high degree of control allowed by micro-structured reactors, make possible the continuous generation of highly monodispersed droplets with infinite applications: nano and microdroplets have been extensively used as closed nanoreactors to speed up chemical transformations, while the high rate of mass transfer between phases, thanks to the high surface to volume ratios, allows for many reactions to happen only the interfaces between immiscible phases.⁶ Again, specific mixer geometries have been studied in order to improve control over droplet shape, with potential applications in the synthesis of polymeric capsules and metallic or semiconductor nanoparticles.⁷

1.1.2 Engineering Aspects

During the present PhD thesis, multiple flow chemistry platforms have been used, depending on the particular application studied and the equipment properties thus needed. The very wide range of synthetic transformations that have been experimented are a proof of the grade of flexibility and availability reached by continuous flow techniques. However, in order to get maximum gain from transition of chemical processes from batch to flow mode, all the equipment should be carefully selected and properly assembled. The following section will give the elements that have to be considered for an accurate and reliable choice of continuous system, as well as some fundamental engineering aspects of performing reactions in continuous flow manner.

1.1.2.1 Construction materials and technologies

Construction materials are of course of high importance when designing and realizing a continuous set-up: glass, silicon, metals, polymeric materials and ceramic are all common

choices. Chemical compatibility will surely be the key parameter while designing a continuous apparatus: a careful choice of materials requires check of requirements in terms of chemical compatibility with the whole productive line. This is particularly true for pharmaceutical industry, where, for example, current Good Manufacturing Practices (cGMP)⁸ specifications usually require metal free plants. Again, if pumping systems are employed for fluid delivery, nature of all wetted parts should be carefully considered. Operating conditions are also very important in the choice of construction materials, in terms of material resistance under stress, high temperatures or pressures, thermal transfer capability and also effective sealing if mobile parts are employed. Finally, once the right base material is selected, suitable construction and assembly techniques should be used in order to assure the right grade of geometrical and dimensional precision, with an eye of course to production cost.

Glass is a material of wide choice thanks to its high chemical resistance to both organic and inorganic reactants, being incompatible only with hydrofluoric acid and concentrated hot bases. Moreover, many well-known techniques for channels imprinting are available, ranging from a combination of photolithography and wet etching to powder blasting. The so far printed devices could be sealed easily by thermal annealing using glass or other materials cover plates, the only drawback consisting in the impossibility to open the reactor once closed. Glass, however, has the advantage of allowing visual inspection of the channels during reactions, as well as compatibility with optical applications.⁹ If special glasses are used, namely borosilicate, very good thermal and mechanical performances are obtained, whereas if particular optical properties are needed, quartz could be used, even if less resistant and more difficult to handle.¹⁰ Another common choice is silicon: its widespread working for microelectronic purposes has generated a huge amount of etching techniques, both wet and dry, depending on the resolution needed and on the types of structures that should be obtained. Sealing of the device can be easily achieved by thermal meaning when using silicon cover plates or by anodical way if the cover is made by glass.¹¹

Resembling traditional batchwise plants, a large number of reactors have been manufactured using metals and alloys, the more common being stainless steel, nickel and Hastelloy. The incision technique depends only on the type of structure that has to be realized, in particular on aspect ratio, the ratio between channels depth and width. Wet etching techniques allow for quite low aspect ratios, whereas employing of high precision

machining or selective molding techniques results in a very high degree of control over channels shape and dimensions, resulting in straightforward access to rather complex structures that could be also easily stacked together to form multilayer devices by mean of welding, soldering, brazing, clamping, gluing and diffusion bonding. A relatively new type of reactor that is attracting increasingly attention are ceramic devices: ceramic is well suited for realizing chemical reactors thanks to high chemical compatibility and mechanical resistance even at harsh conditions beyond reach of other materials. Ceramic devices are usually realized by sintering of ceramic powders using a 3D mold, or alternatively by injection molding, being aware of shrinkage tendency upon cooling of the sintered material.¹²

More recently reactors have been assembled employing polymeric materials. The key advantages of polymers over the classical construction materials seen above reside in lower costs, higher flexibility of devices and easy assembly. Also, a wide number of different polymeric bases are available depending on chemical compatibility required: the main disadvantage linked to the employment of polymeric devices is in fact the reduced chemical compatibility, as many polymers tend to be dissolved or swelled by organic solvents. Printing techniques encompass injection molding, hot embossing, casting and soft-photolithography. PDMS (polydimethylsiloxane) is widely used for fabrication of devices in research labs, thanks to its unique combination of easy shaping, good chemical resistance, thermal and optical behavior. PMMA (polymethylmethacrylate), Viton and thiolenic resins are used as well, despite the limited compatibility with organics. More resistant polymeric materials are PTFE (polytetrafluoroethylene) and PEEK (polyether ether ketone), widely used for assembly of tubular devices starting from commercially available components; also, techniques for micro-fabrication of PTFE structures have been developed.¹³

During this thesis, some hybrid glass-polymer reactors have been constructed for a wide range of applications. The material of choice was a thiolenic resin (commercial name NOA81) that was patterned by mean of soft-lithographic techniques using UV light, thus giving functional reactors with geometries specifically engineered for the selected application, with a very fast procedures and relatively inexpensive equipments.

1.1.2.2 Reactor sealing, interfaces and connections

As stated above, once channels have been etched in the selected bulk material a suitable sealing method must be used to obtain a complete liquid and gas proof device. Sealing methods may be irreversible or reversible. Irreversible methods includes bonding, welding, soldering, brazing and gluing, affording a surely gas-tight device, whereas reversible methods, based on clamping or use of graphite or polymeric gaskets, are less affordable in terms of leakage prevention but have the undeniable advantage of allowing reactor inspection, cleaning and recovery in case of clogging problems.

Once devices have been sealed, commonly further work is needed in order to provide connection to fluid delivering systems. A usual approach is drilling of access holes in the cover plates that matches fluid delivery lines, following connection of pipes through adhesive ports, gluing or soldering, or providing suitable reactor housing equipped with gaskets and commercially available fittings.¹⁴ An example of connection system will be given in Chapter 3, where construction of hybrid glass-polymer reactors will be described.

Post-functionalization of reactor inner surfaces is very common, in view of both improving chemical stability and corrosion resistance or gaining chemical functionality with active coatings. Thin oxide layers are usually grown over silicon surfaces to improve chemical stability, whereas coatings with Fe-Al alloys have been developed to overcome metal surfaces corrosion problems; sol-gel deposition of fluorinated coatings have been used to prevent fouling inside channels, in particular in presence of catalytic coatings that may undergo poisoning; silanization by sol-gel techniques is commonly employed to improve lifetime of polymeric devices.¹⁵

Thin layer catalytic coatings and monoliths, brushed polymers containing catalytic nanoparticles anchored to surfaces, ceramic or polymeric membranes embossed inside fluidic channels are all common methods employed to exploit the high surface-to volume ratio in microreactors in order to increase the chemical reactivity.

1.1.2.3 Fluid movimentation

Most common approaches used to manipulate reactants and products inside microchannels are electroosmotic flow (EOF) and pressure driven flow.

EOF relies on application of an external electric field to channels walls through electrodes to induce fluid movement. In particular, if the fluid in the micro-channels is an electrolyte that contains dissolved ions or charged molecules, usually small surface charges are produced at the walls, resulting in the formation of an electrical double layer through interaction of opposite charges between fluid and walls. Application of an external electric field promotes migration of the double layers along the walls that results in bulk fluid movement. The advantage of EOF is that no pumps or mobile parts are needed and no pressure is developed inside channels, resulting in wide simplification of set-up and reduced requirements for reactor sealing and connections. The main problem is the lack of general applicability of electronic induced kinetic methods, for which the presence of electrolytic solutions or charged molecules is mandatory.¹⁶

Pressure driven flow, by comparison to EOF, is advantageous as it allows fluid delivery at precise flow rates independently from fluid nature. With the constant improvement of sealing and connection systems, this is so far the most widely employed delivery method, by using syringe, displacement or high performance liquid chromatography (HPLC) type pumps. Such kind of equipment has been used for all continuous reactions performed during this thesis, and, similarly, high throughput pumps are used in industrial applications of flow reactors.

1.2 Micro/Meso Continuous Flow Processing as a Process Intensification Tool

Process Intensification (PI) is an engineering concept referred to rendering a manufacturing or processing design substantially improved in terms of efficiency, cost-effectiveness, quality, waste, safety or more generally enhancement of sustainability. Process intensification focuses on the implementation of radically innovative principles in engineering processes, in order to achieve a “paradigm shift”; PI therefore differs markedly from process optimization as this latter focuses on improvement of performances by following already established concepts and maintaining some process constraints, thus introducing no “new science”. Implementation of continuous flow reactors in chemical

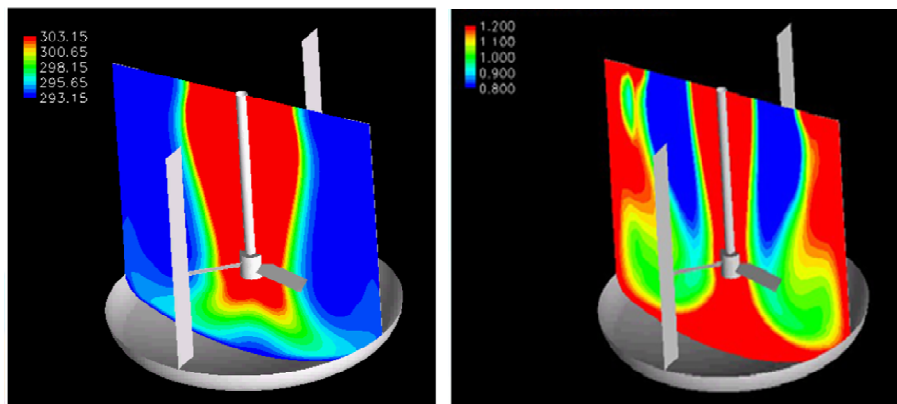
productions, as well as in development stages, is potentially a powerful tool to allow PI: as already mentioned, a key reason of the growing interest on continuous processing is the beneficial effect on reaction performances, made possible by the combination of small dimensions and continuous flow. We will set here a deeper look at such advantages, with particular emphasis on the potential breakthroughs to improvement of process sustainability in industrial and production field.¹⁷

1.2.1 Process Efficiency

As we have seen before, mixing phenomena in flow reactors could be extremely fast, in particular if mixing enhancement devices are employed. This is particularly true if we compare an industrial stirred tank reactor to a continuous flow system. In batch systems, despite the great technological efforts made in improving impellers devices, inhomogeneities along both axial and radial directions are usually obtained (Figure 1.4)¹⁸ as result of both highly chaotic mixing and presence of stagnant zones of fluid. In the case of a synthetic transformation, of course such inhomogeneities result in a diminished control over stoichiometry and reaction times, that usually gives rise to side reactions and formation of unwanted products. This is a major problem in particular for pharmaceutical production, where a strict control over product impurities is needed, and much energy is spent in time and material consuming procedures for product purification. A careful employment of flow reactors can avoid control problems and significantly enhance reaction control, thus allowing for more efficient processes to be carried out also at a production scale.

1.2.2 Process Safety

As for mass transfer, continuous flow reactors have significant improvement potentials respect to batch reactors in terms of heat transfer. In the common laboratory practice, is very usual to deal with reactions that need to be cooled down by immersion in ice bath, or additions of reagents that have to be made drop by drop in very careful manner in order to prevent strong heat releases. When dealing with a few milliliters of reaction mixture, thermal evolution appears to be not a great concern, but when the reactor grows up to a thousand liters scale, temperature control is not so straightforward. As so, it is common in



1 m³ vessel
 Impeller stirred, 500 RPM
 External cooling
 Heat release 55 KJ/mol

Figure 1.4: heat (on the left) and mass (right) gradients determined for a conventional stirred tank reactor.¹⁸

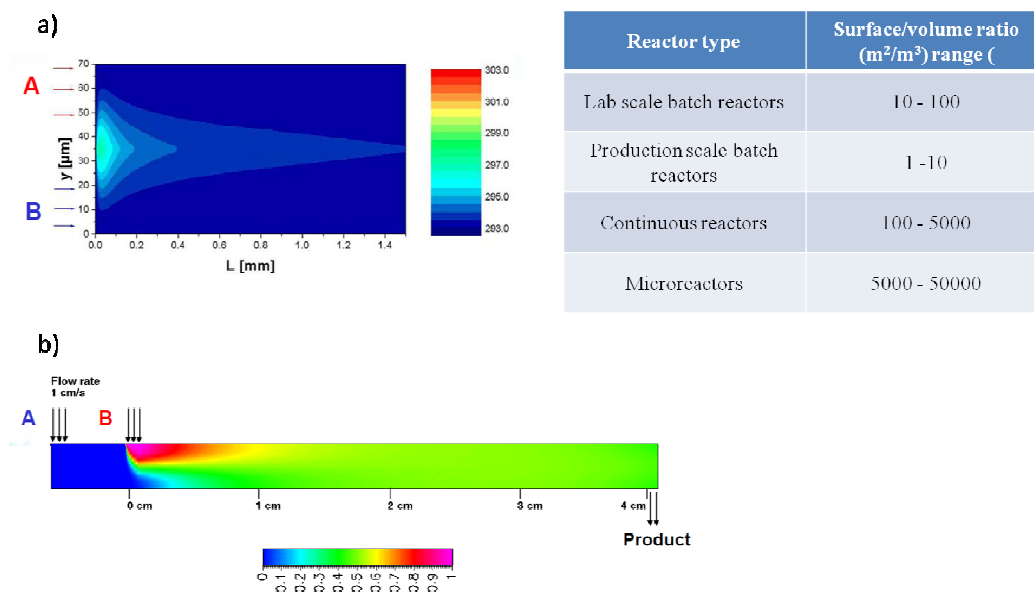


Figure 1.5: heat (a) and mass (b) gradients determined for a continuous flow microstructured reactor and comparison between batch and continuous equipment surface/volume ratios.¹⁸

industrial practice to have a full thermal characterization through calorimetry for a reaction developed on lab scale before going to plant, in order to be well aware of existing exotherms that can cause dangerous runaways. Thus, for safety reasons, many synthetic methods, quite common on research scale, result to be almost unsuited for mass production due to the impossibility to have safe heat control. Even if reactions with very limited heat sensitivity are implemented, the presence of hot spots generated by the reaction or also by

the simple mechanical heating due to impelling process could generate side reactions or unwanted product decomposition. Employment of continuous flow reactors may overcome such limitations: the exceptionally high surface-to-volume ratios found inside micro, and in less extent, meso-channels allow for extremely high heat transfer coefficients with beneficial impacts on both exothermal and endothermal reactions. This means that strong heat releases could be safely controlled, avoiding formation of critical hot spots, whereas the amount of energy needed to cool down reactions, which requires cryogenic conditions, is reduced thanks to higher thermal homogeneity (Figure 1.5).

1.2.3 Novel Process Windows

A direct consequence of continuous flow equipment diffusion in laboratories and production plants is that new synthetic conditions, that were once difficult or rather impossible to be exploited, become now easily available. Thus employment of continuous micro/meso reactors opens up the so-called *Novel Process Windows*, that means operating at extremely harsh conditions in the way to accelerate reactions rate of orders of magnitude while maintaining acceptable selectivities. Such effect could be reached in many ways, the most notably of them being processing at high temperature, pressure or concentration (even solvent free conditions), or by simplifying the process flow through simultaneous processing or function integration. Similar reaction conditions will be far beyond the capabilities of standard batch equipment, at least at a productive scale, whereas they are easily accessible through continuous processing. High surface-to-volume ratios allow for high temperature management with limited power input, while the employment of sealed devices, in combination with pressure driven flow, takes to easily-pressurized equipment in order to perform reactions over solvent boiling point temperature or even at critical conditions. Furthermore, increased process efficiency and safety give chance to limit or completely avoid solvent usage as a control medium, while performing of synthetic steps in a parallel way or integration of functionalities in the reactor equipment are readily obtained thanks to the structural organization of flow devices.¹⁹

Novel Process Windows also open when a combination of continuous flow with other process intensification technologies is performed, in particular microwave heating and ionic liquids processing. Microwave heating in particular has proven to be a valuable tool for increasing rate and efficiency of many synthetic transformations, however, its large

scale application is still far to come, due to the intrinsic difficulties in scaling up of heating systems together with the connected huge power requirements. In a similar way, employment of ionic liquids as reaction medium significantly simplifies work-up procedures and solvent recycling, but their massive implementation is discouraged by the high prices and by supply difficulties. Pairing of such technologies with continuous reactors should, in principle, allow a straightforward implementation to mass production thus overcoming scaling up limitations. Even if important research efforts have been made in such sense, some analysis reveals that both approaches will need further technological improvements in order to be superior to conventionally heated flow systems currently available, and in particular ionic liquids attractiveness is strongly relied on the lowering of supply price.²⁰

1.2.4 Process Monitoring

Many critics to flow technologies in the industrial world usually report that continuous reactors require a much higher expense in terms of control equipment respect to tank reactors, to assure monitoring of critical parameters as pressure, temperature and flow rate. Moreover, a continuous plant optimized for a specific reaction will be in principle far less flexible respect to a traditional batch plant. Both affirmations should be true, even if a high degree of control exerted on continuous reactors also means that a real-time feedback control of reaction is possible. In traditional tanks, reaction course is monitored through sampling and analysis of reaction mixture, but the possibility to repair errors is minimal, and, on consequence, the result will be the loss of tonnes of product due to failure in fulfillment of pharmaceutical specifications. In contrast, in continuous reactor, every change in reaction conditions would be immediately detected by fluctuation of critical parameters (temperature, pressure, flow rate) or by fast in line monitoring, for example using IR, Raman or UV probes, resulting in a real-time and possibly fully automatic correcting intervention. NMR, EPR, GC-MS and HPLC in-line monitoring probes are also available or currently under development.²¹

1.2.5 Productivity and Scale-Up

Continuous reactors allow the real-time measuring of the space-time yield that are usually superior respect to traditional batch reactors of several orders of magnitude. Space-time yield is defined as the amount of material produced per unit time and reactor volume: it gives a numerical indication of how working in continuous way could result in a strong increase of production potential respect to conventional large scale production plants. Moreover, the employment of flow reactors along the whole process development avoid the need for scaling up: in traditional batch approach, transfer of a synthetic reaction from lab to production scale requires usually several steps with a strong effort for re-optimization of reaction conditions in order to fit increased dimensions of reactors. Flow reactors are able to easily increase the throughput by using both the so-called scale-up and numbering-up. First of all, micro-sized reactors could be used for process development, taking advantage of the small volumes to reduce costs and times by rapidly screening for reaction conditions and simultaneously keep low the amount of materials employed and wastes produced. Afterwards, optimized conditions can be readily transferred to meso-sized reactors (scale-up or also called smart dimensioning), with minimal or no need for optimization due to the relatively small increase in reactor dimensions; further increase in production output can be obtained by increasing the number of identical units or devices working in parallel (numbering-up). This dual approach has been only recently proposed as alternative to the simple numbering-up, but is rapidly gaining consideration in industrial field as it allows for high production output by meanwhile maintaining at a minimum the requirements for controlling apparatus and maintenance needed with a large numbers of working units.²²

1.2.6 Energy and Material Savings

Noteworthy, another process intensification feature given by continuous flow reactors is the limited material waste in the process development phase, thanks to the small volume of reactors and the easily monitoring, testing and tuning of the reaction conditions. Moreover, as the transfer of synthetic processes from batch to continuous flow frequently results in higher yield and purity of desired product, lower amounts of solvents are needed both for reaction medium and for work-up or purifications procedures, translating in economical and environmental savings for raw materials as well as for wastes disposal. In addition,

thanks to the easier thermal management important savings in energy for reactor heating and cooling are possible.^{23,24}

1.2.7 Plant Issues

The reduction of continuous flow reactor dimensions suggests how the huge advantages of this quite new technology are not strictly related to chemical efficiency, but also to an engineering efficiency improvement. A flow reactors assembly able to equal productive output of a traditional stirred tank reactor will possess a far lower footprint, even considering the need for discontinuous vessels to prepare feed streams for the continuous reactor and to collect and work-up output stream, besides all the supporting apparatus for fluid delivery and reactor control. A direct consequence of reduction in size of chemical plants, besides an obvious environmental and urbanistic improvement, as well as cost reduction, is the possibility to have delocalized productions. In other words, a plant designed for commodities or fine chemicals manufacturing could easily contain a section dedicated to raw materials on-site production, with an obvious save in terms of transportation expenses and improvement in safety, especially regarding hazardous materials.²⁵

1.3 Perspectives on Industrial Applications

The widespread interest in both academia and industry research labs into development of reliable flow methodologies has leaded in the last years to a huge number of publications. Despite this, so far only a few companies other than big pharma have been able to turn part of their production to continuous flow. Since the main drivers for introducing such new technology are typically economic, namely substantial reductions in fixed and operational costs, a careful evaluation in this sense is necessary and, on consequence, contrasting opinions are spread today.

1.3.1 Application Field

According to the “European Roadmap for Process Intensification”,²⁶ chemical manufacturing could be divided in two major sectors, named PETCHEM (petrochemicals/bulk chemicals) and FINEPHARM (specialty chemicals/pharmaceuticals). Given the rather different orientation of the two gross sectors, different priorities would be assessed: energy saving and cost competitiveness would be main objectives of PETCHEM, whereas priority of FINEPHARM will be improvements in sustainability, selectivity and lead time together with economic competitiveness. Thus potential impact of microreactor technology will be higher for fine production, whereas for bulk chemicals the massive scale economy will somehow limit economical impact of flow technologies to the energy saving aspect.²⁷

One key point to be considered is the range of applicability of continuous processing: a case study was given by Roberge et al from Lonza Company, which examined the reactions portfolio performed in production plant of the company. They found that the 50% of present reactions would have a sufficiently fast kinetic to be applied in flow regime and, for the majority of them (44%) handling by microreactors will be advisable

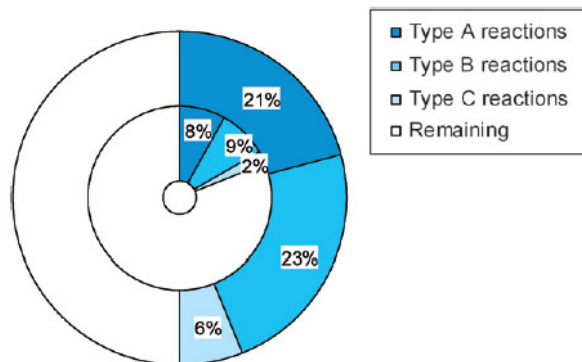
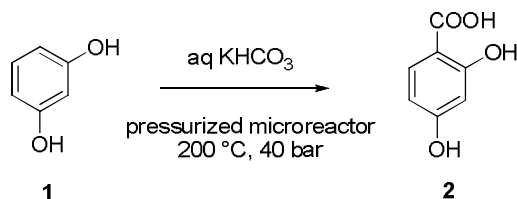


Figure 1.6: classification of reactions portfolio of Lonza Company. Type A: very fast, mixing limited. Type B: fast, heat transfer limited. Type C: other potential benefits by microprocessing, e.g. safety. Outer cycle: all reactions. Inner cycle: reactions with exclusion of gas-liquid and solid-containing processes.

because of difficult mixing or heat control. However, microreactors sensitiveness to solid particle formation cuts off the number of potentially transferable processes to 20% (Figure 1.6).²⁸ A clear consequence is that a strong engineering effort is still needed in optimizing behavior of flow equipments in the presence of heterogenous mixtures.^{29,30,31}

1.3.2 Economic Impact of Continuous Flow Process



Scheme 1.1: aqueous Kolbe-Schmitt flow synthesis of 2,4-dihydroxy benzoic acid.³³

A rough economic analysis of potential impact of microreactor technology for commodities/fine chemicals production has been made by Hassel and co-workers, using as a case study the Kolbe-Schmitt synthesis of 2,4-dihydroxy benzoic acid from resorcinol. Industrially, this synthesis is carried out batch-wise using a potassium carbonate solution and an applied CO₂ pressure of 4.5 bars.³² A variant of the process involves reaction in an aqueous solution of potassium hydrogen carbonate at 200° C in a pressurized microreactor at 40 bar pressure (Scheme 1.1). In such conditions a substantial reduction of reaction time respect to batch was obtained (from some hours to some tens of seconds) whereas a selectivity of 45% was achieved over the possible by-product 2,6-dihydroxy benzoic acid.³³ Employment of continuous flow reactors has thus opened up a novel process window.³⁴

Estimate the fixed costs related to this process is difficult, as they are mainly related to the specific company. For this economical analysis, only product related fixed costs, namely plant costs, were considered but not the raw product purification, resulting in higher incidence of variable costs related to raw materials and labor force. Economic factors were calculated by taking in account a single continuous flow reactor with a theoretical production of 4.4 tons/year. For this particular example, a surprising proportion of 1 euro/Kg of plant related costs versus 91 euro/Kg of operational costs was obtained. Ten-fold process intensification using parallelized flow reactors allows for substantial reduction of costs thanks to cut off the manpower related expenses; if the number of parallel working devices is kept low, only marginally higher costs related to plant will emerge.³⁵ Summarizing, operational (variable) costs should be the main indicator for commercial evaluation of continuous processing, while plant costs should have a minor influence. Continuous flow process intensification could strongly reduce product costs related to labor force with respect to batch, especially for commodities production. In fine chemicals

or especially pharma companies, where highly precious raw materials are employed, and workforce costs are less important, a fruitful application of flow reactors should best rely in a significative improvement of reaction selectivity.³⁶

References

- ¹ C. Wiles and P. Watts, *Micro Reaction Technology in Organic Synthesis*, **2011**, CRC Press.
- ² J. Wegner, S. Ceylan and A. Kirschning, *Chem. Commun.*, **2011**, 47, 4583–4592.
- ³ P. Tabeling, *Introduction to Microfluidics*, **2005**, Oxford University Press.
- ⁴ T. M. Squires and S. R. Quake, *Rev. Mod. Phys.*, **2005**, 77, 977-1026.
- ⁵ W. Eherfeld, V. Hessel and H. Lowe, *Microreactors*, **2000**, Wiley-VCH.
- ⁶ H. Song, D. L. Chen and R. F. Ismagilov, *Angew. Chem. Int. Ed.*, **2006**, 45, 7336 – 7356.
- ⁷ J. L. Steinbacher, D. T. Mcquade, *Journal of Polymer Science: Part A: Polymer Chemistry*, **2006**, Vol. 44, 6505–6533.
- ⁸ EU Legislation – Eudralex, Vol. 4 - *Guidelines for good manufacturing practices for medicinal products for human and veterinary use*.
- ⁹ P. D. I. Fletcher, S. J. Haswell, E. Pombo-Villar, B. H. Warrington, P. Watts, S. Y. F. Wong and Z. Zhang, *Tetrahedron*, **2002**, 58, 4735–4757.
- ¹⁰ P. Beato, R. Kraehnert, S. Engelschalt, T. Frank and R. Schlögl, *Chem. Eng. J.*, **2008**, 135S: S247–S253.
- ¹¹ K. F. Jensen, *MRS Bull.*, **2006**, 31, 101–107.
- ¹² J. J. Brandner in *Microreactors in Organic Synthesis and Catalysis*, T. Wirth (Ed.), **2008**, Wiley- VCH, pp. 1–17
- ¹³ M. G. Alonso-Amigo, *J. Assoc. Lab. Auto.*, **2000**, 5, 96–101.
- ¹⁴ C. K. Fredrickson and Z. H. Fan, *Lab Chip*, **2004**, 4, 526–533.
- ¹⁵ M. Fichtner, W. Benzinger, K. Hass-Santo, R. Wunsch, K. Schubert, *Microreaction Technology: 3rd International Conference on Microreaction Technology, Proceedings of IMRET 3*, **2000**, 90–101.
- ¹⁶ K. A. Comandur, A. A. S. Bhagat, S. Dasgupta, I. Papautsky and R. K. Banerjee, *J. Micromech. Microeng.*, **2010**, 20, 1–12.
- ¹⁷ M. V. Koch, K. M. VandenBussche and R. W. Chrisman, *Micro Instrumentation*, **2007**, Wiley-VCH.
- ¹⁸ *Aldrich ChemFiles*, Vol. 9, No. 4.
- ¹⁹ S. J. Haswell and P. Watts, *Green Chem.*, **2003**, 5, 240.

-
- ²⁰ V. Hessel, D. Kralisch and U. Krttschilb, *Energy Environ. Sci.*, **2008**, 467–478.
- ²¹ J. P. McMullen and K. F. Jensen, *Annu. Rev. Anal. Chem.*, **2010**, 3, 19–42.
- ²² V. Hessel, S. Hardt and H. Löwe, *Chemical Micro Process Engineering – Fundamentals, Modelling and Reactions*, **2004**, Wiley-VCH.
- ²³ B. P. Mason, K. E. Price, J. L. Steinbacher, A. R. Bogdan and D. T. McQuade, *Chem. Rev.*, **2007**, 107, 2300–2318.
- ²⁴ J. J. Lerou, A. L. Tonkovich, L. Silva, S. Perry and J. McDaniel, *Chem. Eng. Sci.*, **2010**, 65, 380–385.
- ²⁵ F. Ebrahimi, E. Kolehmainen and I. Turunen, *Org. Proc. Res. Dev.*, **2009**, 13, 965–969.
- ²⁶ [http://ispt.eu/cusimages/Report European Roadmap for Process Intensification \(December 2007\).pdf](http://ispt.eu/cusimages/Report%20European%20Roadmap%20for%20Process%20Intensification%20(December%202007).pdf)
- ²⁷ V. Hessel, P. Löb and H. Löwe in *Microreactors in Organic Chemistry and Catalysis*, T. Wirth (Ed.), **2008**, Wiley-VCH, pp. 211–275.
- ²⁸ D. M. Roberge, L. Ducry, N. Bieler, P. Cretton and B. Zimmermann, *Chem. Eng. Tech.*, **2005**, 28, 318.
- ²⁹ S. L. Poe, M. A. Cummings, M. P. Haaf, and D. T. McQuade, *Angew. Chem. Int. Edn.*, **2006**, 45, 1544–1548.
- ³⁰ A. Nagaki, Y. Tomida and J. Yoshida, *Macromolecules*, **2008**, 41, 6322–6330.
- ³¹ H. Zhao, J. X. Wang, Q. A. Wang, J. F. Chen and J. Yun, *Industrial Engineering and Chemical Research*, **2007**, 46, 8229–8235.
- ³² *Ullmann's Encyclopedia of Industrial Chemistry, 7th edn*, **2008**, Wiley-VCH.
- ³³ D. K. Hale, A. R. Hawdon, J. I. Jones and D. I. Packham, *J. Chem. Soc.*, **1952**, 3503.
- ³⁴ V. Hessel, C. Hofmann, P. Löb, J. Löhndorf, H. Löwe and A. Ziogas, *Org. Process Res. Dev.*, **2005**, 9, 479.
- ³⁵ V. Hessel, U. Krttschil, P. Löb, H. Löwe, D. Kralisch, G. Kreisel, M. L. Küpper and R. Schenk, *Proceedings of the 2006 AIChE, Annual Meeting San Francisco, CA, November 12–17*, **2006**.
- ³⁶ U. Krttschil, V. Hessel, D. Kralisch, G. Kreisel, M. Küpper and R. Schenk, *CHIMIA*, **2006**, 60, 611.

Chapter 2: Applications of Continuous Flow Technologies

Examples of application of continuous flow techniques in many fields of both organic and inorganic chemistry are growing faster. Here are reported briefly the applications that, in my opinion, better illustrate the advantages of continuous processing over batch methodologies. Since extensive and useful reviews, covering the main application examples on the argument, are readily available to the reader,¹⁻⁵ I will briefly review some exemplificative reactions carried out in both homogeneous and heterogeneous phase, and later focus on the more innovative and peculiar applications that have been recently reported in multistep sequential processes, photochemistry applications and synthesis of molecular materials (polymers and particles), as well as on the more industrially oriented examples.

2.1 Homogenous Chemistry

Since the major part of synthetic transformations performed in chemistry laboratories are essentially solution based reactions, chemistry in homogenous phase has obviously played a leading role during development of continuous flow methodologies. Many examples have been thus reported in literature that largely demonstrate how flow equipment may allow to overcome traditional chemistry limitations. Valuable examples include esterification and amidation reactions, nucleophilic and electrophilic substitutions, Grignard and lithium alkyl chemistry, reductions and oxidations, nitrations and sulfonations, halogenations, Michael additions, carbon-carbon and carbon-heteroatom couplings, Diels-alder reactions, Wittig and Horner-Wadsworth-Emmons reactions.⁶

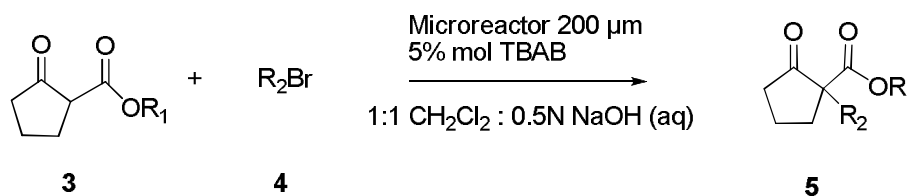
2.2 Heterogeneous Chemistry

For the vast majority of heterogeneous chemical reactions, surface-to-surface interactions between different phases play a key role. In particular, mass transport effects at the interfaces are crucial in determining conversion rate; moreover, many catalyzed transformations involving gaseous components are strongly exothermic, and the presence of high thermal gradient in discontinuous reactor causes both lack in reaction selectivity and potential runaways. As previously cited, one of the main characteristics of flow reactors is the extremely high surface-to-volume ratio, far superior to traditional discontinuous equipment. As direct consequence, reactions involving surface interactions will be potentially accelerated under strict control conditions by using a continuous approach. Typical systems that have been explored in microreactors are thus heterogeneous reactions involving liquid-liquid, solid-liquid, gas-liquid and gas-solid-liquid interfaces

2.1.1 Liquid-Liquid Reactions

Microreactors are a powerful tool in handling systems characterized by two liquid phases, as they favor the formation of homogeneously dispersed flow plugs and segmented flow with significant enhancements in contact area of liquid interfaces. For example, Jovanović and co-workers reported the effective improvement in yield and selectivity in a phase-transfer-catalyzed reaction by using a segmented flow microreactor. The selected model was a neat alkylation reaction of phenylacetonitrile with butyl bromide: aqueous basic solution was used, thus resulting in a two phases aqueous/organic stream, conditions and phase transfer catalysis (triethylbenzylammonium chloride, TEBA). A notable 74% conversion was attained, 1.8 times higher respect to batch conditions, with 99% of selectivity for the monoalkylated product: a 12% improvement respect to batch. Thanks to the high degree of control over flow plugs size granted by the microreactor, a delicate balance was obtained between increase of reaction rate and suppression of consecutive secondary reaction, such as the bis-alkylation. Moreover, precise control over reaction time leads to avoidance of the hydrolysis byproduct, phenylacetic acid.⁷

Ueno and co-workers studied the phase transfer alkylation of 2-oxocyclopentanecarboxylate (Scheme 2.1) catalyzed by tetrabutylammonium bromide (TBAB) as phase transfer agent. Strong improvement in reaction rates and selectivities was achieved by using a micro-structured reactor (200 μm channel width).⁸ Similarly, Hisamoto and co-workers reported the phase transfer diazocoupling reaction between 5-methyl resorcinol and 4-nitrobenzene diazonium tetrafluoroborate.⁹



Scheme 2.1: phase transfer alkylation of 2-oxocyclopentanecarboxylate derivatives.

2.2.2 Solid-Liquid Reactions

In the last decades, strong efforts have been dedicated to the development of solid supported catalysts or reagents for chemical synthesis, as such expedients allow for fast and easy recovery of precious materials and product purification. The same technology could be profitably applied in continuous flow synthesis although, as reported in the precedent chapter, introduction of solid materials in a micro or meso sized channel could result in device blockage. Considerable engineering efforts have developed a vast array of tools for solids immobilization within flow reactors. Functional coatings of channel inner walls has been extensively employed, however capillary type reactors are usually needed in order to assure considerable high surface-to-volume ratios, thus resulting in difficult scalable systems due to low volume and high pressure drops involved. Packed bed reactors have been similarly extensively employed, using metal powders or functionalized Merrifield resins: such devices however still suffer of high pressure drops, together with the tendency to swelling of organic resins in presence of solvents.

Costantini and coworkers reported the growth of a brush polymeric film directly on the inner walls of a microreactor by using atom-transfer radical polymerization. This highly porous material was then used for the *in-situ* formation of catalytic metal nanoparticles, that effectively promoted reduction of 4-nitrophenol in water at room temperature and the Heck coupling between ethyl acrylate and iodo-benzene.¹⁰

Tubular reactors filled with monolithic polymers as support for catalytic materials have been profitably employed, for example in Sonogashira type coupling reactions¹¹ and Knoevenagel condensations.¹² Monolithic materials are, generally speaking, single body structures, obtained usually by polymerization procedures, characterized by a highly porous nature due to presence of interconnected repeating cells or channels. Monolithic type fillings are effective in reducing pressure drops due to high porosity, allowing for relatively high flow rates resulting in good throughputs. Rather different, but very interesting results were obtained by mean of copper made reactors. Zhang and co-workers reported highly efficient Ulmann and Sonogashira couplings and decarboxylation reactions by using an heated copper pipe as flow reactor.¹³ Similarly, Bogdan and co-workers found that an heated copper coil reactor was able to promote the click chemistry cyclization reaction between azides and nitriles. The catalytic effect was correlated to various degree of Cu leaching from the reactor on the reaction stream, depending on reaction solvent.¹⁴

2.2.3 Gas-Liquid and Gas-Solid-Liquid Reactions

Direct fluorination of toluene using elemental fluorine is a typical example of how continuous flow reactors assure high degree of control over reaction times and temperatures, gaining access to rather difficult reaction conditions. Using flow reactors, in fact, formation of unwanted polyhalogenated compounds due to the high reactivity of fluorine is avoided, as well as potentially explosive heat releases.¹⁵

Flow equipment specifically designed for continuous flow metal catalyzed hydrogenations using gaseous hydrogen and packed bed catalytic flow cartridges (Thalesnano H-Cube®) is now commercially available and has become a well-established synthetic tool in many research laboratories all over the world, thanks to high reaction safety and operative simplification.¹⁶ In a similar way, flow reactors have been demonstrated to be effective tools for handling of potentially explosive ozone or ozone/oxygen mixtures in various applications, from ozonolysis of alkenes to oxidation reaction, especially when systems for in-line real-time monitoring of reaction progress are used.¹⁷ Commercial equipment for continuous ozone chemistry are as well currently spreading on the market, allowing chemists at both lab and production scale to safely experiment this useful but rather dangerous chemistry.

Koos et al. have reported the employment of a prototype reactor for gas-liquid continuous flow methoxycarbonylation of aryl and heteroaromatic halogens (Figure 2.1).¹⁸ This system is made by a tube-in-tube assembly, with an inner Teflon tube in which a liquid stream flows, containing the substrate, an homogeneous palladium catalyst and a base, and an outer tube in which instead gaseous carbon monoxide flows. Flow rates of gaseous and liquid feed can be independently regulated, and gas permeability of the inner membrane allows for controlled and effective delivery of the gaseous reactant to the liquid phase, whereas reaction progress was monitored through in-flow quantification of unreacted CO by FT-IR analysis. An analogous system was also reported by Mercadante and co-workers.¹⁹

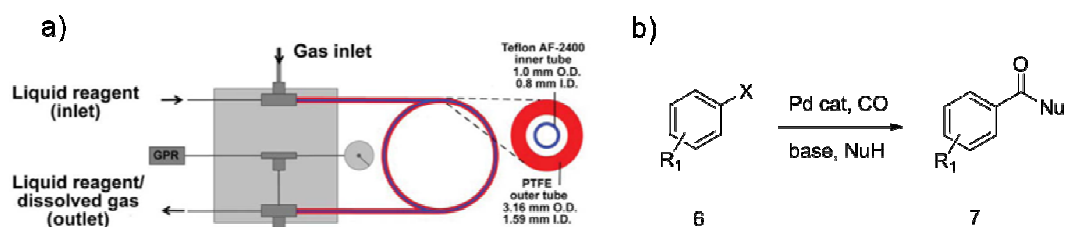


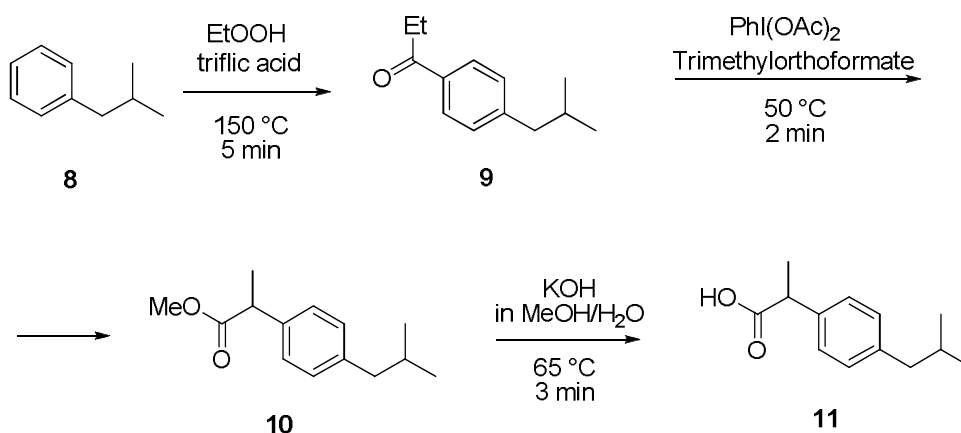
Figure 2.1: a) schematics of a tube-in-tube gas-liquid reactor for gas-liquid continuous chemistry.¹⁸ b) methoxycarbonylation reaction of aryl halides.

2.3 Multistep Synthesis

One of the potential advantages of continuous processing is the operational simplification: many synthetic steps could be performed either in parallel or as a cascade, without need for intermediate isolation as in a batch protocol, thus reducing working time and material and energy investment.

McQuade and co-workers developed a brilliant three steps continuous synthesis of Ibuprofen (Scheme 2.2).²⁰ The synthetic protocol involves a Friedel-Crafts acylation as initial step, followed by a 1,2-aryl migration to afford compound **10**, and finally saponification of the methyl ester moiety. Each single reaction step was optimized separately. Coupling of the three separate steps was however not straightforward: authors found out that strong releases of dissolved gases happened when the hot acylation step output stream (150 °C) was mixed with iodobenzene acetate and underwent aryl migration

in the second reactor kept at 50 °C. Moreover, neutralization of the acidic residues from first step during the final hydrolysis caused, as well, strong heat releases. The continuous flow approach reveals to be essential in overcoming these problems: reaction mixture from first step was thermally quenched and mixed with iodobenzene diacetate in a cooled mixer kept at 0 °C before entering the second reactor, thus avoiding over-pressurization due to gas development. Efficient handling of temperature increase during saponification reaction resulted then in good purity of final product, as side reactions were avoided. Ibuprofen was finally obtained in 51% overall yield and 99% purity by a simple extraction/purification over charcoal purification protocol of the output reaction mixture.



Scheme 2.2: continuous flow protocol for Ibuprofen synthesis.

2.3.1 In-Line Purification and Process Automation

As we have seen in the Ibuprofen synthesis example, performing multistep reactions in continuous flow is a complex task: incompatibilities between sequential reaction steps (acid/basic environments, solvents, precipitation of solids) and carry-over of impurities must be carefully considered. Thus an high effort has been done to develop both solid supported reagents and methods for in line purification between steps. As an example, Lay and co-workers reported the extended use of supported reagents in combination with the so-called catch and release protocol for the synthesis of imines or amines through Staudinger aza-Wittig sequence.²¹ First of all, a solution of alkyl azide is flown over a supported monolithic triphenylphosphine reagent for the Staudinger reaction step to give a solid anchored iminophosphorane, while solvent washing of the solid removes all reaction impurities. Aza-Wittig reaction is then carried out by passing a solution of an aldehyde or

ketone over the monolith, giving an imine solution as output stream. This core sequence can be coupled with both upstream and downstream flow processing, i.e. by generating in flow alkyl azide by either homogeneous or heterogeneous protocol and by flow reduction of imine using supported borohydride. The purification of the resulting amine is performed through catch and release protocol over sulfonic resin: essentially the product is selectively captured on the solid functional support, and soluble impurities are removed by washing with pure solvent. Then a change in composition of flowing solvent mixture or adding of suitable reactive promotes release of the product from the resin and recovery in pure form. The overall sequence has been used for synthesis of secondary amines starting from alkyl bromides with good (65%) to quantitative yields. Moreover, the entire process was fully automated in order to request minimal human intervention, allowing for the facile preparation of compound libraries. Similar systems were reported by the same authors for the synthesis of 5-amino-4-cyano-1,2,3-triazoles, quinoxalines, oxazoles and thiazoles,²² thus proving high flexibility of the method and the potential application of continuous flow chemistry in the drug development process as an alternative to combinatorial approaches, that have proven far less efficient than expected in speeding-up the discovery of new lead molecules.

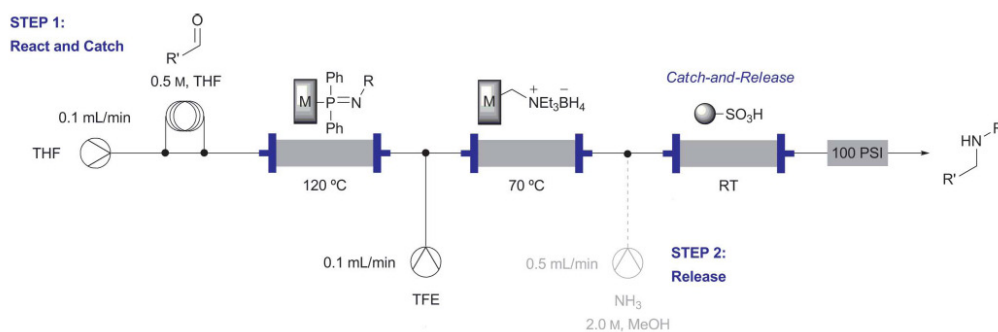


Figure 2.2: continuous flow scheme for automated synthesis of imines and secondary amines.²¹

2.4 Photochemical Reactions

Synthetic organic photochemistry uses light as an energy source to initiate chemical transformations. Light is considered to be a “green reagent” as usually photoinduced

transformations proceed smoothly with good efficiencies and high atom economy; however, excepting for sunlight, clean, safe and power-saving generation of artificial light is still a problem, particularly in large scale, thus relegating organic photochemistry to a secondary role due to difficult application to production of commodities or fine chemicals. Employment of continuous flow micro/meso-sized reactor could overcome such problems: beside the excellent properties of reaction control granted by continuous reactors, the small dimensions usually result in better spatial illumination and increase in efficiency, by contemporary reducing size and power output requirements for light sources. Moreover, systems miniaturization opens the way to employment of LED-based light sources as a flexible, low-energy-dissipation alternative to classical high pressure lamps. The portfolio of photochemical continuous reactions that have been developed so far include both homogeneous and heterogeneous syntheses, among them photoadditions, photorearrangements, photoreductions, photodecarboxylations, photooxygenations and photochlorinations, as well as some production oriented processes, as a demonstration of the high degree of interest in such technological application.²³

Ryu and co-workers developed an high throughput synthesis of a steroidal derivative through continuous flow Barton nitrite photolysis. Reaction conditions were first optimized in a small volume reactor, comparing the performances of both high pressure mercury lamp and UV LEDs as light source: by using this latter, a notable 300 times increase in energy efficiency respect to traditional lamp approach was obtained.²⁴ Optimized conditions were then translated to grams-per day scale production without affecting reaction efficiency.²⁵ Oelgemöller and co-workers compared reaction efficiency in batch and continuous flow for photodecarboxylative reactions of phthalimides, finding out sensible increments in efficiency by using continuous equipment.²⁶ The combined exploitation of photochemistry, slug flow and ultrasonication allowed Horie et al. to develop a continuous flow process for large scale photodimerisation of maleic anhydride with a sensible increase in conversion (70% respect to 26%) and reduction of wasted material respect to batch.²⁷

A huge exploited field correlated to continuous flow photochemistry is the oxidations by singlet oxygen generated through photosensitizers: in such application, use of continuous reactors allow for a substantial process safety increase thanks to very small amount of dangerous oxygenated mixtures that are generated per time unit inside reactors. Maggini and co-workers in particular exploited home-made hybrid glass-polymer reactors to investigate singlet oxygen generation with a fullerene based sensitizers. Excellent yields

(>90%) were obtained for oxidation of α -terpinene and L-methionine methyl ester by using both homogeneous and supported sensitizer and irradiation with traditional lamps and low power consuming white light LED.²⁸

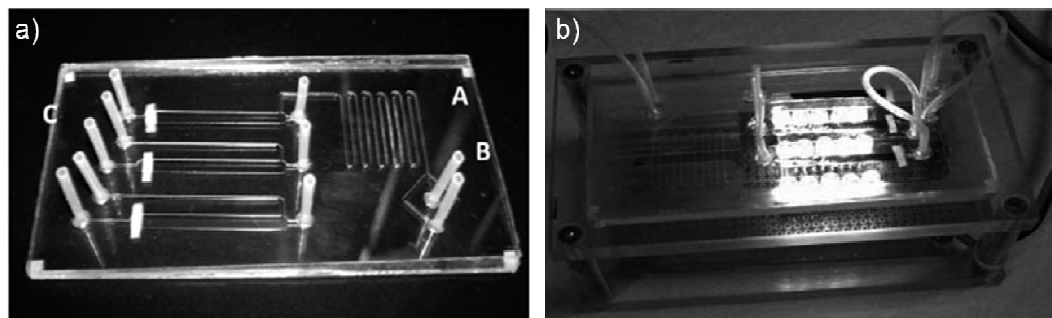


Figure 2.3: a) glass-polymer microreactor and b) white LED working device for continuous flow singlet oxygen photooxidations.

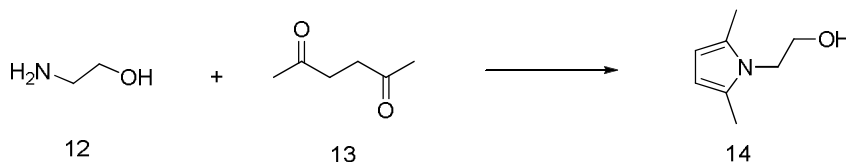
2.5 Preparation of Materials: Polymers and Nanoparticles

The high degree of control over reaction conditions together with the ability to effectively handle emulsions and droplets of various dimensions make flow reactors a powerful tool for material chemistry. Valuable examples in such fields comprise continuous polymerization reactions by cationic, free-radical and ring-opening mechanisms. In particular, Yoshida and co-workers demonstrated that efficient mixing in flow reactors allowed for high polydispersity index polymers to be obtained; in a similar way, efficient heat transfer inside microstructured channels proven to be highly effective in handling heat releases during free-radical polymerizations.^{29,30} By combining emulsification devices or multi-droplet formation geometries, in combination with thermal or photo induced polymerization routes, high control over polymeric particles dimensions and shape was demonstrated. In the same way, microreactors proven to be useful for the preparation of inorganic nanoparticles, such as silica, silver, CdSe, BaSO₄ and palladium. Analogous approaches have been extensively revised for post-synthesis functionalisation of organic molecules, as for example drugs encapsulation for controlled release applications.^{31,32}

2.6 Industrial Applications

Even if many of the examples reported in the previous paragraphs substantially possess characteristics for an industrial application, I will report briefly some examples in which continuous flow equipment has been successfully implemented in existing productive plants or almost operated in an industrial environment.

Togashi et al. reported a 72 tonnes/year productive line for selective phenol mono-nitration, made by twenty quartz microreactors in four banks.³³ Rutjes and co-workers have implemented the continuous flow Paal-Knorr synthesis previously developed by Schwalbe in a four reactor plant able to produce 55 g h⁻¹ of 2-(2,5-dimethyl-1 H-pyrrol-1-yl)ethanol (Scheme 2.3).³⁴ Wille et al. reported the full process development from a laboratory scale single microreactor to a multidevice pilot plant for the synthesis of diazo pigments in far higher yield respect to batch methodologies.³⁵



Scheme 2.3: continuous flow Paal-Knorr synthesis.

Tekautz and Kirschneck have reported the incorporation of a continuous microreactor into an existing two-batch reactors production plant. Replacement of the first reaction step with a continuous protocol allowed for a substantial increase in productivity for the whole process up to 3.6 tonnes per hour.³⁶ DSM instead reported the upgrade of an existing productive site for a Ritter reaction from batch to continuous operation. The reaction, reported in Scheme 2.4, has a very fast kinetic and was characterized by strong heat release upon mixing. Mixing step was then implemented in a continuous system and scaled up to a microreactor stack able of producing 1700 Kg/h of product. The continuous system was then smartly implemented in the existing discontinuous plant with a minimally invasive two steps procedure (see Figure 2.4) by joining with existing pipelines and using the old batch tank as an output stream collector for the flow reactor. By this expedient the

model reaction to develop a continuous system and to give a quantitative comparison of safety conditions between batch and flow, by using Dow's Fire and Explosion Index (that parametrically analyzes safety risks connected to detonations) and Worst case analysis. Continuous peracetic acid synthesis from acetic acid and hydrogen peroxide under H₂SO₄ catalysis was achieved by using a microstructured two unit device with a very short reaction time of *ca.* 300 s and a good product throughput of 10 kg h⁻¹. As may be seen in Table 2.1, the reduced volume of continuous device brought a significative reduction in predictable damage in case of explosion.³⁸ In a similar way, Loebbecke and co-workers reported a completely isolated, remotely operated continuous pilot plant including downstream processing for the synthesis of liquid nitrate esters at 150 g min⁻¹ scale and

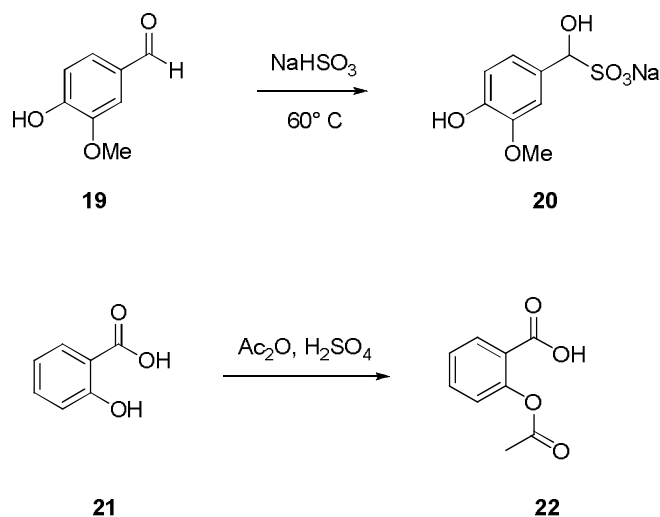
Table 2.1: Critical batch vs flow comparison of risks connected to peracetic acid synthesis.

(a) Dow's Fire and Explosion Index (F&EI)		
<i>Process Unit Risk Analysis</i>	batch	flow
Material factor for 50	40	40
F&EI	226	112
Radius of exposure (m)	58	29
Area of exposure (m ²)	1.05 × 10 ⁴	0.26 × 10 ⁴
Value of area of exposure (\$)	5 × 10 ⁶	5 × 10 ⁵
Damage factor (max. =1)	0.95	0.80
Maximum probable property damage (\$)	5 × 10 ⁶	4 × 10 ⁵
Maximum days outage (day)	75	35
(b) Worst Case and Consequences		
<i>Categories^a</i>		
Material release	4	2
Operating conditions	2	2
Process equipment	4	3
Transportations	5	1
Unpredictable factors	4	2
Total	19	10

a: 5 = Very serious hazard, 4 = serious hazard, 3 = medium hazard, 2

pharmaceutical purity. Jensen and co-workers developed a silicon-pyrex multichannel reactor packed with active carbon catalyst for the continuous preparation of phosgene starting from carbon monoxide and elemental chlorine, with a potential on-site production capacity of 100 kg year⁻¹ of this highly hazardous, although very useful chemical.³⁹

2.6.2 Equipment Flexibility



Scheme 2.5: synthesis of vanisal sodium (**20**) and synthesis of aspirin (**22**).

For a widespread diffusion of continuous technologies in chemical plants, microreactors equipments should demonstrate sufficiently high flexibility of use, besides their well recognized synthetic efficiency properties. In such view, a nice example was given by Ricardo and co-workers that analyzed employment of a Continuous Oscillatory Baffled Reactor (COBR) system for two consecutive production campaigns of, respectively, Vanisal sodium (compound **20** in Scheme 2.5) and aspirin.⁴⁰ A COBR system is made by a tubular reactor containing periodically spaced orifice baffles, that generates eddies in the fluid flow through oscillating motion given by means of diaphragm, bellows or piston at one or both ends of the tube. When operated in continuous, COBR could be assimilated to a Continuous Stirred Tank Reactor (CSTR) thus for sufficiently high number of baffled cells COBR exhibits plug flow behavior in a laminar flow regime, which results in very sharp residence time distributions.

First, COBR reactor system was employed for a 7-days campaign of production of Vanisal sodium (Scheme 2.5), a vanilline derivative employed in soaps and cosmetics manufacture. During operations, reactor output samples were collected and analyzed by HPLC and NMR, assessing an average product purity of 99.94%. The system then underwent cleaning under a Cleaning In Place (CIP) standard procedure: reactor was completely discharged and rinsed with tap water at 60° C, then washed with detergent solution (Liquinox 1%) and finally with United States Pharmacopeia (USP) purified water. The complete cleaning procedure produced 11 L of wastes from a 2 L reactor and at the end the authors found 0.001% residual vanisal sodium, sensibly inferior to accepted industrial limits of 0.1-0.2%. The same system was then employed for a 7-days campaign in which aspirin was produced by standard treatment of salicylic acid with acetic anhydride; the product, collected by filtration upon cooling of reactor output streaming, was analyzed by HPLC, NMR, XRD and SEM giving 99.5% purity and a standard crystal form. Cleaning procedure analogous to vanisal sodium case gave similar results, with a loss upon cleaning in Active Pharmaceutical Ingredient (API) of less as 0.005% of the material produced.

References

- ¹ C. Wiles and P. Watts, *Chem. Commun.*, **2011**, 47, 6512–6535.
- ² J. Wegner, S. Ceylan and A. Kirschning, *Chem. Commun.*, **2011**, 47, 4583–4592.
- ³ C. Wiles and P. Watts, *Eur. J. Org. Chem.*, **2008**, 1655–1671.
- ⁴ B. Ahmed-Omer, J. C. Brandt and T. Wirth, *Org. Biomol. Chem.*, **2007**, 5, 733–740.
- ⁵ K. Tanaka and K. Fukase, *Org. Process Res. Dev.*, **2009**, 13, 983–990.
- ⁶ V. Hessel, *Chem. Eng. Technol.*, **2009**, 32, 1655–1681.
- ⁷ J. Jovanovic, E. V. Rebrov, T. A. Nijhuis, V. Hessel and J. C. Schouten, *Ind. Eng. Chem. Res.* **2010**, 49, 2681–2687.
- ⁸ M. Ueno, H. Hisamoto, T. Kitamori and S. Kobayashi, *Chem. Commun.*, **2003**, 936–937.
- ⁹ H. Hisamoto, T. Saito, M. Tokeshi, A. Hibara and T. Kitamori, *Chem. Commun.*, **2001**, 2662–2663.
- ¹⁰ F. Costantini, E. M. Benetti, R. M. Tiggelaar, H. J. G. E. Gardeniers, D. N. Reinhoudt, J. Huskens, G. J. Vancso and W. Verboom, *Chem. Eur. J.*, **2010**, 16, 12406 – 12411.
- ¹¹ A. Gömann, J. A. Deverell, K. F. Munting, R. C. Jones, T. Rodemann, A. J. Canty, J. A. Smith and R. M. Guijt, *Tetrahedron*, **2009**, 65, 1450–1454.
- ¹² A. El Kadib, R. Chimenton, A. Sachse, F. Fajula, A. Galarneau and B. Coq, *Angew. Chem. Int. Ed.*, **2009**, 48, 4969–4972.
- ¹³ Y. Zhang, T. F. Jamison, S. Patel and N. Mainolfi, *Org. Lett.*, **2011**, 13, 280–283.
- ¹⁴ A. R. Bogdan, N. W. Sach, *Adv. Syn. & Cat.*, **2009**, 351, 849–854.
- ¹⁵ N. de Mas, A. Guenther, M. A. Schmidt and K. F. Jensen, *Ind. Eng. Chem. Res.*, **2003**, 42, 698–710.
- ¹⁶ http://www.thalesnano.com/files/file/brochures/applications/ThalesNano_H_Cube_App_Note.pdf
- ¹⁷ M. O'Brien, I. R. Baxendale and S. V. Ley, *Org. Lett.*, **2010**, 12, 1596–1598.
- ¹⁸ P. Koos, U. Gross, A. Polyzos, M. O'Brien, I. Baxendale and S. V. Ley, *Org. Biomol. Chem.*, **2011**, 9, 6903–6908.
- ¹⁹ M. A. Mercadante and N. E. Leadbeater, *Org. Biomol. Chem.*, **2011**, 9, 6575–6578.
- ²⁰ A. R. Bogdan, S. L. Poe, D. C. Kubis, S. J. Broadwater and D. T. McQuade, *Angew. Chem. Int. Ed.*, **2009**, 48, 8547–8550.

-
- ²¹ C. J. Smith, C. D. Smith, N. Nikbin, S. V. Ley and I. R. Baxendale, *Org. Biomol. Chem.*, **2011**, 9, 1927-1937.
- ²² C. J. Smith, N. Nikbin, S. V. Ley, H. Lange and I. R. Baxendale, *Org. Biomol. Chem.*, **2011**, 9, 1938-1947
- ²³ M. Oelgemöller and O. Shvydkiv, *Molecules*, **2011**, 16, 7522-7550.
- ²⁴ A. Sugimoto, Y. Sumino, M. Takagi, T. Fukuyama and H. Ryu, *Tetrahedron Lett.*, **2006**, 47, 6197.-6200.
- ²⁵ A. Sugimoto, T. Fukuyama, Y. Sumino, M. Takagi, I. Ryu, *Tetrahedron*, **2009**, 65, 1593.-1598.
- ²⁶ A.G. Griesbeck, W. Kramer and M. Oelgemöller, *Synlett*, **1999**, 1169.-1178.
- ²⁷ T. Horie, M. Sumino, T. Tanaka, Y. Matsushita, T. Ichimura and J. Yoshida, *Org. Process Res. Dev.*, **2010**, 14, 405.-410.
- ²⁸ T. Carofiglio, P. Donnola, M. Maggini, M. Rossetto, E. Rossi, *Adv. Syn. & Cat.*, **2008**, 350, 2815-2822.
- ²⁹ A. Nagaki, K. Kawamura, S. Suga, T. Ando, M. Sawamoto and J. Yoshida, *J. Am. Chem. Soc.*, **2004**, 126, 14702-14703.
- ³⁰ T. Iwasaki and J. Yoshida, *Macromolecules*, **2005**, 38, 1159-1163.
- ³¹ K. Torigo, Y. Watanabe, T. Endo, K. Sakai, H. Sakai, M. Abe, *J Nanopart Res*, **2010**, 12, 951-960.
- ³² P.M. Günther, G. A. Groß, J. Wagner, F. Jahn, J. M. Köhler, *Chemical Engineering Journal*, **2008**, 135S, S126-S130.
- ³³ S.Togashi, T. Miyamoto, Y. Asano and Y. Endo, *J. Chem. Eng. Jpn.*, **2009**, 42, 512-519.
- ³⁴ F. P. J. T. Rutjes, R. Segers, P. Nieuwland, K. Koch, H. G. Lelivelt, J. F. D. van den Berg and J. C. M. van Hest, *11th International Conference on Microreaction Technology*, Kyoto, Japan, **2010**, 104-105.
- ³⁵ C. Wille, H. P. Gabski, T. Haller, H. Kim, L. Unverdorben and R. Winter, *Chem. Eng. J.*, **2004**, 101, 179-185.
- ³⁶ D. Kirschneckl and G. Tekautz1, *Chem. Eng. Technol.*, **2007**, 30, 305-308.
- ³⁷ http://www.dsm.com/en_US/downloads/dpp/DSM_Micro_Reactor_Technology_Webinar_Presentation_24Sept09FINAL.pdf
- ³⁸ F. Ebrahimi, E. Kolehmainen, P. Oinas, V. Hietapelto and I. Turunen, *11th International Conference on microreaction Technology*, Kyoto, Japan, **2010**, 404-405.
- ³⁹ S. K. Ajmera, M. W. Losey, K. F. Jensen and M. A. Schmidt, *AIChE J.*, **2001**, 47, 1639-1647.
- ⁴⁰ C. Ricardo and N. Xiongwei, *Org. Proc. Res. Dev.*, **2009**, 13, 1080-1087.

Chapter 3: Overview on Continuous Flow Equipment

In the past chapters we have reviewed chemical, physical and engineering features of continuous flow reactors, together with some useful examples extracted from the abundant literature in the field, with a strong focus on the application of continuous flow techniques in synthetic chemical processes from the development stage to the industrial production.

In the following chapters I will report the results obtained in development of continuous processes for chemical synthesis of derivatives with potential applications in medicinal chemistry and material science. Before, however, I will introduce the tools that made these results possible, by briefly reviewing the flow equipments used during this thesis. Detailed technical descriptions may be found in the experimental sections of each chapter.

3.1 Reactor Types

Equipment employed in this work for continuous flow synthesis is highly varied, as the chemistry that has been performed. Large part of the development work has been carried out using commercially available platforms, specifically designed for such applications. However such systems, despite their high technological content, sometimes lack of flexibility and have to be replaced with more adaptable devices. A major distinction is between tubular type, which is essentially based on reactor coils made by high length, small-size tubes, and modular type based instead on self working modules interconnected by serial or parallel mode.

3.1.1 Tubular Type Reactors

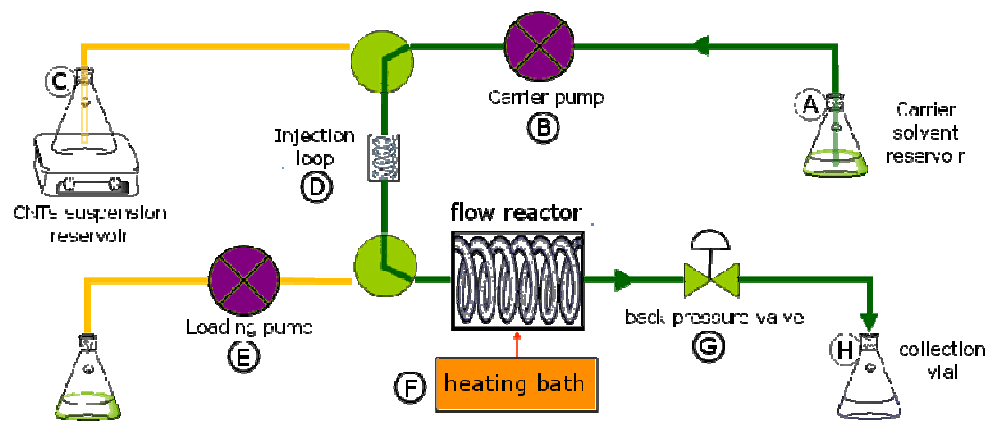
Vapourtec R4 platform¹ for continuous synthesis have been extensively used during this thesis. R4 is a modular system composed by fluid pumping and reactor heating modules. Pumping system is made of two independent HPLC type pumps and fluid lines equipped with selective valves able to switch between reagents and solvent feeds. Heating module has four independent positions able to use independent reactor assembly constituted by either tubular coils (PTFE or stainless steel, SS, with 5 or 10 mL volumes) or cartridge

type reactors for heterogeneous applications. Independently from the type, each reactor is equipped with a thermal mantle for convection heating that also embodies a thermocouple for temperature control. Accessible reactor temperatures range from room temperature to 150 °C (PTFE reactors) or up to 250 °C (SS) and backpressure regulators (BPR) are employed in order to allow operation over solvent boiling point. Electronic control on reaction parameters (temperature, pressure and flow rates) and on flow valves is controlled through informatics interface extensively automated. Relatively large tube dimensions (*ca.* 1 mm) made Vapourtec R4 a typical meso-sized system, characterized by somewhat lower performances in mixing rate and temperature homogeneity respect to other devices. Anyway, high throughput and harshness in reactions conditions made it a valid choice when seeking for translation to continuous of many industrial processes. Examples of Vapourtec R4 employ are reviewed through major parts of the present thesis: in particular, continuous approaches towards synthesis of oncological drugs are described in chapters 6 and 7, whereas in chapter 10 flow functionalisation of a porphyrin derivative is reported.



Figure 3.1: a) fully assembled Vapourtec R4 continuous flow platform and particulars of b) pumping module and c) heating module bearing various reactor modules.

An highly simplified version of such reactor is made by a reactor coil constituted by a pipe assembly made of various materials and provided with suitable fluid connections. Such apparatus strictly resembles common laboratory instruments as HPLCs, and are in fact usually assembled in a very inexpensive way using commercially available equipment. Such approaches, even if not very sophisticated, are usually functional for a wide range of applications or almost in the early stages of flow processes development. Similar equipment has been profitably used in the continuous flow functionalisation of carbon nanotubes, as reviewed in chapter 9.



Scheme 3.1: scheme of the continuous flow apparatus used for functionalisation of carbon nanotubes. A) carrier solvent reservoir; B) main line pump; C) CNTs suspension reservoir; D) injection loop; E) loading pump; F) heater and heating bath; G) BPR; H) collection vial.

Nanotubes are almost insoluble in common reaction mediums, resulting in large aggregates called bundles. However, use of amidic solvents (dimethylformamide, pyrrolidones) promotes bundles disaggregation and produces dispersions that could be processed in a small-size channel. On the other hand, suspensions of solid materials are not suitable to be pumped through traditional HPLC type pumps, as they will cause blockage of pumping pistons. In order to overcome such problem, we designed and realized the flow equipment schematized in Scheme 3.1., made of two main parts. The first one is an injection loop (D) made of a PTFE tubing coil (o.d. = 2 mm) volume of 11 ml and equipped with two switching valves. A stock dispersion of SWNTs and reagents, in the selected solvent, was charged in the sample loop by using loading pump (E). By acting on valves then the plug of nanotubes dispersion was injected into a main line of a carrier solvent (DMF) provided by carrier pump (B); reaction stream passed through the main reactor, a 400 cm segment of polytetrafluoroethylene (PTFE) tubing (i.d. = 800 μ m, total volume 2 ml) submerged into

an oil bath set to 140 °C. Due to gas evolution during functionalisation reaction, a BPR was mounted at reactor exit in order to pressurize the equipment. Reaction mixture is finally collected at reactor output (H). Flow reactor pictured in Figure 3.2 thus allows us to profitably handle solid dispersions of carbon nanotubes. For details on the continuous flow functionalisation reaction see chapter 9.

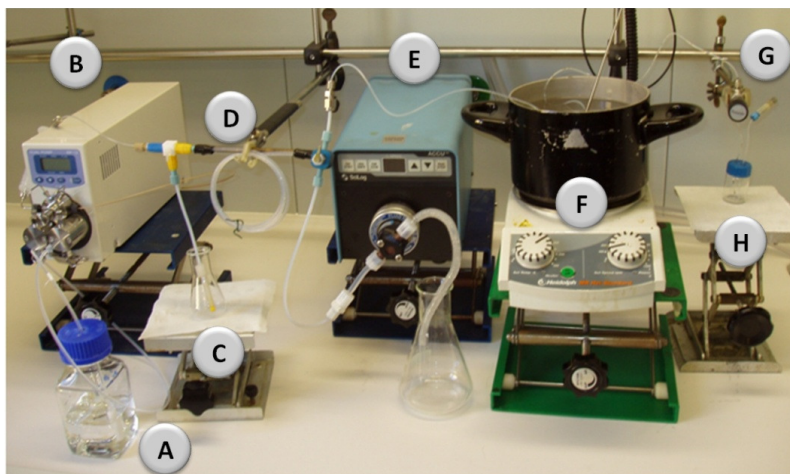


Figure 3.2: Photograph of the continuous flow apparatus for functionalisation of carbon nanotubes. A) carrier solvent reservoir; B) main line pump; C) CNTs suspension reservoir; D) injection loop; E) loading pump; F) heater and heating bath; G) BPR; H) collection vial.

3.1.2 Modular Type Reactors

Classically flow reactors characterized by a modular framework are also hierarchically organized. In such a view, the smallest base unit is usually called *microstructure*: common microstructures are of channel type or similar, even if chambers, pores and static functional elements are also widespread. An assembly of microstructures with a well defined geometrical shape and function is usually called *element*: for example, mixing elements could be constituted by an interdigital channels assembly or by a channel equipped with static elements able to introduce controlled turbulence in the flow path. *Units* are the elements that constitute micro-reactors, and are made of various functional elements interconnected, feeding lines and base supports; units can also be organized in *stacks*, meaning that many identical units are arranged in parallel, with the aim of increasing output. It should be pointed out that neither units nor stacks could be operated alone, as they always require some kind of connections with the external world, namely fluid pipelines or heating/cooling apparatus. Units embedded in proper housing that provides connections, or equipped with connection elements are called *devices* that are the smallest

functional module in micro-reactors. Devices can be used by themselves or more commonly assembled in *systems* by serial, or *banks* by parallel connection of identical or different devices. Finally, the assembly of systems or banks with the proper supporting apparatus, such as distribution systems, controlling elements, pipelines and collecting vessels are referred as *set-up* or *plant*, depending on the size and destination, namely lab or production.²

As already cited, hybrid glass-polymer modular reactors constructed through soft-lithographic techniques have been designed, assembled and used during this thesis. These devices have been fabricated through a procedure, developed by Beers and co-workers,^{3,4} and later improved by others, that exploits commercial thiolene optical adhesives. Accordingly, a layer of thiolene, acting as a negative resist, was poured between two glass plates. Upon partial UV light illumination through a mask containing the desired microfluidic network, the adhesive, in the regions not shielded by the mask, undergoes cross-linking and, on consequence, solidifies. Conversely, the fluid, uncured adhesive can be flushed away with ethanol or acetone through proper interconnects, leaving the microfluidic channels behind. We modified Beers original procedure and introduced a new type of interconnects that greatly simplify the coupling of the microreactor (MR) to the external environment. Our contribution is a versatile press-fit couple composed by a flanged tube (female connector) and another smaller Teflon tube (male connector) with matching inside and outside diameters. Figure 3.3 shows an example of assembled devices provided with interconnections.⁵ Similar reactors have been extensively used in the continuous flow synthesis of a methanofullerene derivative for application in organic solar cells (chapter 8).

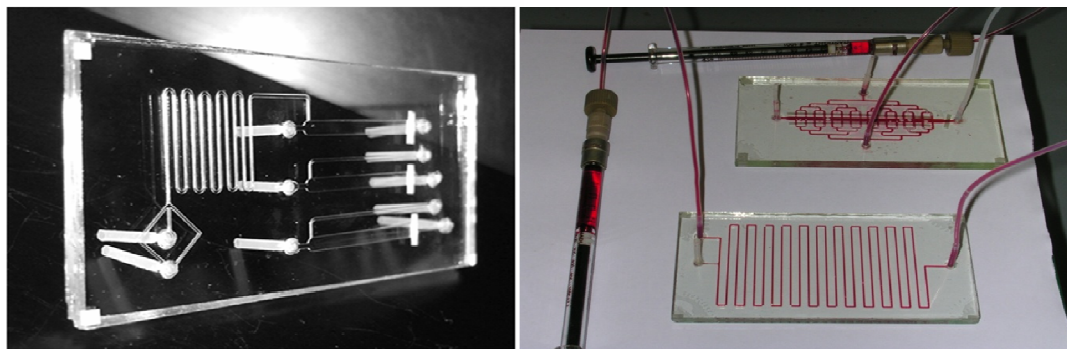


Figure 3.3: examples of polymeric chips assembled using a photocurable thiolenic resin.

During my permanence at CETC of Avon, I extensively used Corning® Advanced-Flow™ Reactors⁶ for the flow experiments. Corning systems are assemblies of glass fluidic modules connected together through appropriate piping and connectors: each module is substantially an autonomous device constituted by a glass unit and a proper housing system equipped with flow connections. In the sequent paragraphs I will show the use of these reactors for the continuous production of diazomethane. Two classes of modules were mainly employed, named *LowFlow* and *GEN1* modules that were grouped into continuous flow synthesis systems by assembling single-injection and residence time modules (Figure 3.4). Single-injection modules mixed two feeds at once and have a heart-shaped glass flow path for optimum phases split/mixing and mass exchange enhancement. Residence time modules have a heart-shaped structure as well.⁷ Typical channel width and height for the GEN1 system were in the 1 mm × 1 cm and in the 600 μm × 1 mm range, respectively, and a total volume up to approximately 10 mL per module. *LowFlow* modules are a compact, low-volume version of GEN1 modules. Typical channel dimensions are 10 times smaller than those of GEN1 modules, with a total volume of 0.45 mL. All modules have an external path for circulating a thermal fluid. Both *LowFlow* and GEN1 systems could be operated from -25 °C up to 200 °C. The limit pressure at 100 °C was 9 and 10 bar for *LowFlow* and GEN1, respectively. The continuous process conditions were first optimized in the small-volume *Low Flow* reactor and then scaled-up into a larger *GEN1* reactor with limited need for further optimization.

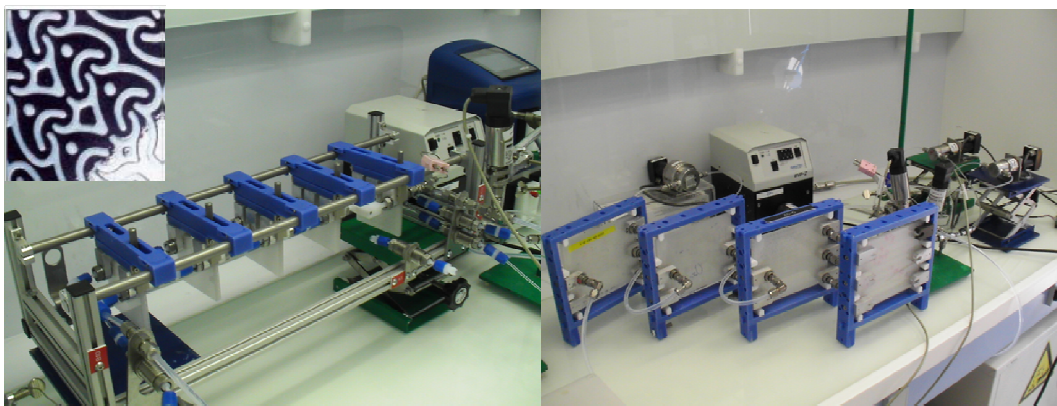


Figure 3.4: Corning® Advanced-Flow™ *LowFlow* (left) and *GEN1* (right) reactor assemblies and example of heart shaped flow elements.⁷

The *LowFlow/GEN1* binomy nicely exemplifies the concept of flow reactors throughput increase by smart dimensioning of the reactors in parallel with numbering up approach.

LowFlow modules for their dimensional characteristics and flow properties (see experimental details in chapter 4) are classical micro-structured devices, marked by low internal volume and high mixing and thermal performances, but poor flow output and solid sensitiveness. They are thus best suited for the process development stage. *GENI* modules at the contrary are high volume meso-structured devices, with somewhat poorer flow characteristics but higher throughput and capabilities for solid handling, as well displayed by their use in slurry hydrogenation reactions. An optimized *GENI* assembly reactor is able to reach high scale productivities, and straightforward increments in such sense can be gained by using both external numbering up (by operating in parallel *GENI* reactors banks) or internal numbering up (by using reactors made of *GEN2* and *GEN3* modules in which multiple parallel stacks are employed) depending on the target production scale (Figure 3.5).⁸

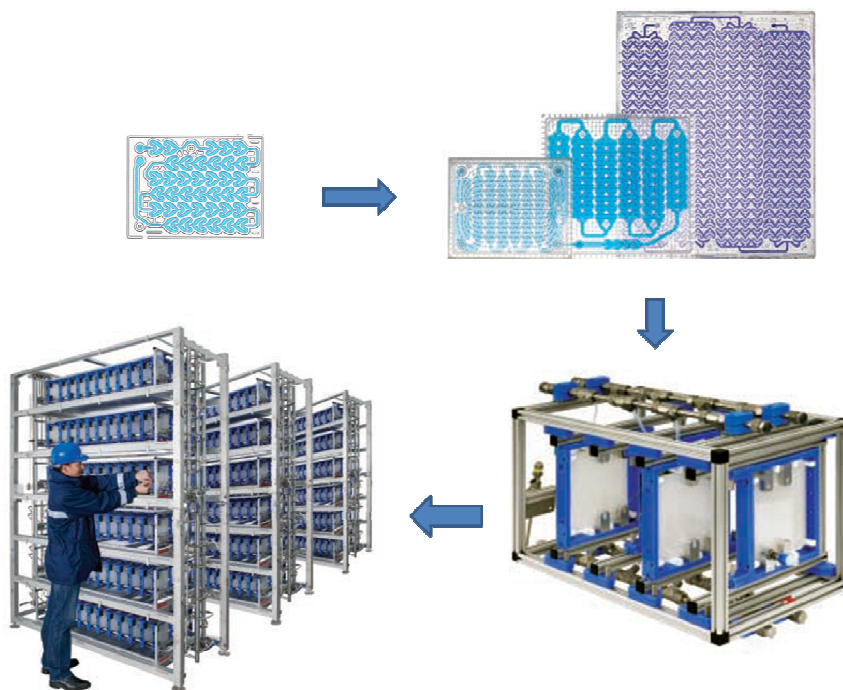


Figure 3.5: continuous process development with Corning Advanced Flow glass reactors: incremental throughput is achieved going from small volume *LowFlow* glass units (upper left) to high throughput *GENX* units through both smart dimensioning and internal numbering up. Selected units are assembled in working reactors (lower right) and finally in production banks by external numbering up.⁸

3.2 Supporting Systems and Fluid Connections

With the exception of Vapourtec R4 platform, that is an all build in bench-top instrument, generally continuous flow set-ups include various pieces of supporting equipments, in particular fluid delivering systems with proper connection, control apparatus and, eventually, special equipments as backpressure regulators or mixing devices.

Proper flow movimentation equipment was selected depending on the specific synthetic application and reactor type. As previously stated, Vapourtec R4 platform is composed by a pumping module which lodges two HPLC type pumps and proper fluid lines. For other applications, independent pumps acquired by various suppliers (FLOM, Encynova, Fuji, see experimental sections for details) were employed. HPLC type pumps are based on a reciprocating piston mechanism and are designed to afford highly reproducible flow rate even at high back-pressures (up to 40 bars). Constant fluid delivery is essential for reliability of continuous flow reactions, as flow pulsation may disrupt laminar flow regime and vanish many of the advantages in terms of control of reaction condition connected to employment of microstructured channels. Capability of working against high back pressure is extremely valuable when temperatures above solvent boiling point have to be reached, or gases are developed during reaction. The major drawback of HPLC type pumps is the high sensitivity to solid particles in the fluid stream, as they would likely result in pump blockage. For applications not requiring harsh conditions, syringe pumps were employed for fluid delivery. Syringe pumps are small infusion pumps that rely on a continuous displacement mechanism to drive the piston of a syringe containing the liquid. This system allows the fluid delivery at extremely precise rates; however, relatively low maximum flow rates achievable and the sensitivity to back-pressure limit employment of syringe pumps to applications in micro-structured reactors. For Corning® Advanced-Flow™ Reactors temperature control was afforded by circulating a thermal fluid through an external chiller/heater unit provided with fluid pump.

Connections between reactors and tubing, as well as connection with pumps, were afforded using commercially available fittings. Swagelok two pieces fittings (nut plus ferrule, stainless steel or PEEK) were used for high pressure applications, whereas Supelco or Upchurch single piece fittings (fingertight, PEEK) were used for low-to-mid pressure applications.

When needed, continuous flow set-ups were equipped with proper equipment for process monitoring, as Pt100 thermocouples and gauge pressure transducers for recording respectively reaction temperature and pressure inside reactors.

Pressurization of reactors was afforded by mounting back pressure regulators (BPR) on reactor output line. These devices work by mechanically reducing channel width, as resistance exerted against flow passage results in back pressure increment. For solid free applications, cartridge BPRs were used, in which flow is forced through a polymeric membrane at controlled porosity: pore size determine flow resistance extent and thus maximum working pressure. In case of streams containing particles, a mechanically regulated needle valve was used.

Tubular reactors were usually equipped with simple T junctions for mixing liquid streams. For special applications, mixing performances were improved by mounting an *Institut für Mikrotechnik Mainz* (IMM) slit interdigital micromixer. This device combines multilamination of feed streams (see section 1.1.1.2), thus reducing diffusion path, and flow focusing for radical enhancing of reagents mixing rate.⁹



Figure 3.6: examples of continuous set-ups and support apparatus: a) a *Low Flow* complete reactor assembly involving also pumping, heating and controlling units. b) on-line probes for temperature and pressure monitoring. c) fluidic modules interconnected through Swagelok fittings and d) an IMM micromixing device.⁹

References

¹ <http://www.vapourtec.co.uk/>

² W. Eherfeld, V. Hessel and H. Lowe, *Microreactors*, **2000**, Wiley-VCH.

³ Z. T. Cygan, J. T. Cabral, K. L. Beers and E. J. Amis, *Langmuir*, **2005**, 8, 3629.

⁴ C. Harrison, J. T. Cabral, C. M. Stafford, A. Karim, E. J. Amis, *J. Micromech. Microeng.*, **2004**, 14, 153.

⁵ T. Carofiglio, P. Donnola, M. Maggini, M. Rossetto, E. Rossi, *Adv. Syn. & Cat.*, **2008**, 350, 2815-2822.

⁶ www.corning.com/reactors

⁷ B. Buisson, S. Donegan, D. Wray, A. Parracho, J. Gamble, P. Caze, J. Jorda and C. Guerneur, *Chemistry Today*, **2009**, 27, 12-16.

⁸ E. D. Lavric and P. Woehl, *Chemistry Today*, **2009**, 27, 45-48.

⁹ http://www.imm-mainz.de/index.php?id=slit_interdigital_micromixer

Chapter 4: A Case Study: continuous flow diazomethane generation

In this chapter I will report personal experience gained in the field of continuous processes development, as a proof of concept of all the potential advantages that microreactors are able to give for chemical industry. Such experience was matured during a period of three months spent at the Corning European Technology Center (CETC) of Avon, France, working with Corning Advanced Flow Reactors; in the frame of a collaboration with a multinational company, Corning Incorporated, aimed to testing of a prototype continuous flow reactor, we studied the continuous generation of diazomethane through the base-induced decomposition of the precursor N-methyl-N-nitrosourea (MNU).¹

4.1 Diazomethane in chemistry

Diazomethane is a highly reactive and selective reagent for the synthesis of pharmaceuticals and fine chemicals.^{2,3,4} However, its acute toxicity and explosive characteristics strongly discourage a large-scale use in synthesis.^{5,6} Discontinuous preparations up to 2–300 mmol of diazomethane, through the reaction of solid nitrosoamides or ureas with bases, has been reported in special safety glassware. Also, strategies for industrial-scale production of diazomethane have been described, although the equipment needed for its safe handling is elaborate and expensive.^{7,8} Trimethylsilyl diazomethane (TMSCHN₂) is reported to be a less hazardous alternative for a wide range of applications, despite the lower reactivity and the formation of byproducts upon decomposition that make it less appealing for pharmaceutical derivatizations.⁹

Important gains can be achieved by transferring the batchwise diazomethane synthesis to continuous-flow processing in microstructured reactors where large surface-area-to-volume ratios allow precise reaction control through efficient heat and mass transfer, while also potentially granting high production throughputs. Struempel and co-workers reported the production of diazomethane in a continuous microreactor setup through the base-

induced decomposition of N-methyl-N-nitroso-p-toluenesulfonamide (MNTS or Diazald, compound **23** in Scheme 3.1)¹⁰ that, in turn, can be prepared in a continuous multistep synthesis starting from p-toluenesulphonyl chloride.¹¹ These studies demonstrated the feasibility of on-site production of diazomethane within microreactors, even if attained productivities were quite low. Ley and coworkers investigated the use of a polystyrene supported MNTS reagent for the flow production of diazomethane to be used in the subsequent preparation of diazoketones, but such solution was finally discarded in favor of direct employment of less hazardous TMSCHN₂.¹² Kim and co-workers developed instead a PDMS microchemical chip based on a dual-channel microreactor: in one of the microchannels gaseous diazomethane was continuously generated by Diazald decomposition and permeated through a porous membrane to the second channel where it could be used for methylation reactions. Despite the very efficient approach, however, effective scalability of the method in an industrial production view results to be difficult.¹³

We resolved to use Corning Advanced-Flow Reactors with the aim of developing a continuous process for generating and reacting diazomethane in large scales. In particular, we first optimized reaction conditions in a small-volume *LowFlow* reactor, then the process was scaled-up into a *GENI* reactor of larger size with limited need for further optimization that, to afford a final processing capability of more than 19 mol d⁻¹ of diazomethane.

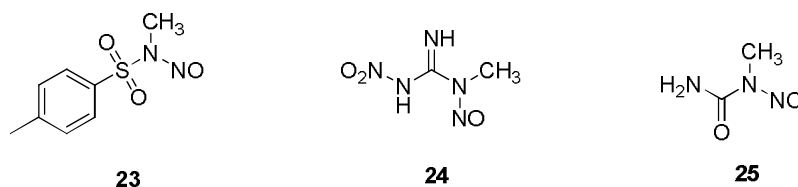
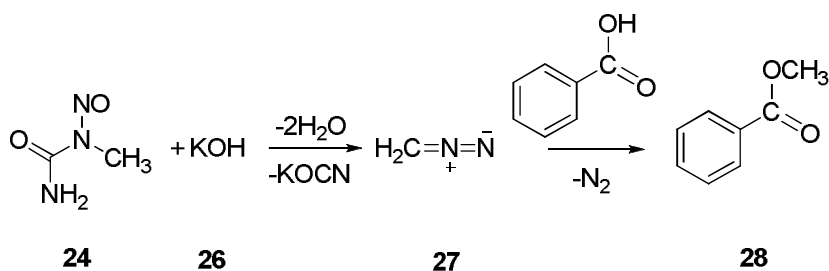


Figure 4.1: Common diazomethane precursors.

Besides Diazald, other common diazo-methane precursors are N-methyl-N'-nitro-N-nitrosoguanidine (MNNG, **24**) and N-methyl-N-nitrosourea (MNU, **25**). MNTS is classified as a self-reacting solid¹⁴ that can undergo explosions by shock, friction, heating, and other sources of ignition,¹⁵ whereas MNU is a flammable solid¹⁶ but is supplied as a water/acetic acid slurry that may reduce flammability during transportation and storage. According to the safety data sheet, MNNG is a nonflammable, nonexplosive solid.¹⁷ On the other hand, toxicity data¹⁸ and price are in favor of MNTS which has a much lower

acute toxicity and is less expensive than MNNG and MNU.¹⁹ However, we believe that the commercial formulation of MNU is safer to transport and store if compared to MNTS²⁰ and may reduce toxicity hazards with respect to MNNG that, as a solid reagent, is affected by an easier exposure route through inhalation. By these reasons, MNU was thus selected as diazomethane precursor for our tests.

4.2 Results and Discussion



Scheme 4.1: Methylation of benzoic acid with diazomethane produced *in situ* by basic decomposition of N-methyl-N-nitrosourea with KOH.

The diazomethane generation efficiency, from the KOH-promoted decomposition of MNU, was demonstrated on the model compound benzoic acid, assuming that the yield of methyl benzoate is equivalent to that of diazomethane.¹⁰ Excess benzoic acid was used to convert diazomethane and to neutralize the excess base from the first reaction step.²¹ To prevent particulate formation and clogging of the flow- reactor, a series of batch tests were carried out to determine the optimum solvent system for the reactions illustrated in Scheme 4.1. From the data reported in Table 4.1, the solvent system reported in entry 6 gave optimal reagent solubility and less particulate formation, with a moderate yield. In particular, a 1:1 mixture of Et₂O and diethyleneglycol diethylether (DEG) solubilized nicely the MNU feed (0.5 M), whereas KOH and benzoic acid feeds were solubilized by water (1.5 M) and ethanol (1.5 M), respectively.^{8,10}

Table 4.1: Solvent tests that were carried out under batchwise conditions at 25 °C. (MNU 0.5 mmol, MNU/KOH/benzoic acid = 1:1.5:3)

Entry	Solvent (MNU)	Solvent (KOH)	Solvent (benzoic acid)	Precipitate	Phases	Yield (%)
1	DEG	2-PrOH	DEG	N	1	33
2	DEG	EtOH	EtOH	Y	1	32
3	THF	EtOH	EtOH	Y	1	19
4	EtOH	EtOH	EtOH	Y	1	19
5	Et ₂ O	EtOH	EtOH	Y	1	70
6	Et ₂ O/DEG ^a	H ₂ O	EtOH	N	2	55

MNU: N-methyl-N-nitrosourea; DEG: diethyleneglycol ethylether; THF: tetrahydrofuran
a: 1:1 v/v

To achieve the continuous-flow synthesis of diazomethane, Corning Advanced-Flow *LowFlow* reactor assembly was first employed to test the optimized conditions of entry 6 (Table 4.1). Figure 4.2 shows the glass microstructured module sequence of the flow reactor, in which each module has a HEART-shaped design, that efficiently handles the liquid–liquid two-phases emulsion created by the solvent combination of entry 6. In the Low Flow, each glass fluidic module has an inner path of 0.45 mL (see Chapter 3). Reactor assembly and experimental conditions were rapidly screened searching for the best values of temperature, reagents stoichiometry and residence time.

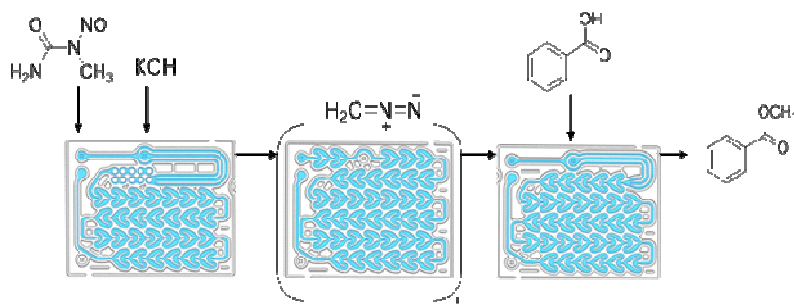


Figure 4.2: Module schematics of Corning Advanced-Flow™ *Low Flow* Reactor.

Under optimized conditions, a constant yield of 75% of methyl benzoate was achieved at room temperature for a residence time of 19 s, a total flow-rate of 3.2 mL min⁻¹ and 1.5 mol. equiv. of KOH (Table 4.2, entry 1). Longer reaction times, obtained by changing either flow rates or the volume of the reactor, probably favor diazomethane decomposition,

whereas higher amounts of base results in extensive saponification of the benzoate ester (Table 4.2, entries 2–6). During all experiments, no clogging problems were encountered.

Table 4.2: Selected Low Flow results at 25 °C (MNU 0.6 M in 1:1 Et₂O/DEG^a; KOH 1.5 M in H₂O; benzoic acid 1.5 M in EtOH).

Entry	MNU flow rate (ml min ⁻¹)	KOH flow rate (ml min ⁻¹)	MNU:KOH	Acid flow rate (ml min ⁻¹)	Residence time 1 ^b (s)	Residence time 2 ^c (s)	Yield (%)
1 ^d	2.0	1.2	1:1.5	2.4	18.7	5.3	75
2 ^d	1.0	0.6	1:1.5	1.2	37.5	10.7	7
3 ^e	2.0	1.2	1:1.5	2.4	39	5.3	15
4 ^e	2.0	1.5	1:1.8	2.4	36.1	5.1	5
5 ^e	2.0	1.0	1:1.2	2.4	42	5.6	33
6 ^e	2.0	0.8	1:1	2.4	45	5.8	6

MNU: N-methyl-N-nitrosourea; DEG: diethyleneglycol ethylether.
a: water 4% (v/v), CH₃CO₂H 0.26% (v/v) from commercial MNU (see experimental section).
b: residence time before addition of benzoic acid.
c: residence time after addition of benzoic acid.
d: total reactor volume 0.9 ml.
e: total reactor volume 1.35 ml.

Once identified the best reaction parameters in the Low Flow system, a scale up was carried out on larger *GENI*-type fluidic modules (see Chapter 3) with minimal adjustments. Under optimized conditions, a nearly quantitative yield of methyl benzoate was obtained at room temperature for a residence time of 28 s, a total flow-rate of 52.8 mL min⁻¹ and 1.3 mol equiv of KOH (Table 4.3, entry 4). One can notice that the optimized conditions for the *LowFlow* and *GENI* systems differ markedly (Table 4.2, entry 1 vs Table 4.3, entry 4). The reason for this variation could be related to a different glass microstructure of the channels that, in turn, determine distinctive flow characteristics within the heart-shaped mixing elements. Mixing is a fundamental process that affects mass transfer rate, hence, the observed difference. It is worth mentioning, however, that the internal volume of the *GENI* system is almost 10-fold that of the *LowFlow* counterpart. In

order to maintain comparable residence times, the flow rates used for the *LowFlow* setup have been increased substantially when diazomethane was prepared in the *GENI* system. In addition, low flow rates in a *GENI* setup may produce flow pulsations that hamper data reproducibility.

Table 4.3: Selected GEN1 results at 25 °C (MNU 0.45 M in 1:1 Et₂O/DEG^a; KOH 1.0 M in H₂O; benzoic acid 1.5 M in EtOH).

Entry	MNU flow rate (ml min ⁻¹)	KOH flow rate (ml min ⁻¹)	MNU:KOH	Acid flow rate (ml min ⁻¹)	Residence time 1 ^b (s)	Residence time 2 ^c (s)	Yield (%)
1 ^{d,e}	25	11.25	1:1.5	31.5	24.6	5.5	29.3
2 ^e	35	21	1:1.3	31.5	16	5.5	40
3 ^{d,e}	33	10.56	1:1.1	29.7	20.5	6.6	55.7
4 ^f	33	19.8	1:1.3	29.7	28.4	5.8	97
5 ^g	33	19.8	1:1.3	29.7	19.2	5.8	87
6 ^g	23.75	14.25	1:1.3	21.37	26.7	8.1	72

MNU: N-methyl-N-nitrosourea; DEG: diethyleneglycol ethylether.

a: water 3% (v/v), CH₃CO₂H 0.18% (v/v) from commercial MNU (see experimental section).

b: residence time before addition of benzoic acid.

c: residence time after addition of benzoic acid.

d: KOH solution concentration 1.5 M in H₂O.

e: total reactor volume 14.86 ml.

Water content in the commercial MNU slurries differs noticeably within different production lots. Product specifications indicate, for instance, a generic acetic acid content ≤5% and an amount of water (by Karl Fischer) ≤ 45%. The MNU employed for *GENI* experiments had a rather different content of water if compared to the lot used with *LowFlow* setup experiments (27% vs 41% w/w). Water was added to MNU stock solutions for the *GENI* experiments to achieve both comparable water content and elimination of particulate. Accordingly, the concentration of MNU (calculated over dry basis weight) decreased. Although the effect of different water content in MNU starting slurries may deserve further studies, it was beyond the scope of this work.

The stability of the process was tested over two hours of continuous operation without observing any clogging of the reactor setup that is shown in Figure 3.2. A mean operative yield of 90% of methyl benzoate was obtained under the optimized conditions reported in entry 4 of Table 3.3. It is worth noting that the production of diazomethane, in the two-phase solvent system described above, is strongly affected by mixing. The highest diazomethane conversions were obtained for a MNU/KOH flow ratio of 1.66 that was kept constant both in the *Low Flow* and *GENI* systems.

3.4 Conclusions

In conclusion, this study has shown the effectiveness of flow reactors to handle the preparation of hazardous diazomethane through a base-induced decomposition of N-methyl-N-nitrosourea. Process scale-up was quickly and efficiently achieved on a modular continuous-flow platform that allowed the production and use of diazomethane up to 19 mol d⁻¹ at a total flow rate of 53 mL min⁻¹, while maintaining the amount of diazomethane itself in the reactor limited to 6.5 mmol. This process productivity could, at least in principle, fulfill the needs of small pharma or fine chemical companies. Best reaction parameters were first developed on a small-volume flow reactor (0.9–1.35 mL) for minimal reagents consumption. Then a 10-fold production improvement was achieved by increasing the flow reactor dimensions (15–25 mL) with a very limited optimization effort. This scale-up procedure complements the so-called numbering-up approach, where a series of identical flow reactors are run in parallel.

3.5 Experimental

All chemicals and solvents were used as received. N-Methyl-N-nitrosourea (MNU, 50–70% aqueous slurry stabilized with 3% w/w acetic acid, Sigma Aldrich) contains a variable amount of water that depends on the production lot as indicated on the package. KOH 86% (Fischer Scientific); benzoic acid (Sigma Aldrich, purity $\geq 99.5\%$); diethyl ether 99.8% (Sigma Aldrich); diethylene glycol 99% (Sigma Aldrich); methyl benzoate 99.5%

(Sigma Aldrich). In the reaction balance, 0.1 equiv of KOH is needed to neutralize the stabilizing acetic acid. MNU concentrations were calculated on dry weight basis.

3.5.1 Batch Reactions

In a 4-mL glass vial MNU (53% dry basis, 100 mg, 0.5 mmol) was dissolved in the selected solvent (Table 4.1, 1 mL) and stirred at 25 °C for 5 min. Then a solution of KOH (0.5 mL, 1.5 equiv) in the selected solvent was added dropwise during one minute with a syringe. After 5 min at room temperature, reaction mixture was quenched with excess benzoic acid (1.5 M, 1 mL). The crude mixtures were analyzed by gas chromatography on a GC Agilent 7890A equipped with an Agilent dimethylpolysiloxane Rtx 50 column (30 m × 320 µm, 0.25 µm film thickness) and FID detector. The product methyl benzoate was identified through a commercial standard reference compound and quantified using toluene as internal standard.

3.5.2 Flow Experiments

Continuous flow studies were carried out in Corning Advanced-Flow *LowFlow* and *GENI* modules that were grouped into continuous-flow synthesis units by assembling single-injection and residence time modules (Figure 4.2). See Chapter 3 for reactor technical description. In all experiments, temperature was kept at 25 °C with the aid of a circulating thermostat that was connected to the external path. The pressure that was recorded during diazomethane production at the various flow rates, reported in Tables 4.2 and 4.3, was in the 4.0–5.0 bar range. The continuous-flow synthesis units were equipped with Pt 100 thermocouples and HD3604T gauge pressure transducers within the reaction and thermal fluid circuits. Temperature and pressure were recorded with an ALMEMO 2590 unit. A three-way gauge was mounted at the outlet of the synthesis units for reactor equilibration purposes and sample collection. Advanced technical information on Corning reactors are available via the web at www.corning.com/reactors. In a typical *LowFlow* experiment, solutions of MNU in a 1:1 diethyl ether/diethylene glycol mixture (0.45 M), KOH in water (1.5 M), and benzoic acid in ethanol (1.5 M) were delivered to the flow reactor through three pumps (two Fuji 211 PEEK HYM super metering pumps for MNU and acid feeds and an Encynova Novasync 2-1 pump for KOH feed). The stock solution of MNU was prepared by dissolving 10.2 g of commercial slurry (water content = 4.2 mL) in 100 mL of ether/glycol mixture. Flow experiments with the *GENI* system were carried out using glass modules of 8.39, 8.53, 8.06, and 6.80 mL that were combined to give the volumes

indicated in Table 4.3. A stock solution of MNU for GEN1 experiments was prepared by dissolving 32.5 g of commercial slurry (water content = 8.7 mL) in 500 mL of ether/glycol. Additional water (5 mL) was added to prevent particulate formation. The KOH was dissolved in water (1.0 or 1.5 M for entry 2, Table 3.3) and benzoic acid in ethanol (1.5 M). The solutions were delivered by means of mzs-7255 pumps.

References

- ¹ E. Rossi, P. Woehl and M. Maggini, *Org. Proc. Res. Dev.*, **2011**, DOI: 10.1021/op200110a.
- ² G. Maas, *Angew. Chem. Int. Ed.* **2009**, 48, 8186-8195.
- ³ H. B. Hopps, *Aldrichim. Acta* **1970**, 3, 9-12.
- ⁴ M. Regitz, G. Maas, *Diazo Compounds-Properties and Synthesis*, **1986**, Academic Press.
- ⁵ J. D. Clark, A. S. Shah, J. C. Peterson, L. Patelis, R. J. A. Kersten, A. H. Heemskerk, *Thermochim. Acta* **2002**, 386, 73-79.
- ⁶ E. B. LeWinn, *Am. J. Med. Sci.* **1949**, 218, 556.
- ⁷ T. Archibald, *U.S. Patent 5,817,778*, **1998**.
- ⁸ A. Warr, *US Pat 0 188 112*, **2002**
- ⁹ T. Shiori, T. Aoyama, T. Snowden, *e-EROS Encyclopedia of Reagents for Organic Synthesis*, **2001**.
- ¹⁰ M. Struempel, B. Ondruschka, R. Daute, A. Stark, *Green Chem.* **2008** 10, 41-43.
- ¹¹ M. Struempel, B. Ondruschka, A. Stark, *Org. Process Res. Dev.* **2009**, 13, 1014-1021.
- ¹² L. J. Martin, A. L. Marzinzik, St. V. Ley, and I. R. Baxendale, *Org. Lett.*, **2011**, 13, 320-323.
- ¹³ R. A. Maurya, C. P. Park, J. H. Lee and D.-P. Kim, *Angew. Chem. Int. Ed.*, **2011**, 50, 5952-5955.
- ¹⁴ www.sigmaaldrich.com/catalog/ProductDetail.do?lang=it&N4=D28000\ALDRICH&N5=SEARCH_CONCAT_PNO\BRAND_KEY&F=SPEC
- ¹⁵ The following statement is reported about diazomethane precursors: “although this material (Diazald) has been kept at room temperature for years without significant change, there has been reported one instance in which a sample stored for several months detonated spontaneously. For long periods of storage, it is recommended that the material be recrystallized and placed in a dark bottle”, in T. J. De Boer, H. J. Backer, N. Rabjohn, *Ed. In Organic Synthesis*; John Wiley & Sons: New York, **1963**; Collect. Vol. IV, p 495.
- ¹⁶ www.sigmaaldrich.com/catalog/ProductDetail.do?lang=it&N4=N4766\SIGMA&N5=SEARCH_CONCAT_PNO\BRAND_KEY&F=SPEC
- ¹⁷ www.sigmaaldrich.com/catalog/ProductDetail.do?lang=it&N4=05343\FLUKA&N5=SEARCH_CONCAT_PNO\BRAND_KEY&F=SPEC
- ¹⁸ <http://toxnet.nlm.nih.gov/cgi-bin/sis/htmlgen?HSDB>. LD50 (Diazald) = 2700 mg/kg; LD50 (MNU) = 110 mg/kg; LD50 (MNNG) = 114 mg/kg. The higher LD50 value is probably the reason why Diazald is usually

preferred for diazomethane preparations. However it is reported that in a favorable environment (i.e. in the stomach) even a weakly or non-carcinogenic compound, such as Diazald, may give rise to strong carcinogenic products via transnitrosation reactions. M. Börzsönyi, K. Saigó, G. Török, A.Pintér, J. Tamás, G. Kolar, B. Spiegelhalder, *Neoplasma*, **1988**, 35, 257.

¹⁹ Cost and toxicity issues should be carefully considered, although the latter concern can be handled by using continuous-flow methodologies.

²⁰ www.unece.org/trans/danger/publi/adr/adr2011/11contentse.html. (ADR 2011, International Carriage of Dangerous Goods) Annex 1, part 1 (1.1.3.6.3 page 10). MNTS (ADR/RID: 3234, transport category 1, maximum quantity per transport unit: 20 kg); MNNG (ADR/RID: 1325, transport category 2, maximum quantity per transport unit: 333 kg); MNU (ADR/RID: 1325, transport category 3, maximum quantity per transport unit: 1000 kg).

²¹ Unreacted MNU or its possible decomposition products were not quantified.



Part II

**CONTINUOUS FLOW SYNTHESIS OF
ONCOLOGICAL DRUGS**

Chapter 5: Basic Principles on Cancer and Chemotherapy

5.1 Cancer

The term “cancer” usually refers to a wide range of diseases (*ca.* 400) entailing commonly the unregulated cell proliferation. In particular in its general meaning such expression indicates malignant forms of tumor, in which ill cells divide and growth uncontrollably giving masses that invade nearby tissues. The process of creation of a cancer is known as *carcinogenesis* or *oncogenesis* or *tumorigenesis*.¹

5.1.1 Biological Bases of Cancer

Cancer is fundamentally a disease of failure of regulation of tissue growth, occurring when normal cells undergo a progressive reprogramming at genetic level resulting in uncontrolled proliferation. Healthy cells growth and replication are physiological processes that occur in almost all tissues and under many circumstances through cell cycle (figure 5.1)², in order to insure replacement of worn-out cells with new cells and maintain proper tissues functionality and body health. The replication process is finely tuned by biochemical control mechanisms, that select

both cellular division extent and rate: enzymatic complexes called cyclin-dependent kinases (CDK) respond to changing levels of various cyclin proteins in cytoplasm by driving the cell through the replication cycle. Biochemical regulators and growth

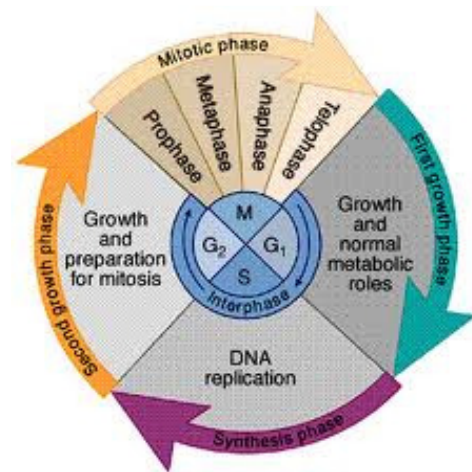


Figure 5.1: cell cycle schematics. From G1 cell may enter quiescence phase G₀ in which cell replication is temporarily disabled.²

stimulators finally induce cells to arrested growth (senescence) and eventually programmed cell death (apoptosis).

In oncological diseases, such fragile chemical equilibrium is broken due to failure of biochemical controllers derived by genetic mutations. During DNA replication process often some errors occurs that may result in alteration of genetic material; however, cells naturally exploit a number of redundant mechanisms for individuation and correction of transcription errors. Unfortunately, such mechanisms may fail due to both external and internal factors, thus resulting in genetic mutations and, as a consequence, cancer. Currently, the single-gene theory, according to which a single mutation could result in a neoplastic disease, has been extensively abandoned in favor of the multiple mutation prerequisite. Genetic pathways that may lead to carcinogenesis are essentially two: Oncogenes over-expression and Tumor Suppressor Genes inhibition.

Oncogenes are cellular regulation genes that derive by an aberration in the expression of proto-oncogenes, normal genes involved in regulation of cell functions. Proto-oncogenes in fact encode many regulation proteins that stimulate cellular growth; in particular, a number of proto-oncogenes code for cell surface receptors, that are involved in communication between cytoplasm and external environment. Mutation to oncogenes usually result in over-expression of control proteins, thus leading to increased cell division, reduced differentiation (cell functional specialization) and inhibition of cell death. Common modification pathways of proto-oncogenes can occur as spontaneous point mutations, inherited germline mutations, chromosomal rearrangements or gene over-expression, that may be stimulated from external triggering mechanisms (exposure to chemical, environmental or viral carcinogen agents).

Tumor Suppressor Genes play a critical role in oncogenes suppression as they are involved in detection of damaged DNA. Tumor Suppressor Genes act in fact at determined checkpoints during cell cycle by stopping multiplication of cells in which genetic material damages have been detected, until such damages are corrected; they may also induce cell death through an apoptosis mechanism. Notable examples of Tumor Suppressor Genes are Retinoblastoma (RB) gene and p53. In particular, diminished or completely lost functionality of p53 activity is usually detected in more than 50% of human tumors.³

Altered functionality of both Oncogenes and Tumor Suppressor Genes results in cells growing and dividing uncontrollably, consuming energy and losing both structure and function because of the inability to properly differentiate. Moreover, abnormal cells proliferation is associated to disabled cell death mechanisms, leading to cell immortality and as consequence to potential genetic instability.

Comprehension of cell replication process and of its regulation mechanisms is of key interest in development of chemotherapeutic agents (chemical substances involved in controlling tumors) as the ability to specifically target biochemical control functions may enhance the capability of arresting tumor growth without critically affecting body life functions, as we will see in following chapters.

5.1.2 Cancer Incidence, Causes and Progression

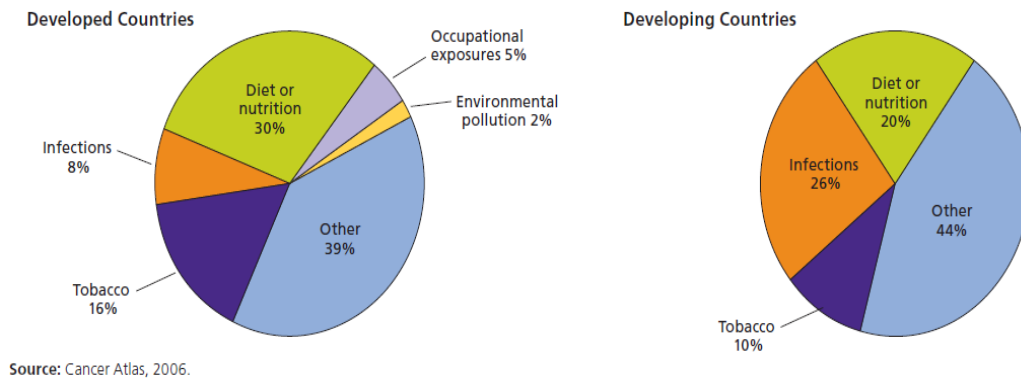


Figure 5.2: proportion of Cancer Causes by Major Risk Factors and Level of Economic Development.⁵

Cancers are generally classified and named on the basis of originating tissue: carcinoma (epithelial origin), sarcoma (muscle or connective tissue), leukemia and lymphoma (hematologic or lymphatic) and glioma (neural).⁴

According to the International Agency for Research on Cancer (IARC), in 2008 a total number of around 12.7 millions cancer cases were detected worldwide, of which 5.6 million in developed countries. Estimated cancer related deaths in the same year were *ca.*

7.6 millions, 2.8 millions in developed countries. IARC projections expect an increase by 2030 to 21.4 millions cases and 13.2 millions deaths due to population aging and reduction of childhood and infections related deaths in countries under development. Diffusion of western world life habits in such countries may eventually result in even higher tumor burden. Most common tumor forms include prostatic, breasts, lung, colon and rectum cancer. In particular, lung cancer is the most fatal. A very small gender-related difference has been noted for such tumors regarding to incidence and mortality, whereas geographical differences in the types or burden of cancers are more marked.⁵

5.1.2.1 Cancer Causes

As previously mentioned, a variety of chemical, environmental and viral factors can trigger cancer formation by mutations induction. DNA viruses and RNA retroviruses have been implicated in human cancer development,⁶ the most known of them being human papillomavirus virus connected to development of skin and cervical cancer, and hepatitis C virus involved in hepatocellular carcinoma. Chemical precipitants of tumors are highly related to occupational cancer risk: well-known and recognized carcinogens are asbestos, which has been conclusively linked to development of lung, pleural and peritoneal neoplasm. Radon is similarly known to induce lung cancer in miners, as in general way exposition to soot and metal dusts. Halogenated compounds as well as aromatic amines are connected to bladder cancer, whereas benzene and aromatics are involved in development of leukemia forms, but many other chemicals result to be confirmed or almost suspected carcinogens. Tobacco and alcohol abuse are well related to arise of a wide range of tumors, mainly lung, oral, liver, pancreatic, stomach, renal, bladder and breast cancers. Exposition to ionizing or ultraviolet radiation may cause leukemia, breast, thyroid, lung and skin cancers.⁷

5.1.2.2 Tumor Progression

The development of cancer occurs usually in four discrete steps. In the *initiation* phase, exposure to carcinogenic agents reported above promotes irreversible genetic mutation. During *promotion* phase, genes modifications originate mutated cells that begin to grow

preferentially respect to healthy cells. Preferential growth may be induced by continuous exposure to carcinogenic agents or from promotion by environmental factors. Fortunately, promotion phase is reversible, so exposure, avoidance or reduction, together with proper changes in diet and lifestyle may avoid tumor genesis. For example, it is reported that smokers who quit experience a 67% reduction in fatal cancer incidence after a 10 years stop. *Transformation* phase occurs in 5 to 20 years and marks out development of cancer cells from mutated ones. Finally, *progression* phase involves cells proliferation, tissue invasion and destruction and metastasis.

Clinically, cancer development is classified on the basis of parameters, as tumor mass size, lymph nodes involvement and metastasis in four classes, ranging from I (localized) to metastatic (IV), by passing through local (II) and regional (III) tissue invasion. Staging is essential in definition of appropriate treatment plan and for prediction of prognosis.

Early detection of tumors is of critical importance for an effective treatment, so particular attention must be paid in symptoms detection, especially for children. Clinical manifestations can vary widely depending on cancer type and stage, but common and warning symptoms are persistent weight loss and severe, unrelenting pain, as well as bleeding or, at advanced stages, detection of masses.⁸

5.2 Cancer Therapy

Cancer treatment may comprise surgery, radiation, antineoplastic (literally against new growth) chemotherapy and/or biological response modifiers, that stimulate patient's own immunological defenses.

Surgery and radiation (that may comprise ionizing radiation or thermal and photodynamic for superficial tumors) are suited for isolated or localized masses, especially in early stages, whereas chemotherapy and biological response modifiers are applied when spread or systemic cancers are present. Chemotherapy is also largely used after surgery or radiation treatment to insure microscopic metastasis removal (adjuvant therapy) as well as prior to surgery to reduce mass and aggressivity of tumors in order to be better handled.

5.2.1 Cancer Chemotherapy

Cancer chemotherapy involves employment of chemical antineoplastic agents against tumor cells. Such agents usually exploit a cytotoxic activity (causing cell death) by interfering with biochemical mechanisms. Preferred mode of action is interference in synthesis or function of RNA, DNA or functional proteins. Since they are specifically designed to kill cell, all antineoplastic agents are toxic and poisonous for the human organism, and must be handled very carefully. In the last decades, many efforts have been spent to design chemotherapeutic compounds that could be specific both for certain tissue types and, more important, only for malignant cells. Thanks to better understanding of biochemical bases of oncogenesis, significative improvements have been made with respect to antineoplastic agents of the very first hour, that were extremely active but highly unspecific.^{9,10} Despite this, research is still far from ideality, and drugs available today are still extremely and generally toxic; for example, the high potential for destruction of sensitive cells as gastrointestinal tract, hair follicles and bone marrow is the main cause of common chemotherapy adverse effects (nausea, vomiting, fatigue and increased sensitivity to infections).

5.2.1.1 Treatment and Response Criteria

Posology and effectiveness of chemotherapeutics are strongly related to disease type and stage, patient general health status and sensitivity to biochemical mechanism of selected agent. Drug dosage must be carefully selected, beneath the limit of daily recommended dose, in order to reach the best ill cells killing rate and minimize treatment period. Treatments are usually performed in several courses or rounds with several days of interval between them in order to permit attenuation of side effects. Rest phase between rounds is an important factor to be tuned on the base of patient strength against adverse effects and tumor progression, and in such optic, the development of chemotherapeutic agents with reduced side effects is of extreme importance. Of course, chronic toxicity effects over organs must be considered during designing or treatment plan.

Effectiveness of chemotherapy treatment is considered complete upon “cure” of tumor, meaning that no signs of relapses are detected for almost 5 years. Unfortunately, a completed cure is seldom achieved, whereas “response”, complete or partial, are more common and leads to high extent of tumor regression. Sensible improvement of patients quality of life is also achieved on a “clinical benefit” response. Failure of chemotherapy approach results in tumor “progression”, meaning worsening of general disease severity.

5.2.1.2 Functional Classes of Antineoplastic Agents¹¹

The very first antineoplastic agent to prove effective against tumors was cortisone in 1940s and later other glucocorticoids. In the same years, study of effects of mustard gases during World War I brought to development of the highly cytotoxic and completely nonselective nitrogen mustards for cancer treatment. Following developments made available chemotherapies based on antimetabolites and antibiotic antineoplastics. In the early 1970s, metal-based antineoplastic agents became available, as well as hormones-based treatments for hormone-dependant cancer forms. Today, the major trend is towards careful design, with the help of rational drug design and high throughput screening techniques, of drugs targeted for specific biochemical factors, with the aim to improve selectivity for diseased cells.

The most widely employed mustards and organometallic complexes, as cis-platin belong to the class of DNA alkylating agents. Such molecules exhibit their activity in several ways by generally promoting alkylation of DNA molecules and eventually cross-linking of DNA strands by double linking. Activity is particularly enhanced during cell cycle late G₁ and S stages, while unfolded DNA molecules are far more vulnerable. Unfortunately, DNA alkylators have high chronic toxicity and potential for inducing carcinogenesis, beside destroying existing tumors. The well-known examples of such agents are Procarbazine, Carmustine, Cisplatin and their derivatives.

Antibiotics antineoplastic are natural or semisynthetic compounds that acts by avoiding DNA replication through intercalation, mutations induction or specific enzymes inhibition. Employed agents belong essentially to the anthracyclines, as Doxorubicin.

Antimetabolites instead of targeting DNA molecules directly inhibit DNA replication by interfering with nucleic acid metabolism. Such compounds act as competitive antagonists of specific metabolites in biochemical synthesis of nucleotides, in particular purine-based (Mercaptopurine, Thioguanine) and pyrimidine-based (Fluorouracil, Methotrexate) nucleotides. Finally other chemical compounds, such as Gemcitabine, enter the nucleotide metabolism and inhibit DNA polymerase enzymes.

Mitosis inhibitors are also widely used as antineoplastic agents, that affect the ability of cells to undergo division by attacking specific structural proteins, for examples tubulines. Taxanes, epothilones (paclitaxel) and Vinca alkaloids are examples of such agents.

5.2.1.3 Development of Resistance in Cancer Cells

Unfortunately, the aggressive character of cancerous cells results often in the development of protection mechanisms against chemotherapeutic agents. Resistance is acquired usually by down-regulating enzymes critical for drug transport or activation, as well by up-regulating enzymes involved in drugs metabolism. Other common protective mechanisms exploited by cancer cells are down-regulation or mutation of drug targeted enzymes and modifications in the metabolic pathway involved in drug uptake and excretion.

The rise of resistant forms of tumors requires a constant effort in improving of activity and optimization of bio-distribution of oncological drugs. Such objective is usually pursued by screening of new potential lead compounds, derived by existing drugs through proper side functionalisation of the active core structures. This highlights the importance, in the drug development phase, of having high throughput synthetic protocols able to readily screen between many molecular structures based on a common scaffold.

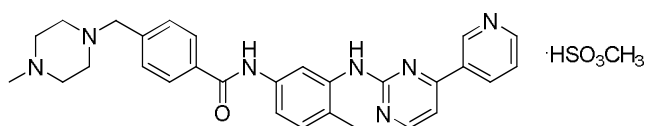
5.3 Tyrosine Kinases Inhibitors: a New Class of Selective Drugs

As stated above, a number of proto-oncogenes are involved in a large part of cell activity through signals transductions. In particular, they encode for many tyrosine kinases

complexes that are found embedded in cellular membranes. Protein Kinases (PKs) are a class of enzymes that exploit a specific activity of chemical modification of other proteins through transfer of a phosphate group from ATP (adenosine-5'-triphosphate) to specific aminoacidic residues that results usually in a structural/functional modification of the target protein by changing enzyme activity, cellular location or association with other proteins. PK acts on hydroxylic functionalities of the aminoacids, as aspecific enzymes in the case of serine and threonine, or specific enzyme for tyrosines and only few PKs are active on all of them. A very limited number of enzymes also promotes phosphorylation of nitrogen atoms in histidine residues.

As previously stated, a number of kinases specific for tyrosine residues are found in transmembrane complexes in association with cell surface receptors. These transmembrane receptors are usually composed by three domains: an extracellular region effectively binds extracellular ligands that act as signal carriers, and such binding causes a change in conformation that is transmitted through a membrane embedded domain to the cytoplasmatic domain. This latter is composed by the kinase enzyme that can work on intracellular proteins and may be activated or inhibited by the structural change affected by extracellular binding phenomena. Many of these complexes are involved in signal transduction through cell growth factors, which activate, upon binding, a chemical signal cascade that promotes cell proliferation. Well-known receptors of such type are for example Epidermal Growth Factor Receptor (EGFR) that is involved in cell-growth regulation and Kinase insert Domain Receptor (KDR) which binds Vascular Endothelial Growth Factor (VEGF) that is involved in angiogenesis, the formation of new blood vassels.

Tyrosine kinases can exploit mutated forms that give rise to deregulation of cell vital cycle causing proliferative disorders and carcinomas. Common examples are the oncogenic over-expressions of the already mentioned EGFR, implied in development of pancreatic and non-small cell lung cancer, and c-KIT for gastrointestinal stromal tumor. Also, over-expressed forms of many human growth factors (VEGF, HER2) stimulate cells multiplication and act by binding to tyrosine kinase receptors.¹²



29

Figure 5.3: Imatinib mesylate, molecular structure.

Specific targeting of transduction mechanisms through tyrosine kinase enzymes is the main mechanism of action of many antineoplastic drugs of very recent development. In particular, Imatinib mesylate **29** was the first exponent of such class of drugs to be developed in the early 2000s for treatment of Chronic Myeloid Leukemia (CML).. CML, differently from other cancer types, is originated by a single genetic alteration, the fusion of a Bcr and an Abl gene, due to chromosomic transmutation. Fused Bcr-Abl oncogenes over-express EGFR receptors thus leading to deregulated cell multiplication;¹³ Imatinib recognizes the cytoplasmatic domain of growth factors receptors and irreversibly binds the ATP pocket, thus blocking the enzyme in the inactive conformation.^{14,15} As the drug specifically targets growth receptors, and these are expressed only in minor extent by healthy cells, the result is an increased selectivity towards aberrant cells and reducing mortality rate of healthy cells respect to more traditional chemotherapeutic agents. Imatinib mechanism of action is exemplified in Figure 5.4.¹⁶

APIs that exploit their activity through inhibition of tyrosine kinases are hence defined as “smart drugs”, together with other highly selective agents of recent development (mainly based on biological, rather than molecular derivation), thanks to their high selectivity of action. Nevertheless, they still present significant levels of chronic toxicity mainly towards cardiovascular and renal systems, especially for cases in which lifelong therapy is needed, or for labour force involved in such drugs preparation and handling. Anyway, advancements on tyrosine kinase drugs represent an important step towards the development of the so-called “magic bullet” against cancer. In such an optic, continuous-flow techniques should actively support new drug development and widespread availability of these important compounds.

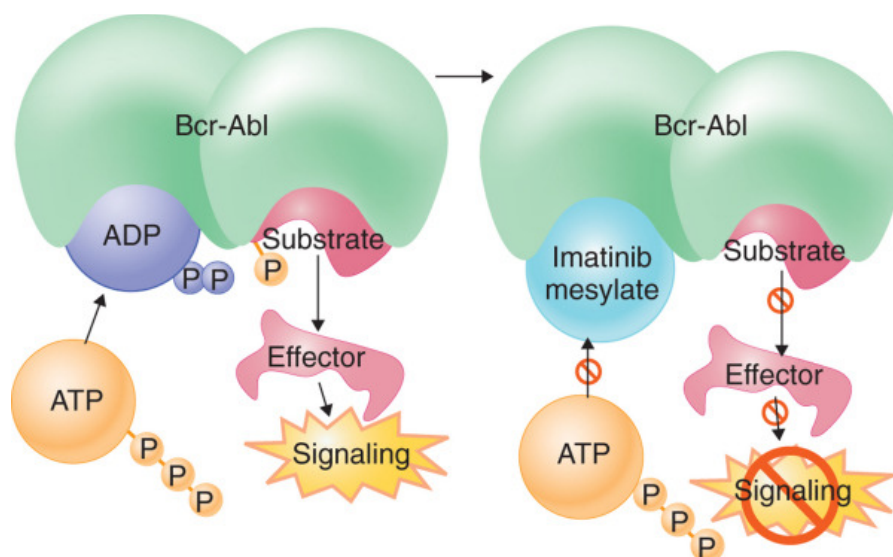


Figure 5.4: Imatinib mesylate mechanism of inhibition of tyrosine kinases.¹⁶

5.3.1 Production Confinement of Oncological Drugs

As we have seen, despite differences in reactivity virtually all antineoplastic agents must be considered as life-threatening substances due to their cytotoxic effects, chronic toxicity against critical organs and high carcinogenic potential. Consequently, production of oncological Active Pharmaceutical Ingredients (APIs, the active molecule contained in a drug) and their formulation in usable drugs must be carefully conducted under strict safety protocols. Massive productions are usually carried out in isolated facilities with controlled atmosphere, and all operators involved in handling of substances during all production stages are likely to be protected from contaminations by wearing sealed suits, equipped with breathing air supplies or attached to proper hoses through which clean air may be pumped. Working in such conditions is a difficult and fatiguing task, as the suits tend to be less flexible than conventional work garments. Therefore, use is usually limited in time to a couple of hours, depending on the difficulty of the work. These toxicity issues must be also accounted during drug development stages, both in industrial and academic laboratories.

Application of continuous flow techniques to the synthesis of oncological APIs should allow the development of more efficient, convenient and safe processes. Overall synthetic efficiency and yield could be enhanced thanks to the advantages of micro/meso flow

systems over traditional batch techniques in terms of precise control of reaction conditions, efficient mass and heat transfer, or possibility to work under super-heating conditions, meaning well above solvent boiling point. Work-up procedures would be reduced by the increased efficiency for each reaction step, or could be performed in flow by using supported reagents or scavengers. Process safety should be greatly improved using continuous technology, as the small foot-print and elevated automation of equipment allows for easy reactor confinement, for example in simple glove-boxes, thus reducing interaction of the operator with the substances. A continuous flow set-up could also promote process simplification by allowing parallel carry-on of building blocks syntheses. Finally, a continuous flow process developed on laboratory scale could in principle be rapidly transferred to production scale with no need of further optimization of reaction conditions.

With such aims in mind, in partnership with a pharmaceutical company, Fabbrica Italiana Sintetici Spa, during the present thesis a study was carried out looking for continuous flow processes for the synthesis of antineoplastic drugs. In particular, our focus was on designing efficient and flexible approaches, with wide range of applicability from high throughput drug development on laboratory scale to mass production. Key improvements sought respect to batch-wise processing was high productivity and easy introduction of structural variations: such flexibility is needed, in fact, for profitable application in screening of new structurally correlated therapeutic candidates. Our molecular targets were tyrosine kinases inhibitors selected in collaboration with the industrial partner. In particular we have focused our efforts in two classes of compounds:

- Imatinib mesylate and its derivatives, bearing a common pyrimidinamine core structure (chapter 6).
- 4-anilino-quinazoline structures as models of various oncological drugs (chapter 7).

References

- ¹J.R. Bertino, W. Hait, *Principles of cancer therapy*. In: Goldman L, Ausiello D, eds. *Cecil Textbook of Medicine*. 22nd Ed., **2004**, WB Saunders, 1137–1150.
- ² A. L. Chanez, *Division of the single mitochondrion in Trypanosoma brucei and its impact on the cell cycle*, thesis, Université de Fribourg (Suisse).
- ³ E.T. Liu, *Oncogenes and suppressor genes: genetic control of cancer*. In: Goldman L, Ausiello D, eds. *Cecil Textbook of Medicine*. 22nd Ed., **2004**, WB Saunders, 1108–1116.
- ⁴ W.H.Woglom, *General review of cancer therapy*. In: Moulton FR, ed. *Approaches to Tumor Chemotherapy*, **1947**, Amer. Assoc Advancement Sci.
- ⁵<http://www.cancer.org/acs/groups/content/@epidemiologysurveillance/documents/document/acspc027766.pdf>
- ⁶ P. M. Howley, D. Ganem, E. Kieff, *Etiology of cancer : viruses: DNA viruses*. In: DeVita VT Jr, Hellman S, Rosenberg SA, eds. *Cancer: Principles and Practice of Oncology*. 7th Ed., **2005**, Lippincott Williams &Wilkins, **2005**, 173–184.
- ⁷ W.J. Blot, *Epidemiology of cancer*. In: Goldman L, Ausiello D, eds. *Cecil Textbook of Medicine*. 22nd Ed., **2004**, WB Saunders, 1116–1120.
- ⁸ P. Calabresi, B. A. Chabner, *Chemotherapy of neoplastic diseases*. In: Hardman JG, Limbird LE, eds. *Goodman & Gilman's The Pharmacological Basis of Therapeutics*. 10th Ed., **2001**, McGraw-Hill 1386–1388.
- ⁹ J.H. Burchenal, *The historical development of cancer chemotherapy*, *Semin. Oncol.*, **1977**, 4, 135–146.
- ¹⁰ E. Chu, *Pharmacology of cancer chemotherapy: drug development* . In: DeVita VT Jr, Hellman S, Rosenberg SA, eds. *Cancer: Principles and Practice of Oncology*. 7th Ed., **2005**, Lippincott Williams &Wilkins, **2005**, 307–317
- ¹¹ D. A. Williams, W. O. Foye, T. L. Lemke, *Foye's Principles of Medicinal Chemistry*, **2002**, Lippincott Williams & Wilkins.
- ¹² P. Yaish, A. Gazit, C. Gilon, A. Levitzki, *Science*, **1988**, 242, 933–935.
- ¹³ Estey EH, Appelbaum FR, eds. *Leukemia and Related Disorders*, **2011**, Humana Press.

¹⁴ B.J. Druker, S. Tamura, E. Buchdunger, S. Ohno, G. M. Segal, S. Fanning, J. Zimmermann, N. B. Lydon, *Nat Med*, **1996**, 2, 561.

¹⁵ I. El Hajj Dib, M. Gallet, R. Mentaverri, N. Sévenet, M. Brazier, S. Kamel, *European Journal of Pharmacology*, **2006**, 551, 27-33.

¹⁶ Dr. J. Fitzakerley, *2011 Antineoplastics*, Lecture at University of Minnesota Medical School Duluth.

Chapter 6: Flow Synthesis of Pyrimidinamine Structures

Imatinib mesylate **29** (Figure 6.1) was the first oncological drug of kinase inhibitors family, approved by FDA in 2001 and commercialized by Novartis as *Gleevec*® in the US and *Glivec*® in Europe.¹ Imatinib exploits a cytostatic activity towards carcinogenic cells by selective inhibition of mutated Bcr-abl trans membrane kinase enzymes expressed in patients affected by myeloid leukemia in the chronic phase.² A slightly modified Imatinib structure, reported below, has been found to be even more active than Imatinib towards diseased cells and has been approved by FDA as Nilotinib **30** (commercial name *Tasigna*®) for treatment of Imatinib resistant mutants.³ Both molecules share a common scaffold, that is a pyrimidinamine moiety, highlighted in red in Figure 6.1. Our efforts in designing a flow procedure for Imatinib synthesis were thus directed to preparation of pyrimidineamines carrying various functional groups.

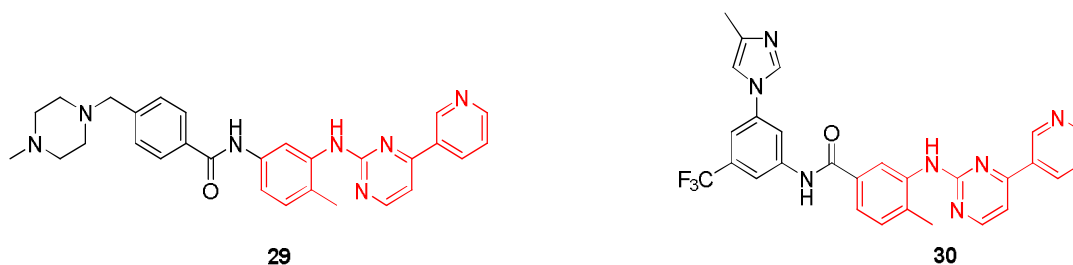


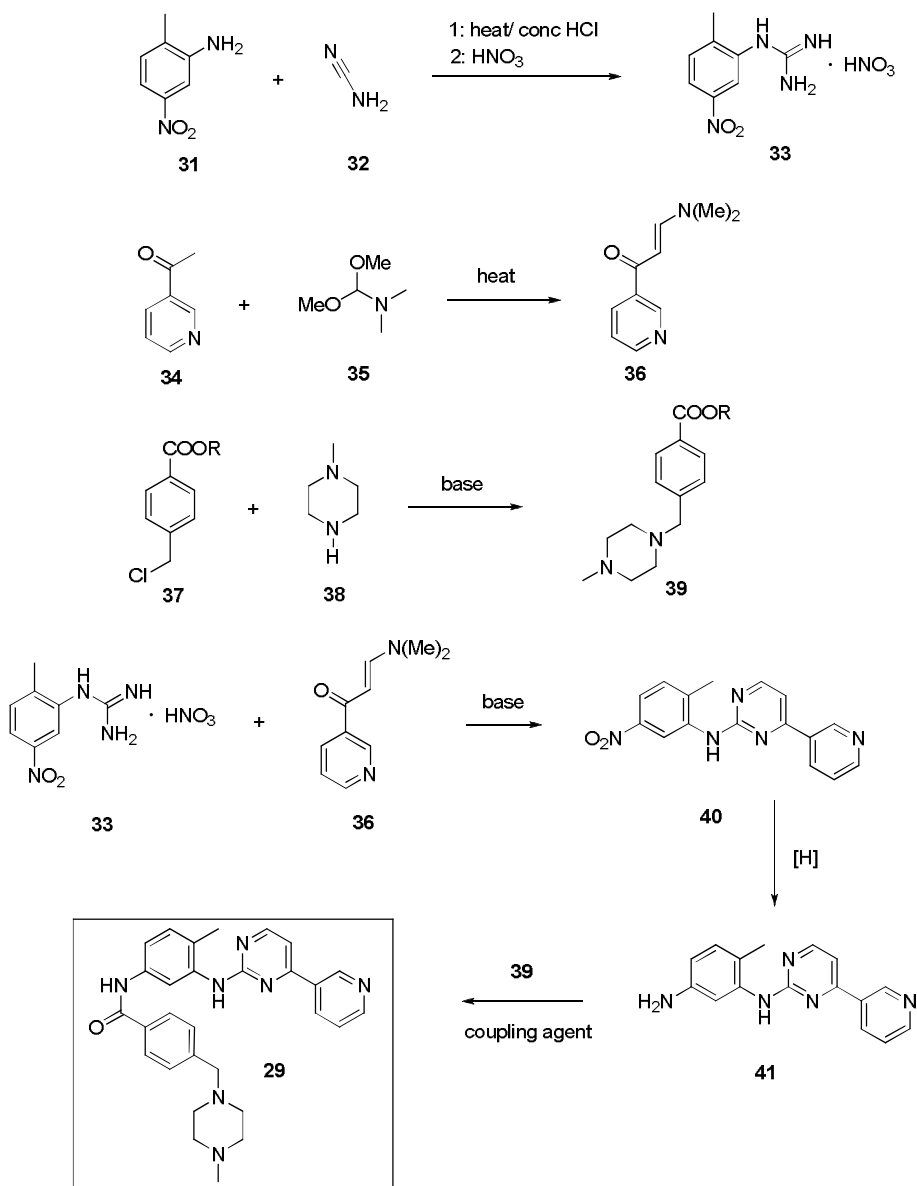
Figure 6.1: molecular structures of Imatinib **29** and Nilotinib **30**. The common pyrimidinamine core structure is highlighted in red.

6.1 Classical Approaches towards Imatinib Synthesis

6.1.1 Classical Batch-Wise Synthesis of Imatinib

The common synthetic route for Imatinib reported in patent literature (Scheme 5.1)⁴ requires several steps and long and difficult work-up procedures. Effective reaction yields for each step are not disclosed, however, the overall yield is believed not to exceed 15%.

This makes the approach not very efficient and economically disadvantageous for industrial scale applications. Furthermore, the high cytotoxic activity of the product and of some intermediates requires the adoption of strict safety protocols: all the operations are performed in special facilities, isolated from the outside, in which the laboratory staff must use protective sealed suits in a controlled environment.



Scheme 6.1: traditional batch-wise approach to Imatinib synthesis.⁴

In this synthetic protocol the three main buildings, namely compounds **33**, **36** and **39** are obtained as depicted in Scheme 6.1. Guanidine derivative **33** is prepared by reaction of the

aniline **31** with cyanamide in presence of concentrated hydrochloric acid, followed by treatment with nitric acid. Enamine **36** is obtained by condensation of 3-acetylpyridine (**34**) with the dimethyl acetal of dimethylformamide (DMF-DMA, **35**) that is used as both *in situ* base developer and reagent. The benzoic acid ester **39** is synthesized by alkylation of the correspondent benzyl chloride **37**.

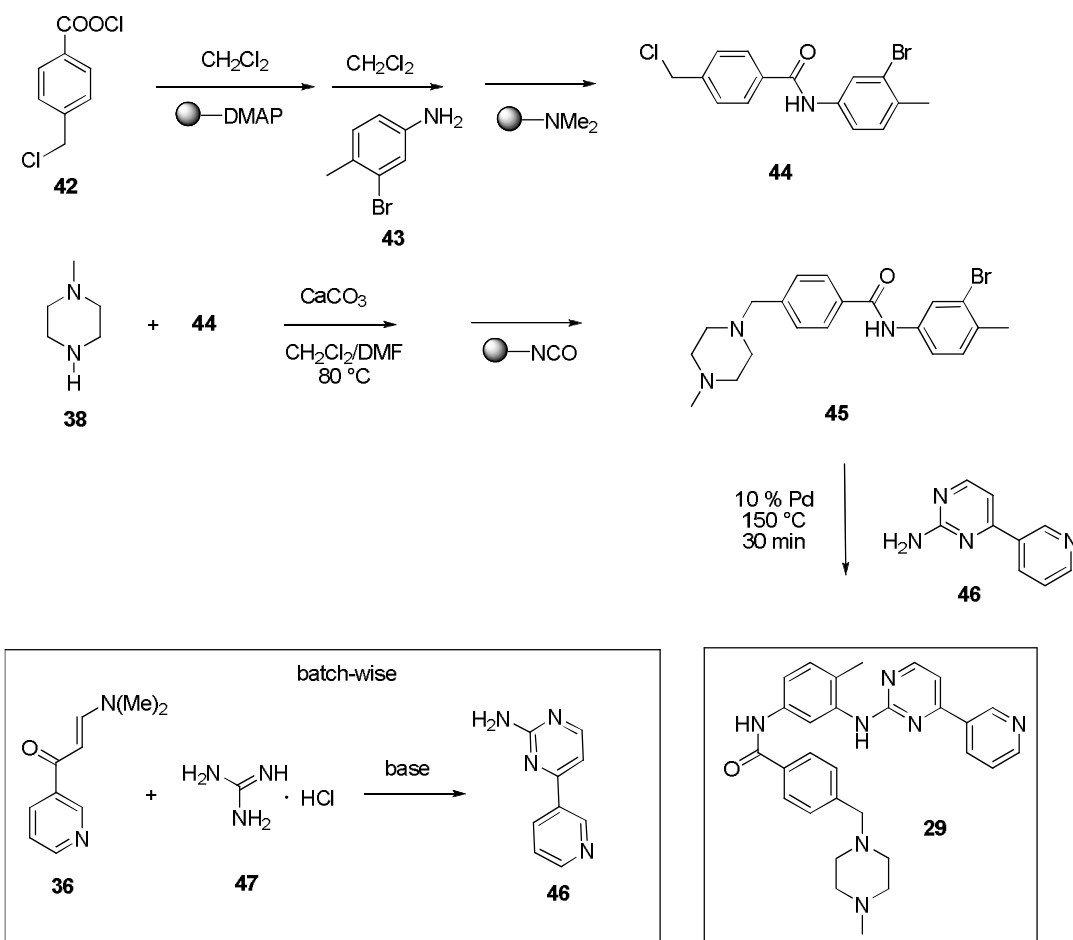
The pyrimidinamine core **40** is formed by condensation reaction of enamine **36** and guanidine **33**, a base is usually needed in order to free the guanidinic acid salt. Reduction of the nitro derivative **40** followed by amidic coupling with derivative **39** yields Imatinib base that is usually isolated in the form of a mesylate salt to increase the bio-availability.

Critical steps of Imatinib synthesis are the preparation of guanidine derivative **33** and enamine **36**. In both cases toxic reagents are used (cyanamide and DMF-DMA). In addition, DMF-DMA is also difficult to handle due to bad odour and high volatility. Moreover enamine **36** is a rather unstable compound that must be rapidly isolated and used immediately for the next step without purification. Compound **41** exhibits biological activity as it bears Imatinib key activity-related structural features, although the absence of amidic side chain limits bio-adsorption. In consequence, the last synthetic steps should be carried out in controlled facilities.

6.1.2 Flow Approaches to Imatinib Synthesis

During course of our studies on the development of a flow approach for Imatinib and related analogues, an elegant flow-based method for Imatinib preparation was reported by Ley and Baxendale.⁵ Such flow protocol (Scheme 6.2) required the formation of amide **44** by reaction of dichloride **42**, pre charged over polymer supported DMAP, with aniline **43** and in presence of dimethylamine scavenger for flow purification. After solvent evaporation, amide **44** was further reacted with N-methyl-piperazine in presence of calcium carbonate to give compound **45**. Flow purification was performed through a polymer-supported isocyanate scavenger and the output stream was directly reacted with amino-pyrimidine **46** (prepared in batch by standard methods reacting enamine **36** with a guanidine salt **47**) through a Buchwald-Hartwig coupling mediated by 10% of palladium catalyst at high temperature. The target compound was obtained in 32% (95% purity) overall yield after automated column chromatography purification.

This notable approach presents however some issues: the low reagents concentration (around 0.1 M) together with the need for a large number of disposable solid supported reagents and scavengers made such synthesis difficult to apply in massive productions in a cost-effective way. Employment of metal catalyst in the last synthetic step is not convenient for an API targeted synthesis: pharmacopeia and cGMP requirements strictly control metal leaching into pharmaceutical ingredients, hence the use of noble metals catalysts requires introduction of additional laborious purification procedures on final product. In a drug development context, such flow approach is surely interesting, however, the potential for introduction of molecular diversity, that is a basic requirement for discovering of new lead compounds, results somewhat limited. This is because of the introduction of substituents on the pyrimidine core is performed batchwise using a two-steps procedure that retains the drawbacks highlighted in classical synthetic route for Imatinib. With this valuable example in hands, we proceeded in the development of our flow approach focusing on overcoming the inconvenients highlighted above.



Scheme 6.2: a continuous-flow approach to Imatinib synthesis.

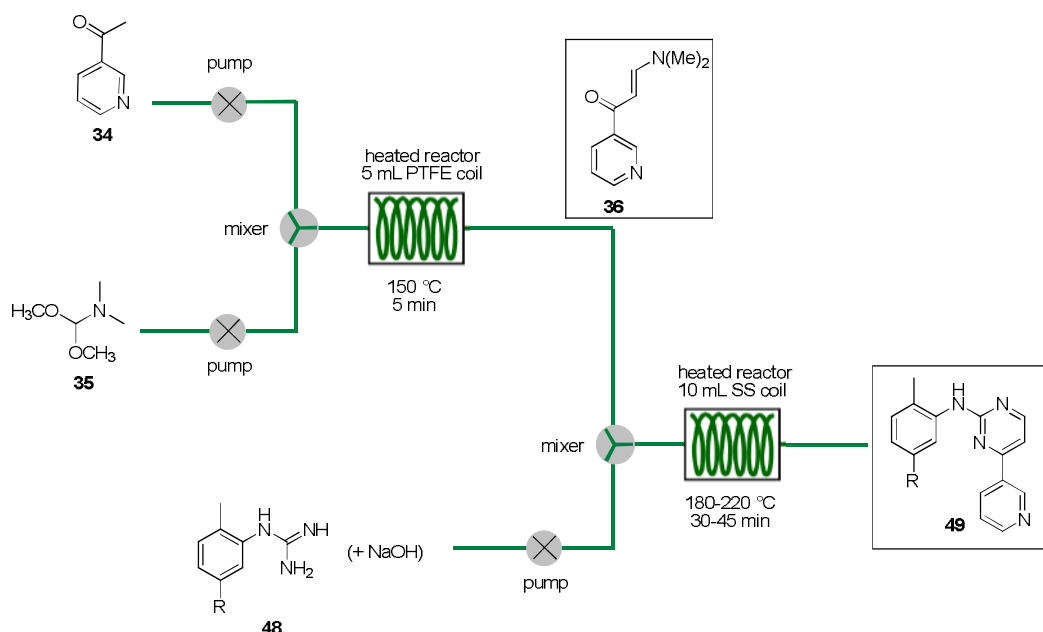
6.2 Continuous Flow Approach to Pyrimidinamines

With the aim of developing a robust, flexible continuous flow method suitable for application in both laboratory and production scale, we chose a rather different approach. We focused on the development of a fast and efficient flow synthesis of the pyrimidine-amine nucleus of Imatinib (**49**, Scheme 6.3) starting from a common enamine, prepared in flow by alkylation of a ketone in a more efficient way respect to batch, and a suitable guanidine derivative prepared in batch. Following this approach, we would be able to prepare many different derivatives, simply changing functional groups on the reagents, with a very simple flow apparatus and a fast optimization of reaction conditions.

The synthetic strategy that has been thus developed relies on two crucial steps:

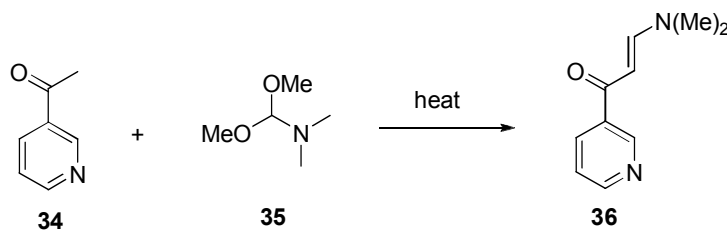
- *in-situ* preparation of the dimethylamino-propenone building block **36** through improvement of reactions conditions respect to batch procedure by using continuous flow, and
- condensation of such building block with a guanidine derivative.

This flow process would confine within a flow reactor some of the reaction steps involving toxic intermediates. In addition, proper pre-functionalisation of the guanidine derivative would allow to introduce a variety of substituents in the final molecule.



Scheme 6.3: flow-scheme for continuous synthesis of pyrimidinamine structures as oncological drugs precursors.

6.2.1 Synthesis of 3-(dimethylamino)-1-(pyridin-3-yl)prop-2-en-1-one (36)

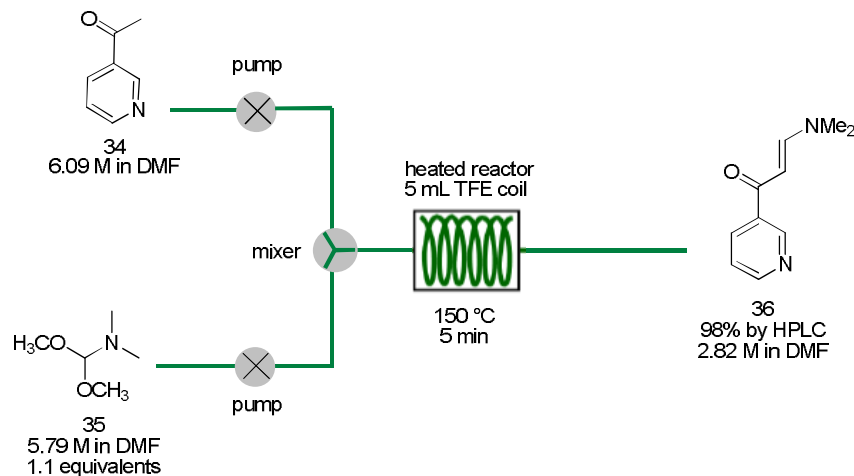


Scheme 6.4: Synthesis of enamine **36**.

Enamine compound **36** was first prepared in batch following established literature protocols,⁴ by condensation of 3-acetylpyridine (**34**) with DMF-DMA (**35**) which serves as both reagent and reaction medium (Scheme 6.4). Distillation of the methanol by-product formed during the reaction was needed to favour complete conversion in a reasonable time (6-8 hours). Solvent removal afforded a red crystal product that was purified by chromatography. Alternatively, upon cooling the reaction mixture and addition of a 2:3 mixture of hexane/diethyl ether the product precipitated and was collected by filtration. Structural characterization was consistent with literature data and the product obtained was subsequently used in following reaction step without further purification.

The batch-wise synthetic procedure described above for the synthesis of enamine **36** was directly transferred to continuous flow using a Vapourtec R4 continuous flow platform for screening and optimization of reaction conditions. R4 system was equipped with a 5 mL Teflon coil reactor heated at 110° C and 3-acetylpyridine and DMF-DMA were dissolved in toluene and charged in the reactor as feed streams. Initial screening of flow reaction stoichiometry resulted in an optimum molar ratio of 1:1.5 respectively in pyridine/acetal. In these conditions, a residence time of only 30 minutes was required for complete conversion, respect to 6-8 hours in batch. HPLC and LC-MS analyses of reaction crude evidenced higher content in target compound respect to batch samples (>95% versus ~85-90%) and lower amount of unidentified impurities. Those good results encouraged us to increase concentration of reagents feeds with the aim of improving reaction output: purity value of the obtained enamine product remained unvaried, however, fouling was noticed during reactor operation, together with some problems related to the fast precipitation of the product upon cooling of reaction mixture at reactor output. Switching the reaction solvent from toluene to DMF increased the solubility of enamine **36**, preventing fouling

phenomena and allowing to increase concentration of feeds solution (respectively to *ca.* 6.1 M for pyridine and *ca.* 5.8 M for DMF-DMA); moreover, higher temperatures (up to 150 °C) could be used. Re-optimization of the process with the new conditions (DMF, 150 °C) resulted in achievement of complete conversion in only 5 minutes of residence time. Moreover, a reduction in consumption of alkylating reagent (DMF-DMA) to 1.1 equivalents respect to pyridine was possible. The solution collected at reactor output contains 3-(dimethylamino)-1-(pyridin-3-yl)prop-2-en-1-one **36** in quantitative yield respect to starting material with a 98% purity (assessed by HPLC) and can be used in the following continuous reaction step without further treatments. Compared to batch, this flow procedure allows for a far higher throughput, whereas experimental procedures are greatly simplified, as no distillation and no product purification are needed; moreover, contact of the operator with toxic volatile compounds (DMF-DMA and pyridine derivatives) is avoided (see Table 6.1).

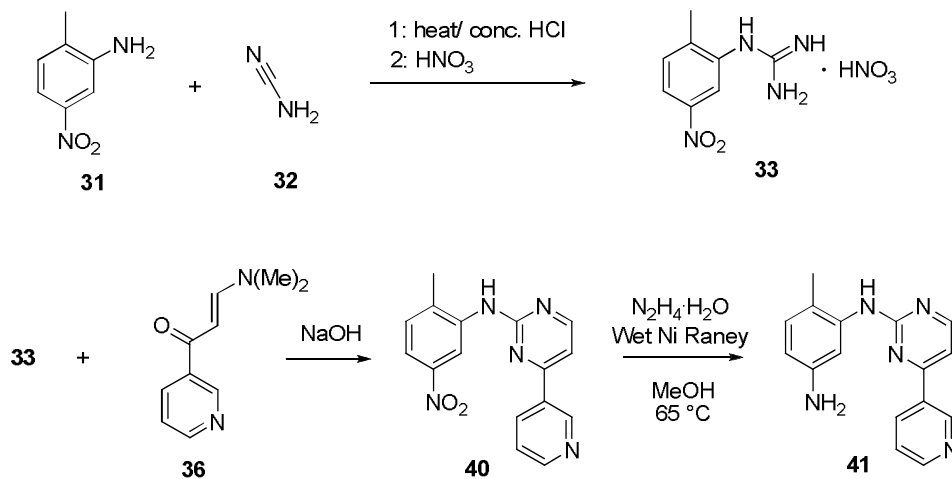


Scheme 6.5: Continuous-flow synthesis of enamine **36**.

Table 6.1: Comparison between batch and flow syntheses of **36**.

Mode	Temperature	Reaction time	Feeds concentration	DMF-DMA equivalents
Batch	110 °C	6-8 hours	~2.0 M	1.5
Flow (toluene)	110 °C	30 min	~ 2.0 M	1.5
Flow (DMF)	150 °C	5 min	~ 6.0 M	1.1

6.2.2 Synthesis of (5-amino-2-methylphenyl)-4-(3-pyridinyl)-2-pyrimidinamine (41)

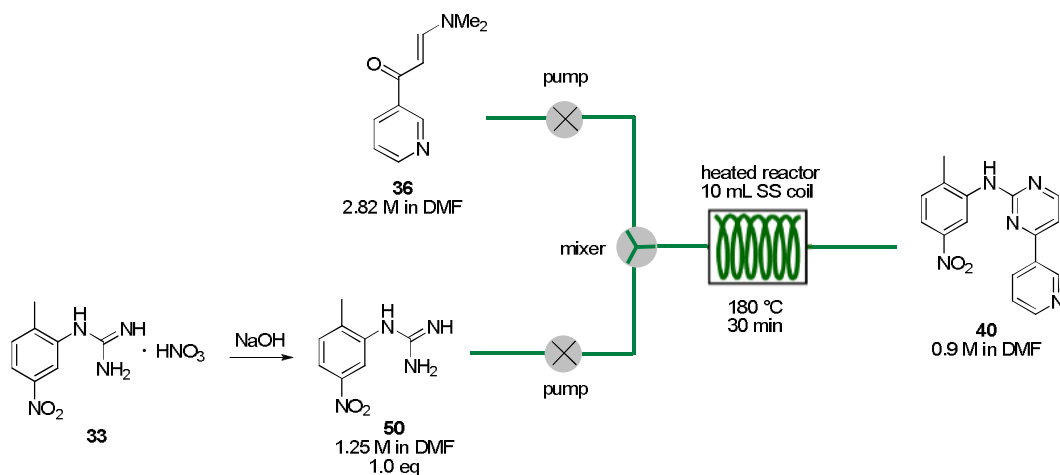


Scheme 6.6: Synthesis of Imatinib precursor 41.

The second synthetic step involves formation of pyrimidine core through condensation of 3-(dimethylamino)-1-(pyridin-3-yl)prop-2-en-1-one **36**, with the guanidine derivative **33**. This latter can be prepared by treating aniline **31** with cyanamide in strong acidic medium. As cyanamide is a toxic and a severe irritant for humans, as well as a potential carcinogen, implementation of this synthetic passage in a flow reactor will be advisable. Unfortunately, solubility problems strongly affect this synthesis, as both reagents and products are highly insoluble in reaction medium, and precipitation usually results in microchannels blockage. Batch-wise, reaction is carried out in alcoholic solvent that is not able to dissolve starting materials below 60 ° C. Attempts to introduce the pre-heated reaction mixture in the flow reactor resulted invariably in extensive precipitation of an untreatable solid upon acid addition. Changing the reaction medium to DMF was not effective, as extensive decomposition of solvent itself in presence of strong acids occurs, resulting in formation of impurities, probably formylated derivatives of aniline **31**. Attempts to replace acid medium with a soluble Lewis acid catalysis were unfortunately not effective. A biphasic organic/water solvent system was employed, but resulted, as well, in a modest reaction yield that was not possible to improve. Despite all our efforts, building block **33** had to be prepared by standard batch techniques (see experimental part) using suitable aniline precursor **31**. However, the optimized synthetic procedure allowed for synthesis of desired guanidine derivatives in high yields, without need of any purification procedure.

Batch synthesis of compound **41** was accomplished using reported procedure. Condensation of compounds **33** and **36** was effected in presence of a stoichiometric amount of base at high temperature (150 °C, 10 h); pouring of reaction mixture in water resulted in precipitation of compound **40** as a yellow solid in 45% yield. Derivative **41** was prepared by reduction of nitro derivative **40** under hydrogen transfer conditions using hydrazine hydrate over Raney Nickel catalyst, with a yield of 92% in final product (5-amino-2-methylphenyl)-4-(3-pyridinyl)-2-pyrimidinamine that is Imatinib precursor compound.

Next we attempted to transfer the process from batch to flow: the solution of enamine **36** obtained in the first continuous step was used as reactor feed together with a DMF solution of guanidine free base **50** (Scheme 6.7) obtained by pre-treatment of the nitrate salt **33** with sodium hydroxide (see experimental section). Vapourtec R4 platform was initially equipped with a 5 mL Teflon coil reactor, for visual monitoring of reaction progress, and afterwards with a 10 mL SS coil reactor for high temperatures investigation. Optimized reaction conditions identified are reported in Scheme 6.7: a residence time of 30 minutes at 180 °C afforded compound **40** in 68% total yield (assessed by HPLC).



Scheme 6.7: Continuous-flow synthesis of pyrimidinamine **40**.

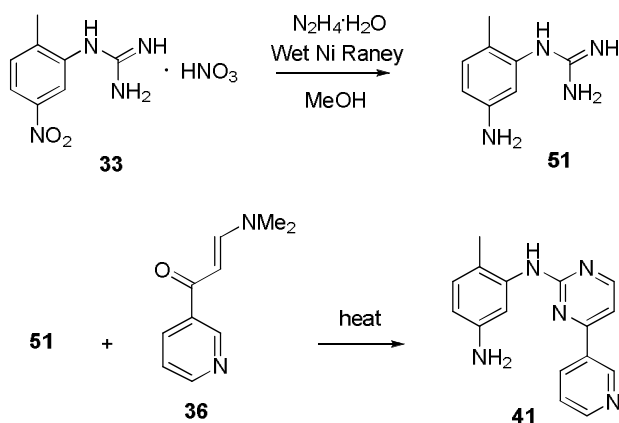
Optimized synthetic flow processes showed in Schemes 6.5 and 6.7 were then sequentially performed with the aim of preparing a massive sample of target compound. (5-nitro-2-methylphenyl)-4-(3-pyridinyl)-2-pyrimidinamine (**40**) was thus isolated from reactor output by pouring in water and filtration of the solid precipitate: isolated product yield was

58% calculated on starting material 3-acetylpyridine. Product purity (96% LC-MS) and chemical structure were confirmed by structural characterization (NMR, LC-MS) and were consistent with literature and batch data. In optimized conditions a total throughput of 3 g/h in product **40** was obtained.

6.2.3 Synthesis of Substituted Pyrimidinamine Structures

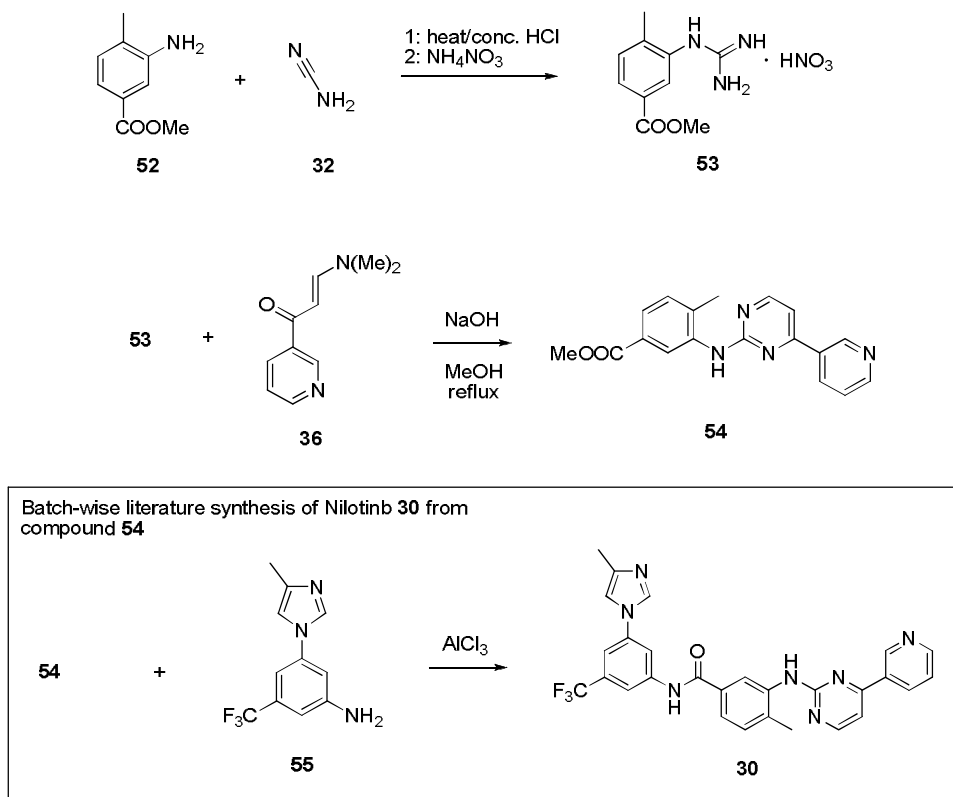
In order to demonstrate the flexibility of the continuous flow methodology, that is a key requirement for the application in a drug development stage, we tested sensitivity of the flow methodology to chemical substituents on the guanidine block. We hence prepared two other guanidine derivatives bearing useful functionalities (NH_2 , COOMe) to be tested as reagents in continuous flow synthesis of pyrimidinamine structures..

1-(2-methyl-5-aminophenyl)guanidine **51** was prepared by reduction of guanidine **33** under hydrazine/Nickel protocol. The aim in using guanidine **51** was exploring influence on reaction performance of a variation in electronic character of the substituent on phenyl ring; moreover, employment of **51** as reactive may afford directly Imatinib precursor **41** in confined environment without need for batch-wise manipulation of the biologically active compound **40**.



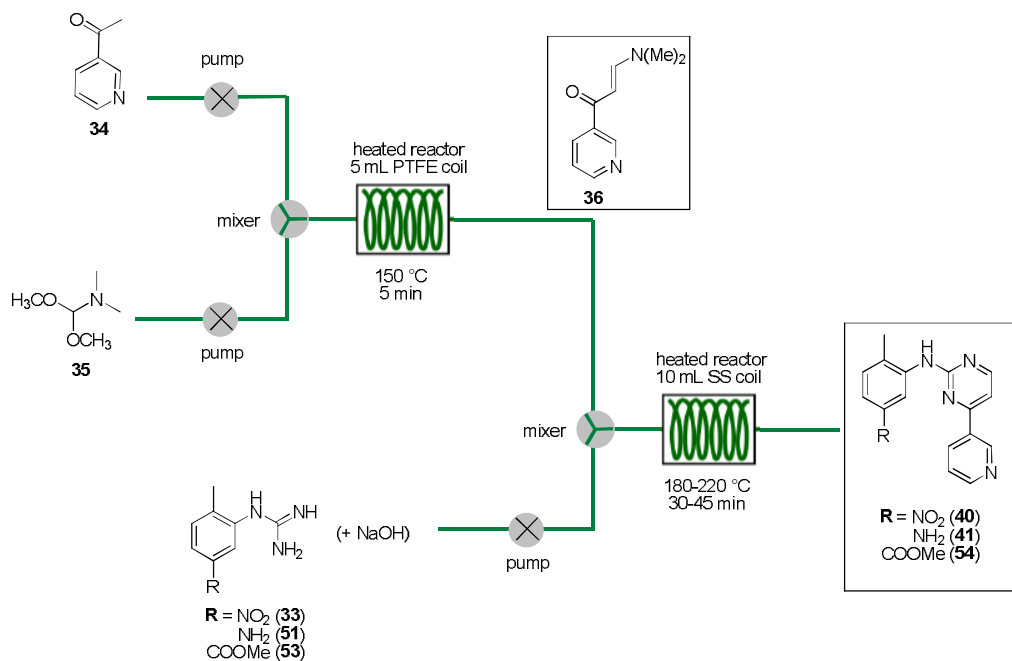
Scheme 6.8: Batch-wise synthesis of guanidine derivative **51** as building block for straightforward construction of pyrimidinamine **41**.

The benzoic ester derivative **53** was synthesised with the aim of opening the way to a continuous flow synthesis of Nilotinib **30** through the precursor compound **54** (Scheme 6.9). Compound **53** was thus prepared batch-wise following our established synthetic protocol. Compound **51** was as well prepared batch-wise following standard literature procedures to afford pure product in 66 % yield.



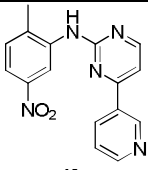
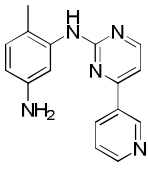
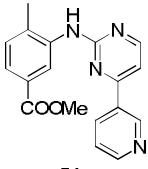
Scheme 6.9: Batch-wise synthesis compound **54** and literature procedure for synthesis of Nilotinib **30** through precursor **54**.

Flow synthesis of derivatives **41** and **54** using process displayed in Scheme 6.10 proceeded smoothly giving target compounds respectively in 75% and 66% isolated yield. Table 6.2 collects optimized reaction conditions and yields obtained for the flow synthesis of compounds **40**, **41** and **54**. In the case of compound **54**, guanidine derivative was directly introduced in continuous reactor as nitrate salt, affording desired product also in absence of the assisting base in 45 min residence time at 220 °C. However, addition of a catalytic amount (10%) of sodium methoxide to the feed mixture resulted in a slightly increased reaction rate, allowing for complete conversion in 30 minutes at 200 °C.



Scheme 6.10: Optimised continuous process for synthesis of pyrimidinamine structures as oncological

Table 6.2: Reaction conditions for continuous flow synthesis of pyrimidinamine structures.

	Temperature	Residence time	Isolated product yield
 40	180 °C	30	58
 41	200 °C	30	75
 54	220 °C (200 ^a)	45 (30 ^a)	66 (61 ^a)

a: with addition of 10% molar NaOMe

6.3 Conclusions

An hybrid batch-continuous flow protocol was established for the multistep synthesis of pyrimidinamine compounds that are functional chemical precursors of well-known oncological drugs, Imatinib and Nilotinib, employed in treatment of chronic myeloid leukemia. The synthetic process involves an optimized procedure for discontinuous preparation of substituted guanidine derivatives; these are then employed for continuous flow condensation with an enamine derivative, prepared in flow as well. Target products are obtained in good final yields and high purities. High throughput together with possibility to readily introduce chemical diversity in final compounds make such flow process suitable for application both in a production scale, with substantially increased process efficiency and safety, and drug development stages.

6.4 Experimental Section

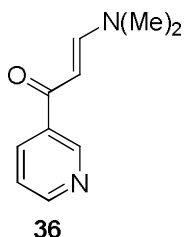
All reagents were purchased from Sigma-Aldrich and used without any purification. NMR spectra were recorded on a Bruker AC-F 250 spectrometer or Bruker Avance 300, using residual solvent signal reference. ESI-MS spectra were recorded in Flow Injection Analysis (FIA) mode on a LC-MSD-Trap-SL (Agilent Technologies, Palo Alto – USA). Samples were dissolved in the indicated solvent ($\sim 10^{-5}$ M) and injected in a stream of the same solvent (with 0.1% of formic acid) at 50 $\mu\text{L}/\text{min}$ (nitrogen nebulizing gas pressure = 20 psi; flow = 5 L/min; T = 325 °C). LC-MS analyses were performed on the same instrument using an Agilent binary pump with attached a Phenomenex Gemini C18 3 μ column. Elution was carried out at a flow rate of 0.6 mL/min using a reverse phase gradient of methanol and water containing 0.1% formic acid. The gradient run is described in the table below:

Min	0.0	10.0	30.0	40.0
% MeOH	30	60	60	60

Standard HPLC runs were performed on a Varian LC-900 instrument in the same conditions reported above. Flow experiments were performed in a commercial available Vapourtec flow platform in standard configuration.

6.4.1 Batch-wise Synthetic Procedures

3-(dimethylamino)-1-(pyridin-3-yl)prop-2-en-1-one (36):



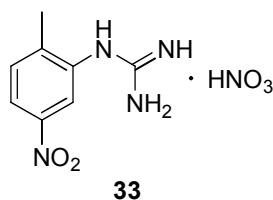
A mixture of 3-acetylpyridine (1.10 mL, 10.0 mmol) and dimethylformamide dimethyl acetal (DMF-DMA, 2 mL, 1.5 eq) in toluene (4 mL) was heated under reflux for 6 hours, disappearance of the product was monitored by TLC; the methanol by-product was removed by distillation during the reaction. After cooling the mixture to room temperature a 2:3 mixture of hexane/ethyl ether was added and the mixture was stirred for 30 minutes. The precipitate was then collected by filtration and washed with hexane/diethyl ether, then recrystallized from toluene to give the pure compound as orange crystals (1.5 g, 85.2% yield).

$^1\text{H-NMR}$ (CDCl_3 , 250 MHz): δ 2.89 (3H, s), 3.11 (3H, s), 5.62 (1H, d), 7.29 (1H, dd), 7.78 (1H, d), 8.12 (1H, dt), 8.60 (1H, dd), 9.02 (1H, d) ppm.

$^{13}\text{C-NMR}$ (CDCl_3 , 62.5 MHz): δ 37.0, 44.83, 91.34, 122.87, 134.58, 135.22, 148.53, 151.04, 154.28, 185.82 ppm.

ESI-MS (methanol): 177.2 m/z ($\text{M} + \text{H}^+$), 199.1 m/z ($\text{M} + \text{Na}^+$).

1-(2-methyl-5-nitrophenyl)guanidine nitrate (33):



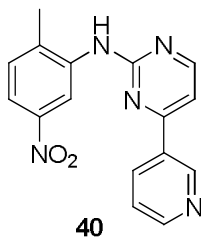
1-(2-methyl-5-nitrophenyl)guanidine nitrate was prepared following a literature procedure. A mixture of 2-methyl-5-nitroaniline (4.00 g, 15.6 mmol) and cyanamide (1.76 g, 2.5 eq) in isopropanol was heated to reflux temperature and 3.6 mL of 37% hydrochloric acid were slowly added. After 2 hours other 1.2 mL of hydrochloric acid were added and heating was maintained for *ca.* 8 hours until no starting material was visible in TLC and HPLC. The mixture was then cooled down to 60°C and 2 mL of 65% nitric acid were added. The mixture was cooled down to room temperature and the product collected by filtration, washed with cold isopropanol and dried to afford 5.19 g (76% yield) of white crystals.

¹H-NMR (DMSO-d⁶, 300 MHz): δ 2.33 (3H, s), 7.43 (4H, s), 7.64 (1H, d), 8.09 (1H, d), 8.15 (1H, dd), 9.5 (1H, s) ppm.

¹³C-NMR (DMSO-d⁶, 75 MHz): δ 17.51, 122.42, 122.69, 132.11, 134.4, 143.6, 146.28, 156.05.

ESI-MS (methanol): 195 m/z (M + H⁺).

(5-nitro-2-methylphenyl)-4-(3-pyridinyl)-2-pyrimidinamine (40):



1-(2-methyl-5-nitrophenyl) guanidine nitrate (0.9 g, 3.5 mmol) and of 3-(dimethylamino)-1-(pyridin-3-yl)prop-2-en-1-one (0.6 g, 1.0 eq) were dissolved in DMF (20 mL) and the solution was heated to reflux. Meanwhile 0.31 g of NaOH was dissolved in 0.7 mL of water and 0.4 mL of this solution (1.0 eq) was added to the mixture. Reaction evolution was followed by HPLC. After 10 hours the mixture was quenched by adding cold water (10

mL) and then poured in 100 mL of water. The precipitated product was collected by suction filtration, washed with water and dried at 40°C under vacuum. 0.48 grams (yield 45%) of title compound as brownish solid was obtained.

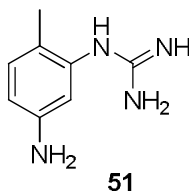
¹H-NMR (DMSO-d⁶, 300 MHz): δ 2.43 (3H, s), 7.55 (3H, m), 7.89 (1H, dd), 8.48 (1H, dt), 8.62 (1H, d), 8.71 (1H, dd), 8.8 (1H, d), 9.22 (1H, s), 9.32 (1H, d).

¹³C-NMR (DMSO-d⁶, 75 MHz): δ 18.26, 108.79, 117.4, 117.86, 123.77, 131.14, 131.79, 134.21, 138.66, 138.8, 145.74, 148.07, 151.53, 159.6, 160.21, 161.52.

ESI-MS: 308 m/z (M + H⁺).

HPLC:

1-(2-methyl-5-aminophenyl)guanidine (51):

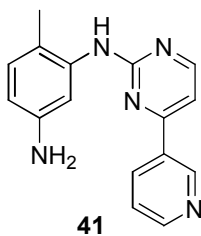


1-(2-methyl-5-nitrophenyl)guanidine nitrate (6.51 g, 25.6 mmol) was dissolved in methanol (250 mL). Wet Nickel Raney (0.6 g) was added and the mixture was heated to reflux under stirring. A solution of *ca.* 40% hydrated hydrazine in methanol (4.8 mL of hydrazine in 5 mL of methanol) was slowly added. After 30 minutes, the same amount of hydrazine solution was added and the heating was maintained for *ca.* 8 hours. Reaction was followed by TLC and mass spectroscopy till disappearance of the reagent. The mixture was cooled down to room temperature and filtered on a pad of celite; the pad was washed with methanol, the filtrates were collected and the solvent evaporated. Excess hydrazine and water were removed by azeotropic distillation with toluene. The product was then dissolved in the minimum amount of HPLC methanol, heated to reflux and treated with active carbon. The mixture was filtered over celite and the solvent removed to give 4.13 g (99.3% yield) of the product as a yellow solid.

$^1\text{H-NMR}$ (DMSO-d_6 , 300 MHz): δ 1.89 (3H, s), 4.56 (4H, s), 5.99 (1H, d), 6.06 (1H, dd), 6.72 (1H, d).

ESI-MS (methanol): 165 m/z ($M + \text{H}^+$).

(5-amino-2-methylphenyl)-4-(3-pyridinyl)-2-pyrimidinamine (41):



Method A: (5-nitro-2-methylphenyl)-4-(3-pyridinyl)-2-pyrimidinamine **40** (0.4 g, 1.3 mmol) was suspended in methanol (20 mL). Wet Nickel Raney (40 mg) was added and the mixture was heated to reflux under stirring. A solution of *ca.* 40% hydrated hydrazine in methanol (0.5 mL of hydrazine in 0.5 mL of methanol) was slowly added. After 30 minutes, the same amount of hydrazine solution was added and the heating was maintained for *ca.* 8 hours. Reaction was followed by TLC and mass spectroscopy till disappearance of the reagent. The mixture was cooled down to room temperature and filtered on a pad of celite; the pad was washed with methanol, the filtrates were collected and the solvent evaporated. Excess hydrazine and water were removed by azeotropic distillation with toluene. The product was then dissolved in the minimum amount of HPLC methanol, heated to reflux and treated with active carbon. The mixture was filtered over celite and the solvent removed to give 0.33 g (92% yield) of the product as a yellow solid.

Method B: A mixture of 1-(2-methyl-5-aminophenyl)guanidine (0.58 g, 3.5 mmol) and 3-(dimethylamino)-1-(pyridin-3-yl)prop-2-en-1-one (0.6 g, 1.0 eq) in DMF (20 mL) was heated to reflux for 8 hours. After cooling the mixture was poured on water and extracted twice with dichloromethane. Combined organic phases were washed with brine and dried over sodium sulphate. Active carbon was then added to the solution and the mixture was heated to reflux for 30 minutes. The carbon was removed by filtration and the solution concentrated to a small volume and poured over a pad of silica gel. The pad was washed with 100 mL of a mixture of dichloromethane/ethyl acetate 1:1, than with ethyl acetate

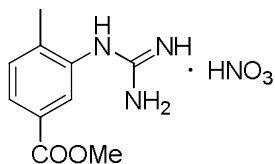
(200 mL). The acetate solution so obtained was concentrated in vacuo to obtain 0.47 g of title compound (48% yield) as yellow crystals.

$^1\text{H-NMR}$ (DMSO- d_6 , 300 MHz): δ 2.06 (3H, s), 4.84 (2H, br), 6.33 (1H, dd), 6.79 (1H, d), 6.87 (1H, d), 7.36 (1H, d), 7.53 (1H, dq), 8.40 (1H, dt), 8.46 (1H, d), 8.66 (1H, s), 8.69 (1H, dd), 9.24 (1H, dd).

$^{13}\text{C-NMR}$ (DMSO- d_6 , 75 MHz): δ 17.09, 106.94, 110.8, 110.98, 119.19, 123.67, 130.18, 132.18, 134.12, 137.82, 146.63, 147.99, 151.18, 159.21, 161.18, 161.36.

ESI-MS (methanol): 278 m/z ($\text{M} + \text{H}^+$).

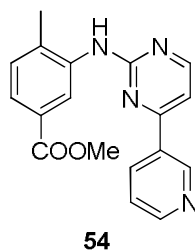
Methyl-(3-guanidinio-4-methyl)benzoate (53):



53

Methyl-(3-amino-4-methyl)benzoate (13.8 g, 83.5 mmol) and cyanamide (7.7 g, 183.0 mmol) were suspended in 50 mL methanol and the mixture was heated to reflux. Under stirring, 11 mL of concentrated hydrochloric acid was added dropwise and the mixture was refluxed overnight. Reaction mixture was then left cooling to room temperature, the solvent was removed and solid residue treated with water (50 mL) and cooled to 0 °C under stirring. A solution of ammonium nitrate (13.5 g, 169.0 mmol) in 40 mL water was added dropwise, followed by additional 80 mL of iced water. The white suspension was stirred under cooling for 30 minutes, filtered and the solid product washed with iced water (50 mL) and diethyl ether (2 x 50 mL), and finally dried to afford 18.78 g (83 %) of white crystals.

N-(5-(2-methyl)methylbenzoate)-4-(3-pyridinyl)-2-pyrimidinamine (54):



Methyl-(3-guanidinio-4-methyl)benzoate **53** (4.3 g, 15.9 mmol) and 3-(dimethylamino)-1-(pyridin-3-yl)prop-2-en-1-one **36** (2.81 g, 1 eq) were suspended in methanol (30 ml). Powdered NaOH (0.68 g, 17 mmol) was added and the mixture was heated to reflux for 24 h, until disappearance of starting material (assessed by TLC). Upon evaporation of the solvent, the orange solid residue was partitioned between water and ethyl acetate. Aqueous phase was extracted twice with ethyl acetate (50 mL), combined organic layers were dried over sodium sulphate and dried. Finally solid product was crystallized from hot methanol to afford 3.38 g (66 %) of product as yellow crystals.

¹H-NMR (DMSO-d⁶, 300 MHz): δ 2.3 (3H, s), 2.5 (1H, m), 3.9 (3H, s), 7.4 (1H, d), 7.5 (2H, m), 7.7 (1H, dd), 8.4 (2H, m), 8.5 (1H, d), 8.7 (1H, dd), 9.0 (1H, s), 9.3 (1H, d).

6.4.2 Continuous Flow Syntheses

Flow synthesis of 3-(dimethylamino)-1-(pyridin-3-yl)prop-2-en-1-one **36:**

Vapourtec flow system was equipped with a 5 mL internal volume, PTFE tube coil reactor and a 100 psi back pressure regulator. Solvent line was charged with DMF, whereas reagents lines were charged with stock solutions prepared by dissolving 10 mL of 3-acetylpyridine in 5 mL of DMF (6.08 M, line A) and 10 mL of DMF-DMA and 3 mL of DMF (5.79 M, line B). System settings were: pump A 0.46 ml/min flow rate, pump B 0.54 ml/min, reactor temperature 150° C. Reactor output was collected in a vial and directly employed for further synthetic steps.

Flow synthesis of (5-nitro-2-methylphenyl)-4-(3-pyridinyl)-2-pyrimidinamine:

1-(2-methyl-5-nitrophenyl)guanidine free base was obtained by treating a DMF solution of the correspondent nitrate salt with 1.0 eq of soda solution. The resulting orange suspension was filtered over magnesium sulphate to remove salts and charged as stock solution in pump A in Vapourtec flow systems, equipped with a 10 mL internal volume, stainless steel tube coil reactor and 250 psi BPR. In pump B was charged the solution of 3-(dimethylamino)-1-(pyridin-3-yl)prop-2-en-1-one collected from the flow system as reported above. System settings were: pump A 0.46 ml/min flow rate, pump B 0.54 ml/min, reactor temperature 150° C. Analogous conditions were used for synthesis of pyrimidinamine structures.

References

- ¹ R. Capdeville, E. Buchdunger, J. Zimmermann and A. Matter, *Nature Reviews, Drug Discovery*, **2002**, 1, 493-502.
- ² P.W. Manley, S.W. Cowan-Jacob, E. Buchdunger, D. Fabbro, G. Fendrich, P. Furet, T. Meyer and J. Zimmermann, *European Journal of Cancer*, **2002**, 38, S19–S27.
- ³ W. Breitenstein, P. Furet, S. Jacob, P. W. Manley, International Patent WO 2004/005281.
- ⁴ W. Szczepek, W. Luniewski, L. Kaczmarek, B. Zagrodzki, D. Samson-Lazinska, W. Szelejewski, M. Skarzynski, International Patent WO 2006/071130.
- ⁵ M. D. Hopkin, I. R. Baxendale, and S. V. Ley, *Chem. Commun.*, **2010**, 2450–2452.



Chapter 7: Flow Synthesis of 4-anilino-quinazoline Structures

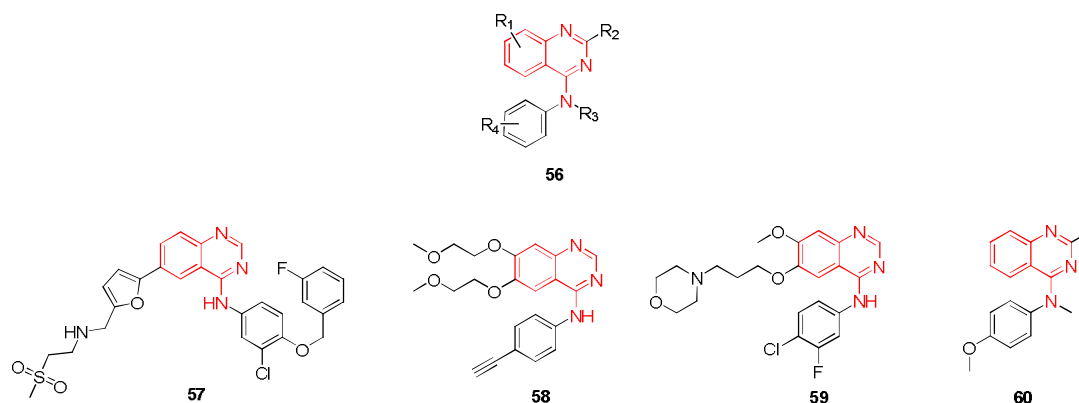


Figure 7.1: molecular structures of some approved chemotherapeutic agents based on a 4-anilino-quinazoline moiety (general structure **56**, core scaffold highlighted in red): Lapatinib **57**, Erlotinib **58**, Gefitinib **59** and Verubulin **60**.

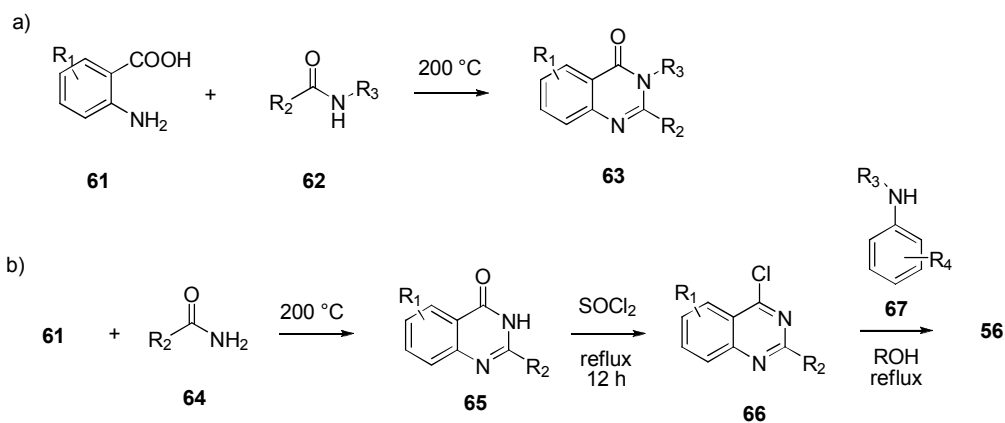
7.1 Classical Approaches towards Quinazoline Synthesis

The second class of oncological drugs considered for flow studies involves molecules containing 4-anilino-quinazoline core. The basic chemical structure of the quinazoline moiety consists in a two fused aromatic rings: benzene and pyrimidine. Derivatives of quinazoline have been extensively used in medicine as antimalaric agents and, more recently, antitumoral agents.¹ In particular molecules carrying a 4-anilino-quinazoline moiety (general structure **56** in Figure 7.1) that resembles ATP (adenosine-5'-triphosphate) have been discovered to possess high cytotoxic activity, mainly through a mechanism of inhibition of tyrosine kinases similar to Imatinib. Valuable examples are Lapatinib and Erlotinib, already approved by FDA for clinical use. Lapatinib is commercialized by GlaxoSmithKline in the form of a ditosylate salt under the name of *Tykerb/Tyverb*® for treatment of resistant forms of mammalian tumors. Lapatinib is used as third line treatment in patients that have previously responded negatively to Herceptin (an intravenous administrated monoclonal antibody), taxanes and anthracyclines.² Erlotinib in a similar way is commercialized by Genentech under denomination of *Tarceva*® and used in combination with gemcitabine in treatment of advanced metastatic pancreas tumors.³ Gefitinib (Iressa, *AstraZeneca*®) exhibits a similar structure and is employed in many

countries as first line treatment for non-small lung cancers.⁴ Finally, Verubulin (*Azixa*TM) is an investigational new drug developed by Myrexia, Inc. for treatment of advanced primary and metastatic glioblastoma and metastatic melanoma. Verubulin possess a 4-anilino-quinazoline core structure, although its action is based on microtubule destabilization rather than kinases inhibition, differently from the other drugs here presented. Verubulin is also a potent vascular disrupting agent (VDA) able to reduce blood supply to the tumor. Importantly, in non-clinical studies, *Azixa* has demonstrated the unique ability to effectively cross the blood-brain barrier and accumulate in the brain.⁵

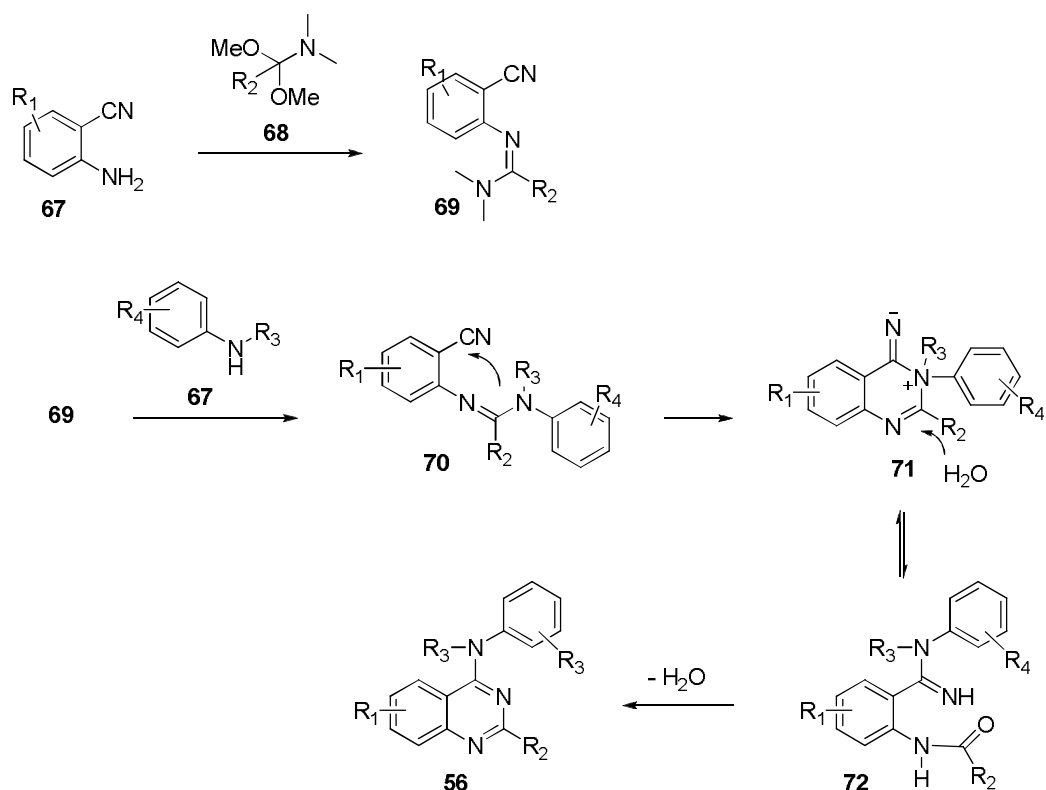
7.1.1 Classical Synthetic Route for 4-anilino-quinazoline Moieties

Traditionally, synthesis of 4-anilino-quinazoline functions involves quinazolin-4(3*H*)-ones of general structure **63** (Scheme 7.1) as reaction intermediates.⁶ Many synthetic protocols are available in literature, highlighting the wide interest in such functional derivatives. Mainly, quinazolin-4(3*H*)-ones are prepared using the so-called Niementowski synthesis, by reaction of anthranilic acid derivatives with formamide under acidic conditions at high temperature (Scheme 7.1).⁷ Harsh reaction conditions often result in decomposition paths that reduce yields; in addition, sensitive substituents on starting materials result often to be incompatible with synthetic conditions, thus extensive recourse to protecting group is needed. Even if method improvements have been proposed, it still remains a poorly effective way.⁸ In addition, synthesis of 4-amino substituted derivatives requires preparation of the highly unstable intermediate 4-chloro-quinazolines **66** by treatment of quinazolin-4(3*H*)-ones with corrosive reagents, as thionyl chloride/phosphoryl chloride.



Scheme 7.1: a) general mechanism of Niementowski synthesis of quinazolin-4(3*H*)-ones. b) synthetic protocol for preparation of 4-anilino-quinazoline structures via quinazolin-4(3*H*)-ones.

In the past years, an alternative approach has been proposed for easy two-step preparation of 4-anilino-quinazoline moieties by mean of Dimroth rearrangement (Scheme 7.2): an anthranilonitrile derivative of structure **67** is firstly reacted with an amide acetal **68** at high temperature to give the reactive formamidine intermediate **69**. In presence of an aromatic amine and under acidic conditions, intermediate **69** undergoes a cascade reaction to finally afford the target 4-anilino-quinazolin compound of general formula **56**. Reaction mechanism is supposed to involve initial substitution of dimethylamine moiety by aniline to give compound **70**, followed by formation of a pyrimidine compound **71**; hydrolysis of the iminic bond causes ring opening, followed by rotation of a carbon-carbon bond and finally ring closure to afford the product compound (see Scheme 7.2).⁹



Scheme 7.2: general mechanism for preparation of 4-anilino-quinazolin structures by a two-step synthesis involving Dimroth rearrangement.

This latter approach represents a huge simplification of synthetic procedure for obtaining quinazoline derivatives, however, criticisms still subsist: high temperatures and long reaction times result in chemical by-products; moreover, first synthetic step often involves employment of the toxic compound DMF-DMA (Chapter 6, Section 6.2.1) or analogous derivatives. To overcome selectivity and efficiency problems, a microwave enhanced

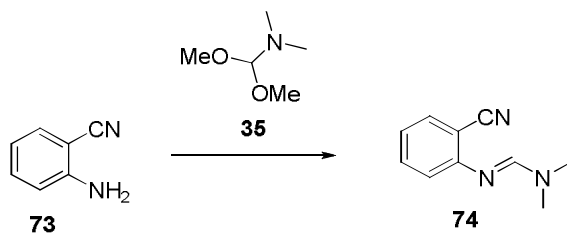
methodology for such synthesis has been recently proposed.¹⁰ Despite the substantial increase in efficiency thus obtained, the method results almost impossible to be scaled up due to the well-known problematics related to scalability of microwave heat sources.

Continuous flow approach has already proven to be useful in handling difficult reaction steps, with the concomitant advantage of inducing higher reaction rates and productivities thanks to better control on reaction conditions and implementation of novel process windows. Moreover, reaction conditions very similar to microwave enhanced chemistry might be obtained by using high temperature continuous flow equipment under conventional heating, with the key advantage of gaining straightforward scalability. With this in mind, we afforded to develop a robust, flexible flow based approach to the synthesis of highly substituted 4-anilino-quinazoline derivatives.

7.2 Continuous Flow Approaches to 4-anilino-quinazolines

7.2.1 Synthesis of N'-(2-cyanophenyl)-N,N-dimethylformamide (74)

Initially, we focused on preparation of highly reactive dimethyl formamide derivatives from suitable 2-amino-benzonitrile precursors. As a proof of concept, we used a simplified model system for continuous flow implementation. We hence selected the commercial anthranilonitrile (2-amino-benzonitrile **73**) as inexpensive starting material. Batch-wise preparation of dimethyl formamide derivative **74** upon treatment with excess DMF-DMA in toluene under continuous distillation of methanol by-product afforded the desired compound in good yield in 4-6 hours (Scheme 7.3).



Scheme 7.3: synthesis of N'-(2-cyanophenyl)-N,N-dimethylformamide **74**.

Process translation to continuous flow was dealt in a similar way to the previously reported example of Imatinib analogues synthesis (Chapter 6), by using Vapourtec R4 platform charged with DMF solutions of reactives. Optimization of flow methodology was done by means of Design of Experiment (DoE). DoE is a statistical method used to deduce the critical parameters of a chemical process and to plan optimized experiments. Differently from a classical optimization procedure, that reiterates experiments by varying one parameter at a time in a trial-and-error mode, DoE reduce the number of experiments by changing more than one parameter at a time. By using a careful design based on a statistical method, parameters critical for process performances could be identified, while contemporary deducing possible second order interaction between different parameters, undetectable with a classic approach. As a result a smaller experimental effort is needed and a better process efficiency and knowledge are obtained.

For our purposes, DoE screening was performed considering six reaction parameters that were believed to be influencing on process performance; for each parameter a two level value was selected, meaning a lowest and an highest value defining a suitable applicability range. Eight experimental conditions sets were designed and corresponding experiments were performed twice in a randomized order, with the aim of minimizing external factors influence on results. The pool of parameters selected, boundary values and an example of experimental sets are reported in Tables 7.1 and 7.2. Reaction yields in desired product were determined by HPLC and are also reported in Table 7.2. Among the parameters screened, together with temperature, residence time, stoichiometry and acetal molar concentration, also reactor engineering parameters were checked, as the reactor volume, that directly affects flow rates and mixing efficiency, and employment of a micromixing device of slit interdigital type instead of a simple T junction.

The main effects plot of obtained results reported in Figure 7.2 shows up the weight factor for each experimental value on reaction total performance: the more pendant the plot, the higher the influence on process output. As it is possible to notice, reaction times and reactor volume have a very low impact on reaction behavior; on the contrary, temperature, number of equivalents and molar concentration of DMF-DMA have the highest influence.

Table 7.1: Set of parameters and relative boundary values used for DoE screening of reaction conditions.

Factor	Entry	-1	+1
temperature	A	100° C	150° C
DMF-DMA equivalents	B	1.0	1.5
Residence time	C	5 min	10 min
Reactor volume	D	5 mL	10 mL
Micromixing device	E	No	Yes
DMF-DMA concentration	F	Ca. 5.6 M	Ca. 7.5 M (neat)

Table 7.2: example of experiment set for DoE screening.

Run order^a	exp	A	B	C	D	E	F	Yield (%)^b
2	1	+1	-1	-1	+1	-1	+1	99,1
4	2	+1	+1	-1	-1	+1	-1	79,8
1	3	+1	+1	+1	-1	-1	+1	99,0
7	4	-1	+1	+1	+1	-1	-1	74,5
5	5	+1	-1	+1	+1	+1	-1	33,4
8	6	-1	+1	-1	+1	+1	+1	52,4
3	7	-1	-1	+1	-1	+1	+1	54,7
6	8	-1	-1	-1	-1	-1	-1	52,7

a: experiments performed in randomized order to minimize external influence.

b: mean values over repeated experiments and analytical determinations (HPLC).

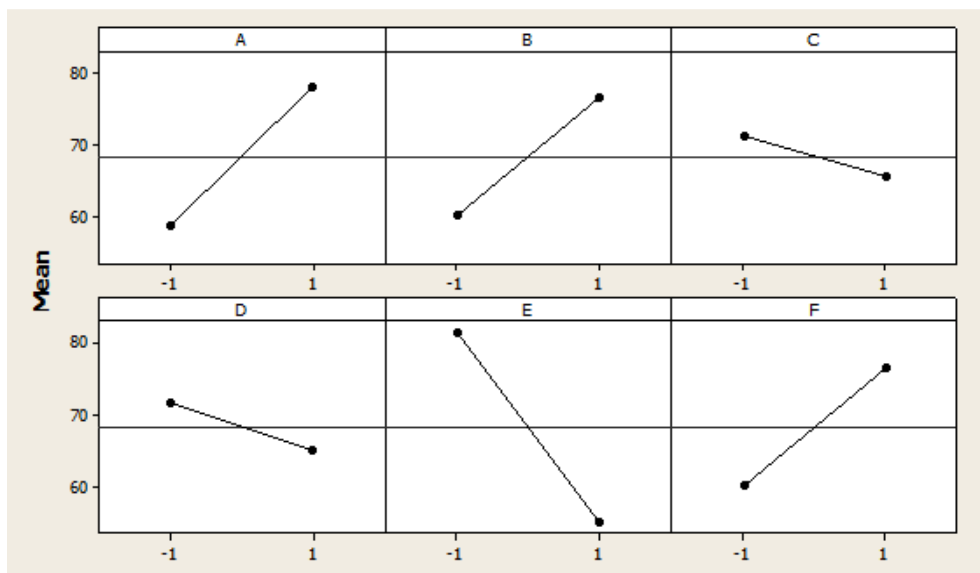
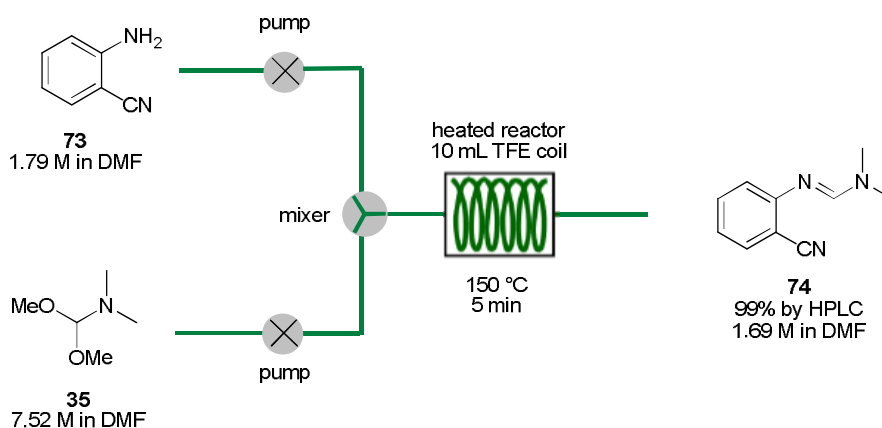


Figure 7.2: main effect plot calculated for DoE screening of reaction parameters.

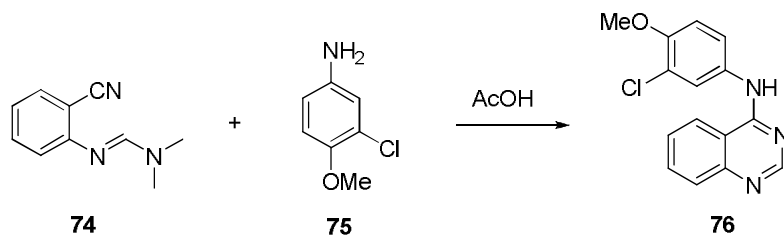
Optimum reaction conditions were found to be 1.0 eq. of neat acetal at 150 °C, 5 minutes of residence time allowed for a quantitative yield in formamidine intermediate **74**, determined by HPLC. No further optimization of the process or determination of second order parametric influence was attempted at this step. Reactor type and mixing device resulted to have low impact on process behavior. 10 mL Teflon coil reactor was then adopted in order to improve process throughput; whereas the micromixer device was avoided in view of engineering simplification. Optimized process for the flow synthesis of N'-(2-cyanophenyl)-N,N-dimethylformamidine is shown in Scheme 7.4.



Scheme 7.4: Continuous-flow synthesis of N'-(2-cyanophenyl)-N,N-dimethylformamidine. Anthranilonitrile **73** feed solution was employed at maximum achievable concentration.

7.2.2 Synthesis of 4-(3'-chloro-4'-methoxyanilino)-quinazoline (76)

Following our aim of designing a model flow process, we focused on the second synthetic step of our protocol, the condensation/Dimroth rearrangement reaction of formamidine intermediate **74** with a suitable aniline. As model compound for the aniline derivative, we selected 3-chloro-4-methoxyaniline **75** as its structure basically mimics the side chain of the oncological drug Lapatinib (compound **57** in Figure 7.1).

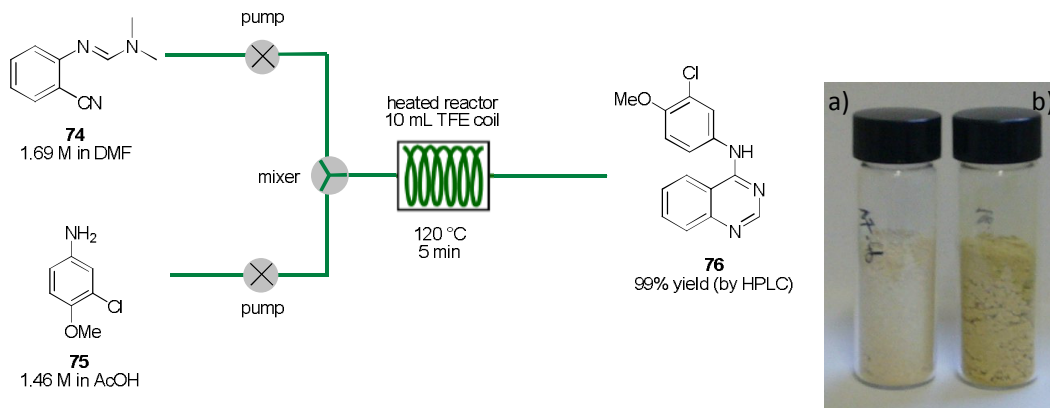


Scheme 7.5: synthesis of 4-(3'-chloro-4'-methoxyanilino)-quinazoline (**76**).

Initial batch-wise synthesis was performed by suspending a mixture of formamidine **74** and aniline **75** in acetic acid and heating to reflux for several hours. Upon cooling of the reaction mixture, product **76** was recovered by filtration and purified by crystallization.

Addition of DMF to the reaction mixture resulted in a more homogeneous mixture. On the other hand, a more complex final mixture was obtained, as solvent decomposition in acidic environment promotes parasite reactions. Chromatographic purification was required in order to remove by-products, and compound **76** was thus obtained in a good yield of 65%

The synthetic procedure was readily transferred to continuous, feeding the reactor with an acetic acid solution of aniline **75** and the formamidine **74** solution collected from reactor output in the first synthetic step. Aniline concentration (maximum achievable value of 1.5 M) and stoichiometric ratios between reagents (1:1) were kept fixed for the first set of experiments, as well as reactor volume (10 mL). A nearly quantitative yield in product (determined by HPLC) was obtained independently from reaction temperature (screened between 120 and 220°C) and reaction time (from 2 to 60 minutes). A flash heating protocol was thus applied setting a 5 minutes residence time at 120 °C.



Scheme 7.6: left) continuous-flow synthesis of 4-(3'-chloro-4'-methoxyanilino)-quinazoline. Right) comparison between 4-(3'-chloro-4'-methoxyanilino)-quinazoline obtained by continuous flow process (a) and by batch procedure (b). Off white colour is symptomatic of lower amount of impurities.

Sequential flow processes were carried out in order to afford a preparative sample of compound **76**. Reactor output was collected and cooled, then toluene was added to help precipitation of the product; the solid was recovered by filtration and washed with either toluene or diethyl ether to afford the target compound as white crystals in 94% yield.

In such conditions a total productivity of 24 grams per hour of product is potentially accessible; moreover, product obtained by continuous flow mode has a clearly lower content of colored impurities (Scheme 7.6): colored compounds are in fact commonly produced as by-products in chemical processing and are thus good indicators of product purity. Higher purity respect to batch-wise prepared product is a parameter that can be of great importance in view of industrial application of such process.

7.2.3 Synthesis of a Libray of 4-anilino-quinazolines

With the optimized flow procedure developed on the simple model compound in hand, we focused on extending applicability range to the preparation of highly substituted derivatives. This aim was pursued through two main routes: first, introducing preformed functionalities on the benzonitrile precursor, or suitable anchor points for downstream functionalisation; second, varying the structure of the aniline in second flow step.

First of all we managed to handle the benzonitrile building-block: in many examples of biological active quinazoline derivatives, the 6 ring position is the one most bearing chemical functionalities. With this in mind, we selected two simple functional derivatives as starting materials for further synthetic work, 5-nitro **77** and 5-bromo anthranilonitrile **78**.

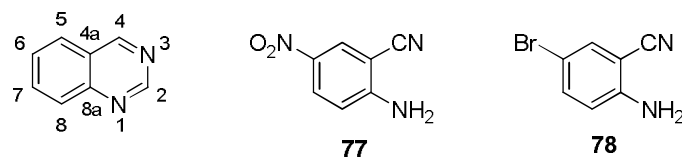
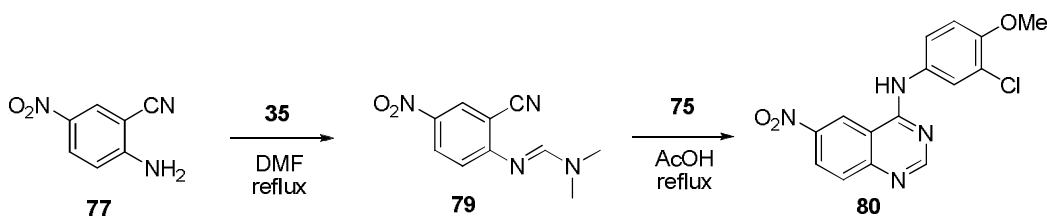


Figure 7.3: scheme of substitutions on quinazoline rings: introduction of functionalities on position 6 was accomplished by using 5-substituted benzonitrile derivatives **77** and **78**

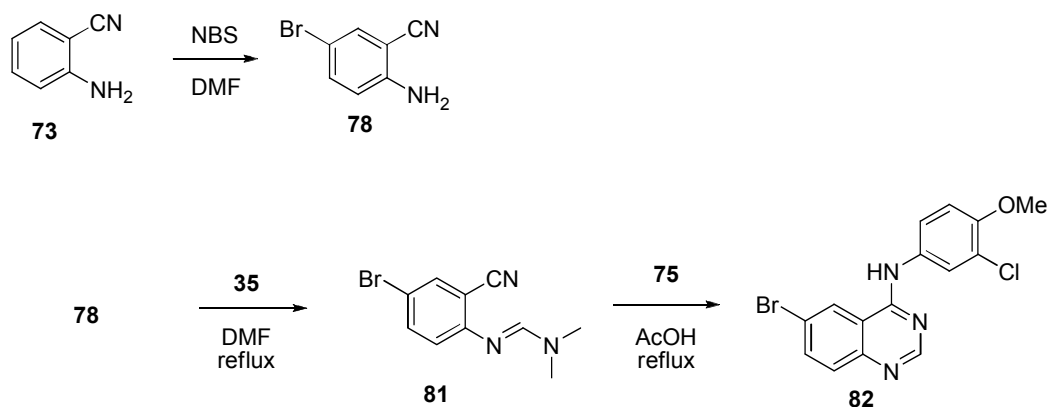
5-nitro anthranilonitrile **77** is commercially available, and the nitro group can easily be reduced to amino thus opening good functionalization perspectives. Moreover, derived 6-thioureido and 6-ureido-4-anilino-quinazoline derivatives have recently attracted much interest as both antimalaric and anticancer drug candidates. Batch-wise synthetic protocol analogous to the model compound anthranilonitrile was applied to derivative **77**, affording the correspondent formamidine **79** and 4-anilino-quinazoline derivative **80** in moderate yield.



Scheme 7.7: Batch-wise synthesis of 6-nitro-4-anilino quinazoline derivative.

5-bromo-anthranilonitrile **78** similarly affords good opportunities of chemical post-functionalization through a wide range of carbon-carbon metal catalyzed cross-coupling protocols or substitution paths. This derivative was successfully prepared batch-wise in high yield by selective mono-bromination of 2-amino-benzonitrile with N-bromo-

succinimide (NBS) in DMF solution and used for preparation of the correspondent



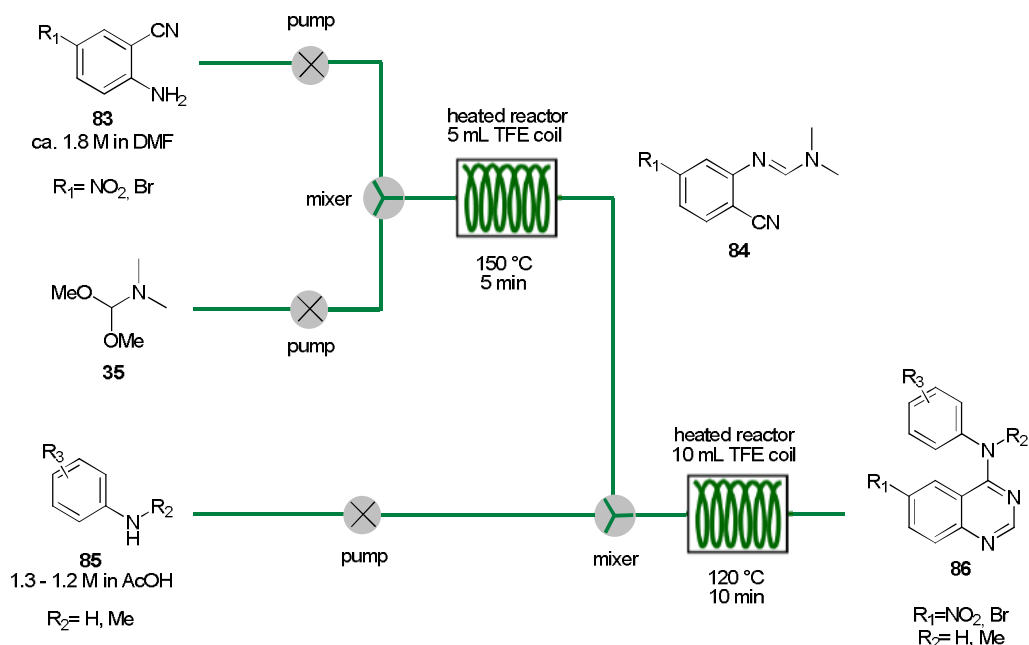
Scheme 7.8: Batch-wise synthesis of 5-bromo-anthranilonitrile (**78**) and correspondent quinazoline **82**

quinazoline derivative **82** in 51% yield.

Flow procedure analogous to that reported in Scheme 7.6 similarly afforded the target compounds with an only moderate yield of nearly 60% in isolated product. A fast re-optimization of reaction conditions was performed, leading to the increment of reaction time for the second synthetic step from 5 to 10 minutes. Moreover, an influence on reaction yield from aniline molar concentration was detected: an optimum range between 1.3 and 1.2 M was determined, probably due to the amount of acetic acid needed with respect to substrate in order to effectively promote molecular rearrangement. By using these new parameters, product yield was improved to a more acceptable value of 71 % for the nitro derivative and 76 % for bromo derivative.

The optimized flow process joining the two single steps is reported in Scheme 7.9: this general procedure has been applied for the synthesis of a library of compounds. Bromine benzonitrile derivative **78** has been selected as main starting material, being the more flexible derivative, but also the more sensitive to reaction conditions being highly reactive itself and likely to present carry-over of synthetic impurities. Reactive anilines were selected by taking into account the electronic nature of substituents (electron-donor/electron-withdrawing groups) and the structural analogy to molecules that have already shown high biological activities. The employed derivatives were acquired from commercial sources when possible, or prepared through batch-wise procedures derived

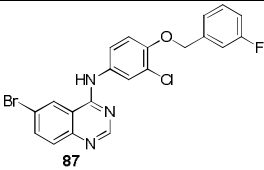
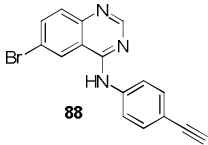
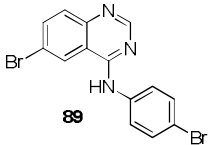
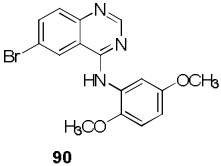
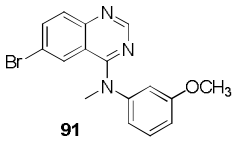
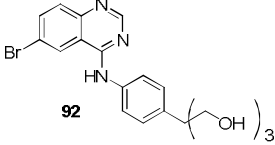
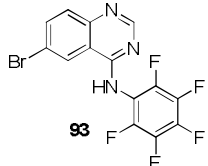
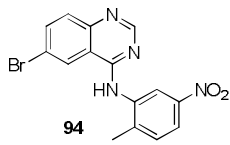
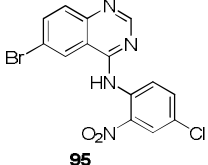
from established literature protocols (see Experimental Section). Details on aniline synthesis and isolation of various quinazoline derivatives are reported in the experimental part. Results obtained in the synthesis of various substituted derivatives are summarized in Table 7.3.



Scheme 7.9: Continuous-flow optimized protocol for the synthesis of 6-substituted-4-anilino-quinazolines.

Table 7.3: Summary of results for the synthesis of substituted 4-anilino-quinazoline derivatives.

Entry	Structure	Experimental conditions	Isolated yield
1		Step 1: 150 °C, 5 min. Step 2: 120 °C, 10 min	76%
2		Step 1: 150 °C, 5 min. Step 2: 120 °C, 10 min	71%

3	 <p>87</p>	<p>Step 1: 150 °C, 5 min.</p> <p>Step 2: 120 °C, 10 min</p>	68%
4	 <p>88</p>	<p>Step 1: 150 °C, 5 min.</p> <p>Step 2: 120 °C, 10 min</p>	65%
5	 <p>89</p>	<p>Step 1: 150 °C, 5 min.</p> <p>Step 2: 120 °C, 10 min</p>	85%
6	 <p>90</p>	<p>Step 1: 150 °C, 5 min.</p> <p>Step 2: 120 °C, 10 min</p>	73%
7	 <p>91</p>	<p>Step 1: 150 °C, 5 min.</p> <p>Step 2: 120 °C, 10 min</p>	10%
8	 <p>92</p>	<p>Step 1: 150 °C, 5 min.</p> <p>Step 2: 120 °C, 10 min</p>	traces
9	 <p>93</p>	<p>Step 1: 150 °C, 5 min.</p> <p>Step 2: 120 °C, 10 min</p>	n.d
10	 <p>94</p>	<p>Step 1: 150 °C, 5 min.</p> <p>Step 2: 120 °C, 10 or 30 min</p>	n.d
11	 <p>95</p>	<p>Step 1: 150 °C, 5 min.</p> <p>Step 2: 120 °C, 10 or 30 min</p>	n.d

As may be noticed, good to excellent yields were obtained for 4-anilino-quinazoline derivatives bearing electron-rich groups, especially alkoxides and common halogens like bromine and chlorine (entry 1-6). Perfluorinated anilines and derivatives bearing nitro-groups gave hardly any reaction, as confirmed by mass analysis of reaction crudes; increase of reaction time for the second step was attempted with no effective result (entry 9-11). This was probably due to electron-withdrawing effects that reduce nucleophilic character of aniline nitrogen atom, thus inhibiting both the formation of the pyridine intermediate and subsequent rearrangement (see scheme 7.2); lack of reactivity of such compounds has been also suggested previously in literature.¹⁰ Similarly, methylation of aniline nitrogen results in substantial lack of reactivity, and only poor yield of the correspondent quinazoline compound **91** were obtained (entry 7). Compound **92** (Table, 7.3, entry 8) bearing a polyhydroxyl function, was designed as a functionalized derivative to be anchored on inorganic nanoparticles, based on silica or metal, that have been suggested to be excellent platforms for controlled drug delivery. In this case reaction yield was equally poor, and only traces of desired product were identified in final reaction mixture. Such result arises from the high liability of the polyhydroxilic moiety, that often requires protection in order to avoid structural rearrangements. Further work in such sense is needed.

7.3 Conclusions

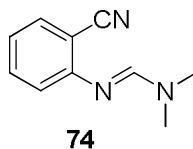
A continuous flow two step synthesis of 4-anilino-quinazoline derivatives was developed, starting from simple derivatives of 2-amino-benzonitrile and functionalized anilines. The first reaction step, involving the synthesis of an highly reactive dimethyl formamidine intermediate, was readily optimized using a model compound in conjunction with a Design of Experiments approach that allowed for fast and reliable process development, thus demonstrating the power of such designing method. Optimization efforts on the second synthetic step, a condensation/Dimroth rearrangement reaction, using both model compound and more structurally complex derivatives resulted in a powerful continuous method for production of target molecules, with high throughput capability and potential for allowing structural variation.

7.4 Experimental Section

All reagents were purchased from Sigma-Aldrich and used without any purification. NMR spectra were recorded on a Bruker AC-F 250 spectrometer or Bruker Avance 300, using residual solvent signal reference. ESI-MS spectra were recorded in Flow Injection Analysis (FIA) mode on a LC-MSD-Trap-SL (Agilent Technologies, Palo Alto – USA). Samples were dissolved in the indicated solvent ($\sim 10^{-5}$ M) and injected in a stream of the same solvent (with 0.1% of formic acid) at 50 $\mu\text{L}/\text{min}$ (nitrogen nebulizing gas pressure = 20 psi; flow = 5 L/min; T = 325 °C). HPLC runs were performed on a Varian LC-900 instrument equipped with a Phenomenex Gemini C18 3 μ column. Flow experiments were performed in a commercial available Vapourtec flow platform in standard configuration.

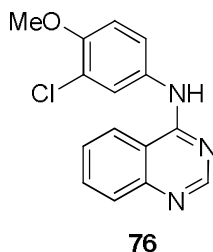
7.4.1 Batch-wise Synthetic Procedures

N'-(2-cyanophenyl)-N,N-dimethylformamidinium (74):



2-amino-benzonitrile and dimethylformamide dimethyl acetal (DMF-DMA, 2 mL, 1.5 eq) in toluene (4 mL) was heated under reflux for 6 hours, disappearance of the product was monitored by TLC; the methanol by-product was removed by distillation during the reaction. After cooling the mixture to room temperature a 2:3 mixture of hexane/ethyl ether was added and the mixture was stirred for 30 minutes. The precipitate was then collected by filtration and washed with hexane/diethyl ether, then recrystallized from toluene to give the pure compound as orange crystals (1.5 g, 85.2% yield).

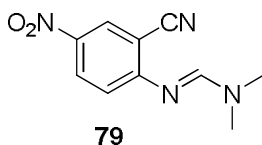
4-(3'-chloro-4'-methoxyanilino)-quinazoline (76):



Method A: N'-(2-cyanophenyl)-N,N-dimethylformamide (10 mmol) and 3-chloro-4-methoxy aniline (10 mmol) were suspended in 5 ml acetic acid and the mixture refluxed for 8-12 hours. Upon cooling of the reaction mixture solid precipitated was filtered and washed with toluene or diethyl ether to afford product as a yellowish solid (75%).

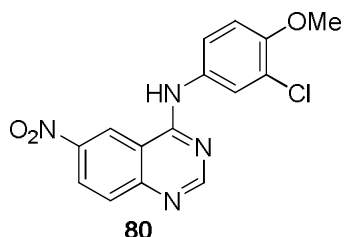
Method B: Solution of N'-(2-cyanophenyl)-N,N-dimethylformamide in DMF (2.82 M, 1 mL) was added to 3-chloro-4-methoxy aniline (1.0 eq) in 5 mL acetic acid and the mixture refluxed for 16 hours. Cooled reaction mixture was poured in water and extracted with ethyl acetate. Organic layers were dried, filtered and the solvent evaporated. Solid residue was purified by column chromatography to afford title compound (65%).

N'-(5-nitro-2-cyanophenyl)-N,N-dimethylformamide (79):



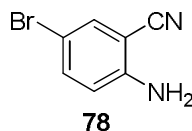
5-nitro-2-amino-benzonitrile and dimethylformamide dimethyl acetal (DMF-DMA, 2 mL, 1.5 eq) in toluene (4 mL) was heated under reflux for 6 hours, disappearance of the product was monitored by TLC; the methanol by-product was removed by distillation during the reaction. After cooling the mixture to room temperature a 2:3 mixture of hexane/ethyl ether was added and the mixture was stirred for 30 minutes. The precipitate was then collected by filtration and washed with hexane/diethyl ether, then recrystallized from toluene to give the pure compound as orange crystals (81% yield).

6-nitro-4-(3'-chloro-4'-methoxyanilino)-quinazoline (76):



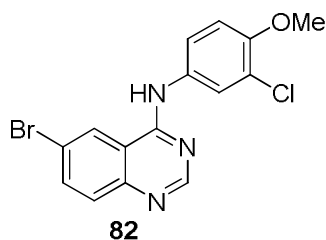
N[']-(5-nitro-2-cyanophenyl)-N,N-dimethylformamidine (10 mmol) and 3-chloro-4-methoxy aniline (1 eq) were suspended in 5 mL acetic acid and the mixture refluxed for 8-12 hours. Upon cooling of the reaction mixture solid precipitated was filtered and washed with toluene or diethyl ether to afford product as a yellowish solid.

5-bromo-2-amino-benzonitrile (78):



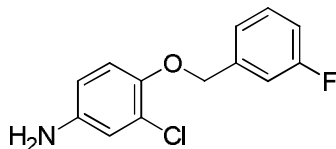
2-amino-benzonitrile (150 mmol) was dissolved in DMF (100 mL). A solution of N-bromo-succinimide (NBS, 150 mmol) in DMF (60 mL) was slowly added under vigorous stirring. Reaction mixture was protected against light and left under stirring at 35 °C overnight. Solvent removal afforded a reddish residue that was partitioned between water and diethyl ether, and aqueous phase was extracted twice with ether. Combined extracts were dried, filtered and evaporated to dryness. The solid obtained was dissolved in hot ethanol, treated with active charcoal and filtered over celite pad. The filtrate was cooled to 0 °C and the precipitate filtered, washed with ethanol and dried to afford title compound as colorless to slightly brown crystals.

6-bromo-4-(3'-chloro-4'-methoxyanilino)-quinazoline (82):



N¹-(5-bromo-2-cyanophenyl)-N,N-dimethylformamide (10 mmol) and 3-chloro-4-methoxy aniline (1 eq) were suspended in 5 mL acetic acid and the mixture refluxed for 8-12 hours. Upon cooling of the reaction mixture solid precipitated was filtered and washed with toluene or diethyl ether to afford product as a reddish solid.

3-chloro-4-oxy-(3-fluoro-benzil) aniline:



2-chloro-4-nitro-phenol (10 mmol) and 3-fluoro-benzilbromide (10 mmol) were dissolved in DMF (50 mL), potassium carbonate (2.5 eq) was added, and mixture was refluxed overnight. Hot mixture was filtered over celite and filtrate cooled, and solvent evaporated. Solid residue was dissolved in ethanol (100 ml), acetic acid (50 mL) and powdered iron (2 g) were added. Mixture was stirred at 80 °C for 5 hours, then cooled, and a 1:1 mixture of water/ethyl acetate was added. Aqueous layer was extracted three times with ethyl acetate, extracts reunited, dried, filtered and evaporated. Solid residue was chromatographed to afford title compound as yellowish/brownish solid in 54% yield.

References

- ¹ J. P. Michael, *Nat. Prod. Rep.*, **2005**, 22, 627.
- ² G. M. Higa, *Expert Rev Anticancer Ther.*, **2007**, 7, 1183-92.
- ³ Li Z, Xu M, Xing S, Ho W, Ishii T, Li Q, Fu X, Zhao Z, *J Biol Chem*, 2007, 282, 3428–32.
- ⁴ W. Pao, V. Miller, M. Zakowski, *Proceedings of the National Academy of Sciences of the United States of America*, **2004**, 101, 13306–11.
- ⁵ MPC-6827, a Small Molecule Inhibitor of Microtubule Formation with High Brain Penetration: Absorption, Distribution, Metabolism, Excretion, and Clinical Considerations. *96th Annual Meeting of the American Association for Cancer Research (AACR)*, **2005** in Anaheim, California.
- ⁶ D. Lednicer, *Strategies For Organic Drug Synthesis And Design*, **2009**, John Wiley & Sons, Inc.
- ⁷ C. L. Yoo, J. C. Fettingner, M. J. Kurth, *J. Org. Chem.* **2005**, 70, 6941.
- ⁸ F. Li, Y. Feng, Q. Meng, W. Li, Z. Li, Q. Wang and F. Tao, *Arkivoc*, **2007**, 40-50.
- ⁹ V. Chandregowda, G. V. Rao, and G. C. Reddy, *Org. Proc. Res. Dev.*, **2007**, 813–816.
- ¹⁰ A. Foucourt, C. Dubouilh-Benard, E. Chossona, C. Corbière, C. Buquet, M. Iannelli, B. Leblond, F. Marsais, T. Besson, *Tetrahedron*, **2010**, 4495-4502



Part III

**CONTINUOUS FLOW FUNCTIONALISATION OF
MOLECULAR NANOSTRUCTURES**

Chapter 8: Continuous-Flow Synthesis of a Methanofullerene Derivative

8.1 Introduction to Carbon Allotropes: Fullerene

For many decades, elemental carbon has kindled a low interest for chemists. Charcoal, the main amorphous form under which carbon could be found, played a major role during all human history and in particular in the industrial age as primary combustible, but it had only a few other uses other than as energetic source. For the synthetic chemist elemental carbon was a quite useless material: contrary to other elements, carbon can't be combined directly in chemical reactions to give useful compounds. The two other carbon allotropic forms more common in nature, graphite and diamond, have been long known and used for various technological applications, for example cutting tools, coatings, conductive materials and optical applications, but were similarly been of low interest for chemical synthesis purposes.¹ The situation has changed abruptly as in the recent past, new carbon allotropes have emerged, that possesses totally new properties and intriguing chemical features and hence offer wide possibilities for chemists to challenge their abilities.

The first of the new carbon allotropes, fullerene, was discovered in 1985. Differently to diamond and graphite which are extended-network solids, fullerene presents a definite molecular structure, made in the most common form of 60 carbon atoms disposed in interconnected hexagons and pentagons: the shape of the molecule closely resembles the classic soccer-ball. Chemical properties of fullerene are completely different from, for example, graphite: molecules can be solubilised in various solvents and undergo many chemical reactions. In the last years, a wide chemistry have been constructed on C₆₀ fullerene and its higher homologues (mainly C₇₀ and C₈₄) giving rise to many new compounds with high technological interest in many applications.

8.1.1 Historical Background

Theoretical existence of the ball shaped carbon cage was already predicted in the late 1960s; however, the first experimental evidences came in 1985 when Kroto and Smalley

identified C_{60} by mass-spectrometry on the plasma generated by laser ablation of graphite. For such discovery they were also awarded of the Nobel Prize together with Curl in 1996.² The first production of fullerene in macroscopic amounts was instead achieved by Kratschmer and Huffman in 1990 through graphite vaporization in an inert atmosphere. Since then the technology connected to fullerene production and purification has constantly improved, allowing scientists to gain access to large amount of material to study its structure, physical and chemical properties.

The name of fullerenes derived by the well-known architect Buckminster Fuller, inventor of the geodesic dome, because of the characteristic form of geodesic spheroid of fullerene molecules. The fullerenes family is thus usually referred to as buckminsterfullerenes or also buckyballs.

8.1.2 Fullerene Structure, Properties and Uses

Each fullerene contains $2(10 + M)$ carbon atoms corresponding to exactly 12 pentagons and M hexagons. C_{20} is the smallest theoretically allowed fullerene, whereas the smallest stable compound is soccer-ball shaped C_{60} (Fig.8.1).

Energetic considerations force some basic requirements for structure stability: the Isolated Pentagon Rule (IPR) suggests that the more thermodynamically stable structure is the one with all pentagons surrounded by

hexagons; bonds at the junctions of two hexagons (6-6 bonds) are shorter than the bonds at the junctions of a hexagon and a pentagon (5-6 bonds) and 6-6 bonds length is close to a carbon-carbon double bond, whereas 5-6 bonds resembles single bonds. This structure is the lowest in energy and implies that no double bonds are enclosed in the pentagonal rings. In order to account for molecular sphericity and bond distribution, an intermediate hybridization of carbon atoms between sp^3 and sp^2 must be considered, which results in high tensional strain of the molecule and partial overlap of p orbitals. As a result, fullerenes possess only partial aromatic character, whereas strain release drives molecular reactivity.

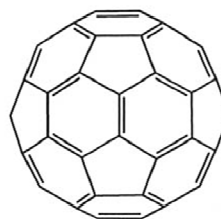


Figure 8.1: molecular model of C_{60} .

Fullerene possesses a high electronegativity, as it readily and reversibly accepts up to six electrons. Diversely from graphite it is an electrical insulator due to high band gap values, but can be turned to conductor or even superconductor by doping. Fullerene is sparingly soluble in most common organic solvents, as halogenated solvents or alkanes, whereas it exhibits appreciable good solubility in aromatic solvents such as benzene (1.7 mg/ml), toluene (2.8 mg/ml) and chlorinated derivatives as chlorobenzene (7.0 mg/ml) and dichlorobenzene (27 mg/ml).

Chemical reactivity of fullerene is largely driven by release of strain energy associated to bond pyramidalization, hence reaction at 6-6 double bonds are thermodynamically favoured and molecular reactivity strictly resembles an electron-deficient polyolefin. Main synthetic transformations include reduction/oxidation, hydrogenation, addition of radicals, carbenes and nucleophiles, cycloadditions, halogenations and interaction with alkali and transition metals. As potentially all double bonds are equally reactive, fullerene functionalization almost always results in formation of poly-addition products, thus reaction conditions must be carefully controlled. Functionalization of fullerene has been performed both exohedrally, meaning on the outside of the shell, or endohedrally, with foreign atoms located inside the fullerene cage.

Explored applications of fullerene in nanotechnology, superconductivity, heat resistance and optic limitation fields have been very wide. At the present time, however, major uses of fullerene and related compounds are essentially two: (i) photosensitizer for efficient generation of singlet oxygen and (ii) material for Organic Photovoltaic Devices (OPVs). The ability to generate the highly reactive singlet oxygen has been exploited both in chemical synthesis, as green oxidant, and in medicine, as antimicrobial and photodynamic therapy agent for tumors treatment. High electronegativity character makes fullerene an efficient electron-acceptor component for polymer based solar cells. In particular, efficient functionalization of pristine fullerene cage with proper organic pendants, in order to gain material processability while maintaining electronic properties, is today of great importance.³

8.2 Organic Photovoltaics

Photovoltaics is offering an important contribution to the quest of alternative energy sources that replace conventional fossil fuels through a variety of solar cell devices based on inorganic semiconductors.⁴ Since this technology, in its current stage of development, is not economically viable to allow a wide diffusion of solar energy conversion in the absence of government incentives, the last few years have seen huge efforts to introduce organic materials^{5,6} as an alternative to inorganic semiconductors. Organic Photovoltaic Devices (OPVs) offer indeed the prospects of low manufacturing costs (i.e., casting or printing technologies using solution-processable materials), large area coverage, and compatibility with flexible and light-weight substrates.^{7,8} In particular, the great potential of organic semiconductors is the tunability of their physical and chemical properties by rational sequential structure modification, which justify the tremendous increase in OPV power conversion efficiencies (PCEs), now surpassing 8%.⁹

8.2.1 OPV Functioning and Architecture

Organic solar cells belong to the class of photovoltaic cells known as excitonic solar cells. Photocurrent generation is due to formation, after excitation with light, of strongly bound electron–hole pairs (excitons).¹⁰ Excitonic states exist in these materials as a consequence of the low dielectric constants in the organic components, that differently from high dielectric inorganic counterparts do not allow direct electron–hole dissociation. Such dissociation occurs, in excitonic solar cells, almost exclusively at the interface between two materials of differing electron affinities: the electron donor (D) and the electron acceptor (A). Dissociated charges must then percolate through D/A materials network, minimizing recombination phenomena, till reaching electrodes. Thus, in order to generate an effective photocurrent in these organic solar cells, an appropriate donor–acceptor pair and device architecture must be selected.

Two main approaches have been explored in the effort to develop effective devices: the donor–acceptor bilayer,¹¹ commonly achieved by vacuum deposition of molecular components,¹² and the so-called bulk heterojunction (BHJ).^{13,14}

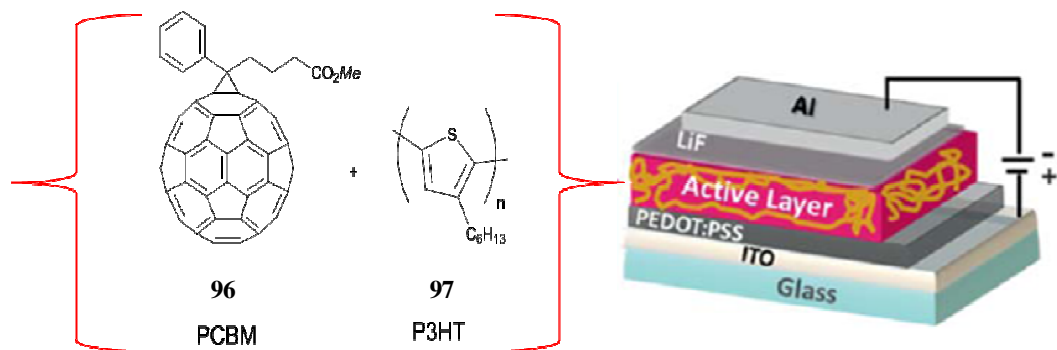


Figure 8.2: schematic of polymeric solar cell based on a classical BHJ architecture and its constituents.

The active layer of BHJ solar cells consists of an acting as an electron-donor, and an electron-accepting component. This latter is typically based on methanofullerene derivatives, commonly C_{60} or C_{70} PCBM¹⁵ ($[C_{60}]PCBM = 6,6\text{-phenyl-}C_{61}\text{-butyric acid methyl ester}$, colloquially named PCBM, compound **96**, Figure 8.2). The donor and acceptor phases should self-organize to form nanodomains with dimension comparable to the exciton diffusion length (10–20 nm) to ensure that all excitons are harvested at the interface. Once the exciton is dissociated, the electron and hole must drift separately to the electrodes through the bicontinuous pathways for an efficient charge collection. Nevertheless, creating an optimal BHJ is a delicate balancing act: having an homogeneous components blending limits the formation of separate polymer and fullerene networks, but, on the other hand, a phase segregation leads to the formation of unconnected islands that can act as carrier traps. Thus, one key to improving BHJ device performance is controlling the nanometer-scale morphology of the interpenetrating organic networks.¹⁶ Several groups have focused the attention on the control of nano-morphology of active BHJ layer based on P3HT (poly-(3-hexylthiophene) **97**) and PCBM. PCEs up to ~5% have been achieved by macroscopic device-processing conditions (i.e., thermal treatments, mixture of solvents, additives, and vapour annealing) which could promote the molecular re-organization by controlling the kinetics of segregation and crystallization of the components.¹⁷ An alternative way to induce an optimal self-assembling of the semiconducting components is the molecular approach. It is known that the morphology is largely affected by the chemical/structural nature of the donor and acceptor materials, in particular by their solubility and mutual affinity or intermolecular interaction, so the molecular design could play a crucial role in controlling the nanoscale self-organization as well as the intrinsic properties of the single material.¹⁸ For instance, replacing conventional fullerene electron

acceptors (PCBM) with other functionalized analogues has been reported to affect the processability, HOMO and LUMO energy levels, and self-assembly/phase segregation capability in active BHJ layer.¹⁹

8.2.2 The Active Fullerene Component

So far, PCBM (C_{61} or C_{71}) remain one of the best performing fullerene derivatives for organic photovoltaic, thanks to their large solubility in organic solvents that allow easy handling and optimum interaction with the polymeric material. However, a wide variety of new soluble fullerene derivatives have been synthesized and tested in P3HT-based BHJ solar cells, although only a few novel materials afford better OPV performance with respect to the reference P3HT:PCBM system.²⁰ Recent studies, focused on fullerene-based acceptors, demonstrate that fine structural modifications and changes in the correlated physical parameters, such as solubility, super-saturation thermodynamics, precipitation kinetics and miscibility with donor material, strongly affect the nano-morphology and the resulting OPV response.¹⁵

The prospects of BHJ cells as valid candidates for solar energy conversion would be further reinforced if a scalable and high throughput chemical synthesis of PCBM or of a similar fullerene-based active material would be available. The conventional flask synthesis of PCBM and related compounds generally involves generation and addition to [60]fullerene of 1-phenyl-1-(3-(methoxycarbonyl)propyl)diazomethane through the base-induced decomposition of the corresponding sodium salt of methyl-4-benzoylbutyrate tosylhydrazone at *ca.* 70 °C. This synthetic step is usually carried out *in-situ* by heating a suspension of tosylhydrazone and sodium methoxide in pyridine. Upon addition of diazocompound to fullerene, essentially one of the possible [5,6]-open fulleroids is formed and then converted into the thermodynamically more stable [6,6]-closed isomer by thermal processing.²¹ The use of the highly reactive diazoderivative seriously limits process scale-up, whereas process economy is seriously affected by the high energy input required for both thermal decomposition of tosylhydrazone salt and the later product isomerization, in particular when considering that final yields in PCBM usually does not exceed 35%. A continuous-flow process will effectively help in overcoming such inconveniences. To this end, we managed to develop a continuous flow approach using a micro-structured flow-reactor (MFR) setup. Given the small MFR channels dimensions, we considered that decomposition of tosylhydrazone salt may cause a few technical problems due to presence

of suspended solids. We thus resolved to use a rather different approach for diazoderivative generation, based on de-hydrogenation reaction of unsubstituted hydrazones promoted by metal oxide salts. Chemical incompatibility of the methyl ester moiety with such new reaction conditions forced us to choose a different fullerene derivative, very similar to the benchmark compound, PCBtB ([6,6]-phenyl-C61-butyric acid tert-butyl ester). PCBtB synthesis, first reported in 1995²², could in fact be easily transferred from batch-wise to continuous mode. The resulting continuous process would potentially be of importance not only for [60]fullerene, but also in view of the functionalization and screening of less abundant fullerenes (C₇₀, C₈₄) or endofullerenes (Sc3N@C₈₀, Lu3N@C₈₀).²³

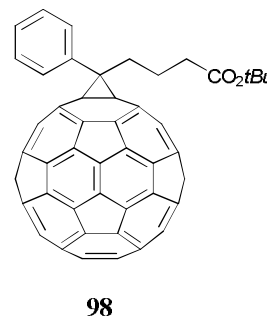
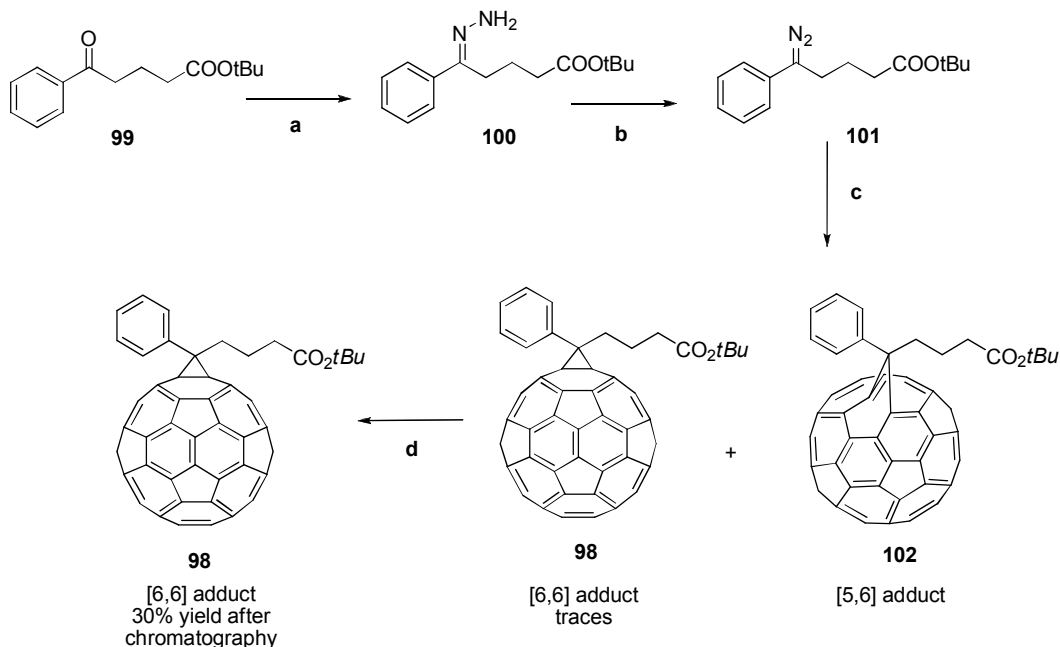


Figure 8.3: [6,6]-phenyl-C61-butyric acid tert-butyl ester, PCBtB.

After publication of our work (2011), Wong and co-workers reported an effective method for continuous flow production of PCBM²⁴: solubility problems were resolved by selecting 2,2,6,6-tetramethylpiperidine (TMP) as alternative to sodium methoxide, that results in an homogeneous reaction mixture. Using a meso-structured flow system based on Vapourtec R4 platform, improved yields in PCBM (59%) respect to batch procedure were obtained, together with high product throughput. This process is very interesting, even if still retains some problems in process economy: TMP reagent results to be more expensive respect to other bases, and extensive thermal treatment required for product isomerization is still high power-consuming, despite being far lower respect to discontinuous systems. For such reasons, a careful economic evaluation of the process should be made. We believe that our approach, that makes use of a renewable metallic reagent for diazocompound production, whereas isomerization step is carried out by photochemical way using a low-power LED source, results in a lower economical and environmental impact. Moreover, PCBtB based organic solar cells have proven to have power conversion efficiency comparable to the benchmark PCBM, without need for high temperature annealing of the device. Such step is in fact usually needed in order to critically improve efficiency of the classically assembled photovoltaic systems.

8.3 Results and Discussion

8.3.1 Flow Synthesis of PCBtB



Scheme 8.1: Synthesis of PCBtB: a) excess hydrazine hydrate, EtOH, reflux, 4h, 81%. b) NiO₂, Na₂SO₄, ODCB, 0° C, 15 min. c) C₆₀, ODCB, 6 min, rt, 37% (HPLC). d) photochemical isomerization, ODCB, rt, 30% isolated yield of **98** after chromatographic column.

Scheme 8.1 shows the sequence that has been used to carry out the synthesis of PCBtB in batch, whereas Figure 8.4 shows microfluidic reactor assembly. As previously stated, we used an alternative approach to diazoalkanes by using a metal oxide reagent for dehydrogenation of suitable hydrazone compounds. In particular, diazo compound **101** was produced through metal oxide promoted oxidation of tert-butyl-4-benzoylbutyrate hydrazone **100** at room temperature. In particular, we found out nickel peroxide (NiO₂) to be a far more efficient system for this step respect to classical manganese dioxide. This latter in fact should be used in large excess in order to assure complete conversion of the hydrazone to the corresponding diazo derivative. Addition of sodium sulfate in order to remove water formed during reaction was needed, whereas long reaction times resulted in the need for cooling reaction mixture, in order to avoid diazo product decomposition.

Nickel peroxide instead can be used in stoichiometric amounts, and reaction temperature kept at 25 °C without significant loss in product. NiO₂ can be efficiently loaded into cartridges for serial processing in flow and the exhausted material, after the oxidation, can be renewed with 6% sodium hypochlorite solution.²⁵ In this way, it can be repeatedly

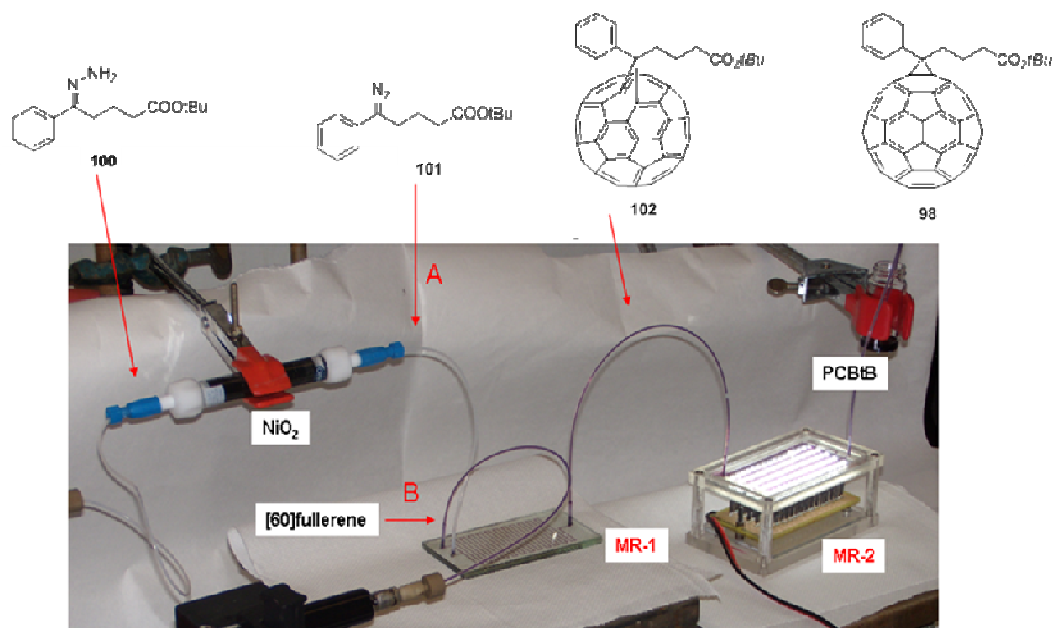


Figure 8.4: microfluidic assembly for the synthesis of PCtB.

employed with a definite economic and environmental advantage. In turn, compound **100** was prepared, under batch-reactor conditions, from tert-butyl-4-benzoylbutyrate and hydrazine hydrate in 81% yield. It should be recognized that the choice of tert-butyl substituent, and thus the departure from PCBM, has been dictated by the well-known reactivity of n-alkyl esters towards hydrazine. The same is in the case of methyl-4-benzoylbutyrate which is the substrate for PCBM synthesis. On the other hand, the bulky tert-butyl ester does not react with hydrazine, yielding eventually PCtB. Hydrazone **100** was used for the next oxidation step, after evaporation of the solvent, without further purification. Oxidation of a solution of **100** in *ortho*-dichlorobenzene (ODCB), performed at room temperature into a flow tube packed with NiO₂, gave diazoester **101**. Reaction progress was monitored off-line by FT-IR spectroscopy, following disappearance of characteristic hydrazone band (3400 cm⁻¹), due to N-H stretching, and increasing in the diazo signals (2030–2080 cm⁻¹, N-N stretching).

The solution of **101** was introduced through inlet A into the MR-1 whereas a solution of [60]fullerene in ODCB was added through inlet B (Figure 8.3). 1,3-Dipolar cycloaddition of **101** to [60]fullerene (molar ratio [**101**]/[C₆₀] = 1.2) gave fulleroid **102** in 37% yield (assessed by HPLC) in only 6 minutes at room temperature, along with unreacted [60]fullerene and traces of polyaddition by-products. The yield of **102** could be increased up to 53% working with an excess of diazoester **101** ([**101**]/[C₆₀] = 4.9). However, the

amount of fullerene polyadducts rises up to 6% as well, resulting in loss of valuable starting material that could be eventually recovered during purification step. The fulleroid-to-methanofullerene **98** conversion was carried out into the photochemical MR-2 connected in series through the outlet of MR-1 (Figure 8.5). As previously demonstrated in Chapter 2, MFRs represent an interesting alternative to conventional photoreactors because the small size of fluidic channels leads to higher spatial illumination homogeneity and better light penetration through the entire reactor depth. As a result, the **101** to **98** conversion proceeded smoothly under white light emitting diodes (LEDs) as a cold, low-power illumination source. Both MR-1 and MR-2 were hybrid glass-polymer devices assembled in our lab by mean of photolithographic techniques, as previously reviewed. Reactor geometries were thus optimized for the specific synthetic task. In particular, MR-1 was equipped with a T junction for combining the two feed streams and a serpentine micro-structured channel to promote efficient continuous mixing of the solution. Gas evolution (nitrogen) was noticed during operation, but due to limited extent do not resulted in over-pressurization problems. MR-2 was instead equipped with sequential high width chambers in order to promote better illumination power distribution.

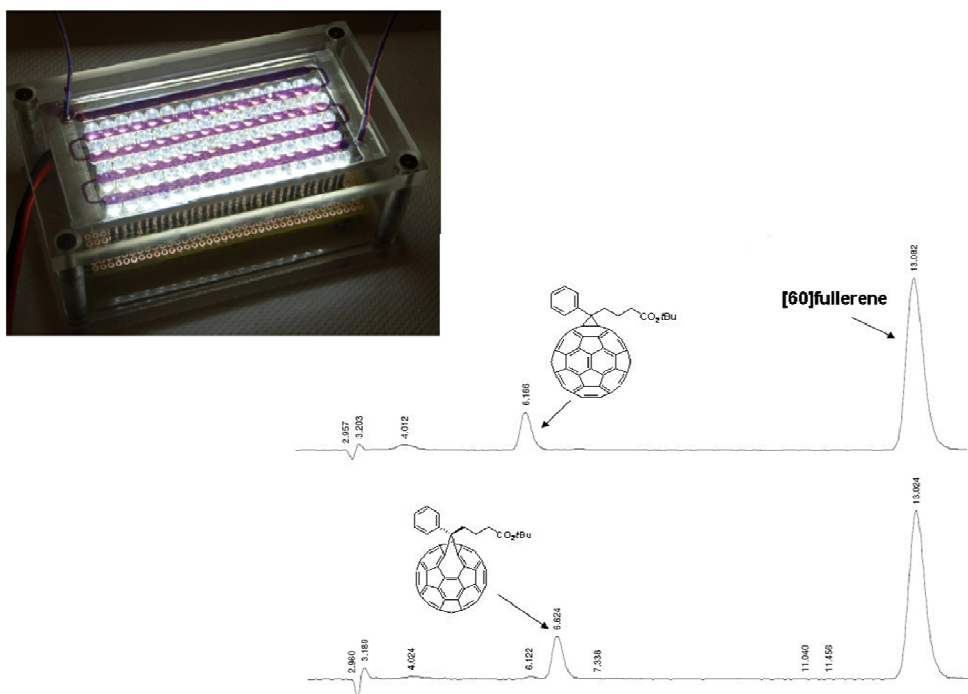


Figure 8.5: photochemical MR-2 for isomerization of (5-6)/(6-6) PCBtB crude mixture and HPLC traces of reaction mixture at reactor outlet and inlet.

With a total flow rate of 1.5 ml h^{-1} the productivity was about 6 mg of crude mixture per hour. However, achieving high productivity was not the scope of this investigation. Higher productivities could be obtained through the optimization of the operating conditions, MFR design or by the addition of more identical MFRs in parallel.²⁶

8.3.2 PCBtB as Component of BHJ Solar Cells

8.3.2.1 Solar Cells Assembly and Characterization

The potential of PCBtB as acceptor material in OPV devices was investigated in bulk-heterojunction (BHJ) solar cells using P3HT as the electron donor (D) counterpart. Solar cells assembly and characterization work was carried out in collaboration with the CNR-ISMN unit of Dott. Michele Muccini (Bologna, Italy). For comparison, BHJ solar cells based on P3HT and commercial PCBM were also fabricated. The device structure employed was a classical BHJ architecture made of glass/ITO/PEDOT:PSS/P3HT:Acceptor/LiF/Al. Details of the device fabrication and characterization are given in the Experimental Section. Summarized photovoltaic response data including VOC (Open Circuit Voltage), JSC (Short Circuit Current Density), FF (Filling Factor) and PCEs (Power Conversion Efficiency) are reported in Table 88.1. Representative OPV current density–voltage (J–V) plots under standard illumination AM1.5G are shown in Figure 8.6.

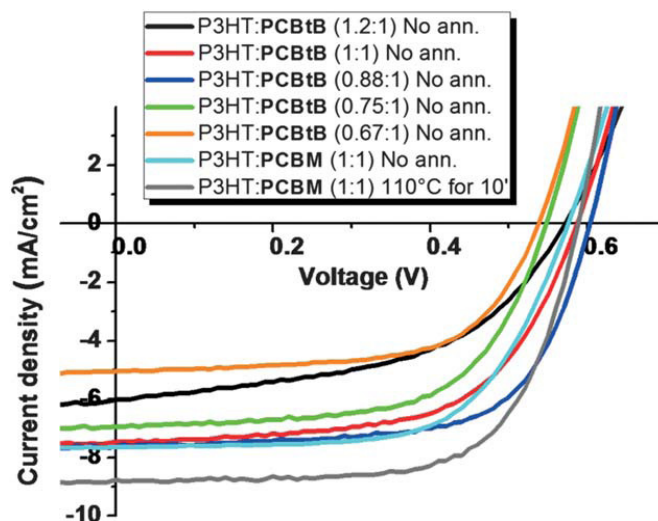


Figure 8.6: J–V plots, under illumination, of optimized P3HT:PCBtB as a function of D:A (w/w) composition, and 1 : 1 (w/w) P3HT:PCBM-based BHJ solar cells.

As shown in Figure 8.6 and Table 8.1 the main difference between OPV devices based on P3HT:PCBtB and P3HT:PCBM films is represented by the short-circuit current density values, which reflects the gap in the overall PCEs.

For reference, in the PCBM-based devices, the JSC ranges from 7.70 to 8.85 mA cm⁻² with a maximum PCE of 3.48% obtained for a D/A w/w ratio of 1:1 and upon thermal annealing: such procedure in fact frequently improves the efficiency of P3HT-based BHJ solar cells. Using the same blend ratio, the as-cast P3HT:PCBtB-based device exhibits VOC, JSC, FF and PCE of 586 mV, 7.47 mA cm⁻², 61% and 2.66%, respectively.

The OPV performance of P3HT:PCBtB-based solar cells resulted to be strongly dependent on the blend composition as substantial improvements were obtained upon increasing the relative PCBtB amount in thin films, with the best value obtained for the device based on 0.88:1 (w/w) blend ratio. The resulting as-cast solar cell gives a PCE of 3.03% with VOC, JSC, and FF of 603 mV, 7.64 mA cm⁻² and 66%, respectively. Noteworthy, these values

Table 8.1: Bulk-heterojunction photovoltaic parameters of representative P3HT:PCBtB (or PCBM) based solar cells.

Active layer D:A ratio (w/w)	Total conc./ mg mL ⁻¹	Tann/ °C ^a	VOC/ mV	JSC/ mA cm ⁻²	FF (%)	PCE (%)
P3HT:PCBtB (1.2 : 1) ^b	37.0	—	572	5.98	50	1.73
P3HT:PCBtB (1.2 : 1) ^b	37.0	110	432	2.89	48	0.60
P3HT:PCBtB (1 : 1) ^c	34.0	—	586	7.47	61	2.66
P3HT:PCBtB (1 : 1) ^c	34.0	110	479	5.44	55	1.43
P3HT:PCBtB (0.88 : 1) ^d	32.0	—	603	7.64	66	3.03
P3HT:PCBtB (0.88 : 1) ^d	32.0	110	441	4.19	51	1.00
P3HT:PCBtB (0.75 : 1) ^e	29.8	—	547	6.94	62	2.35
P3HT:PCBtB (0.75 : 1) ^e	29.8	110	361	5.60	50	1.00
P3HT:PCBtB (0.67 : 1) ^f	28.4	—	538	5.03	63	1.71
P3HT:PCBtB (0.67 : 1) ^f	28.4	110	476	4.31	41	0.84
P3HT:PCBM (1 : 1) ^g	36.0	—	575	7.70	63	2.80
P3HT:PCBM (1 : 1) ^g	36.0	110	588	8.85	67	3.48

a: Annealing time: 10 min; b: d = 205 nm; c: d = 165 nm; d: d = 160 nm; e: d = 120 nm; f: d = 95 nm; g: d = 200 nm.

are greater than those obtained for as-cast optimized PCBM-based devices, highlighting the potential of PCBTB as new acceptor material able to induce a good nano-morphology of the active layer during the deposition–drying process. Moreover, nice charge transport properties in the organic network are confirmed by good FF values (Table 8.1) and charge mobility values, without the need of additional thermal treatments.

Further increase in PCBTB content in the active blend (0.75:1, and 0.67:1 w/w ratio), as well as increase in the donor content (1.2:1 w/w) resulted in poorer device performances. Observed discrepancy in open-circuit voltage values for PCBM and PCBTB based blends at different D:A compositions can be ascribed to different morphological features which is known to influence the VOC.²⁷

Several efforts to optimize the thin-film nano-morphology of PCBTB-based devices were carried out, but no significant improvements were achieved. Different solvents (e.g., chlorobenzene and toluene) were used to spin-cast the blends, but poor quality films were obtained as a consequence of the low PCBTB solubility. The most continuous and most electrically uniform films were obtained from ODCB solutions, resulting in the best OPV performance.

Thermal annealing treatment of PCBTB devices was attempted in order to improve device performances: annealing over the range 80–150 °C, for different times, before and after device completion, invariably resulted in unusual film degradation, limiting VOC (<500 mV), FF, and, consequently, the overall device performance. It is well-known that annealing increases the crystallinity of P3HT, but the effects on the fullerene network are less clear.²⁸ Probably, the thermal treatments could promote undesirable phase segregation on the PCBTB network which adversely affects the VOC and FF values. Degradation of PCBTB during the annealing process at 110 °C has been ruled out on the basis of thermogravimetric analysis (TGA, Figure 8.7) that shows a first weight loss above 200 °C. It is reasonable to assume that at the annealing temperature only morphological rearrangements take place, as discussed below.

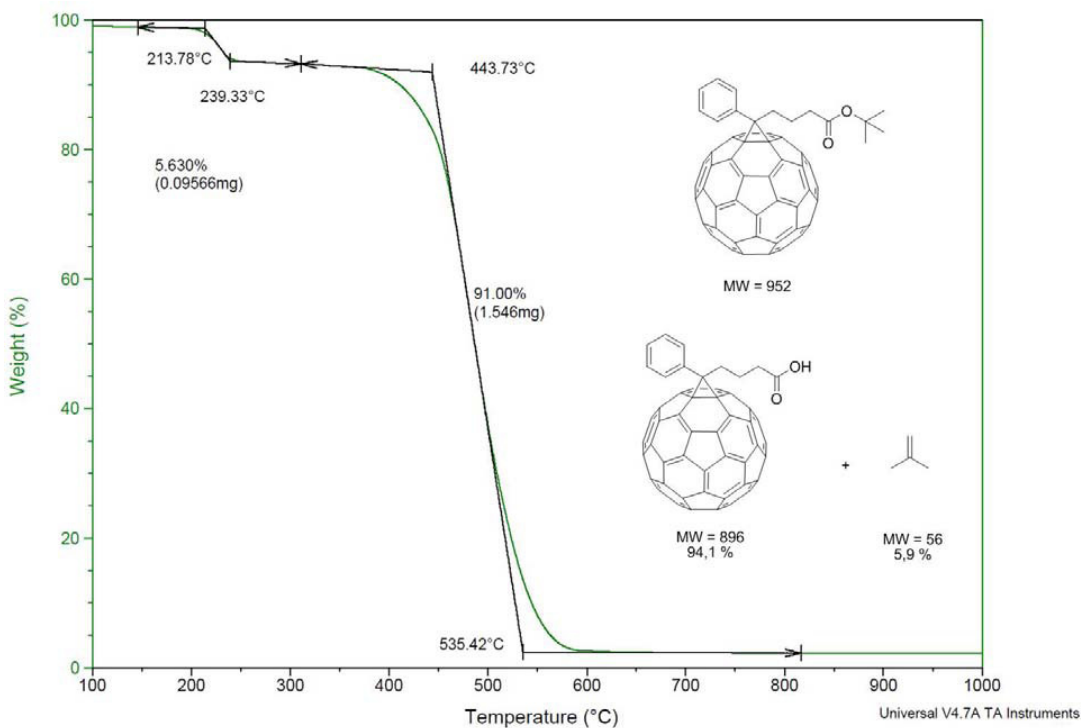


Figure 8.7: TGA analysis of PCBtB. From the TGA data it is proposed that the first transition that starts at ca 214 C is due to the loss of isobutylene.

8.3.2.2 Morphology

Thin film spectroscopy measurement of pristine PCBM and PCBtB confirmed that no relevant differences in electronic properties are present. Measurements on mixed polymer/fullerene films as well resulted in P3HT:PCBtB-based films not showing significant changes in the optical absorption properties compared to P3HT:PCBM films. Therefore, PCBtB plays a crucial role at the molecular level affecting other parameters such as nano-scale self-organization and charge carrier transport.

Morphological differences of P3HT:PCBtB (or PCBM) blend films were investigated by tapping-mode AFM and near-infrared photoluminescence (NIR-PL) spectroscopy. As might be noticed, the scale of film segregation depends on the P3HT:PCBtB w/w blend ratio: high concentration of P3HT (1.2:1 w/w ratio, Figure 8.8A) generates larger domains which are gradually reduced in terms of size by decreasing the D:A composition to 1:1, 0.88:1 and 0.67:1 w/w ratio (Figures 8.8B, C and D, respectively). A similar trend was observed for the surface roughness, with a substantial decrease going from high to low P3HT contents. This effect might be attributed to the progressive intercalation between the components producing smoother nano-structured films. Correlation of determined OPVs electronic characteristics to film morphology is straightforward: for high donor contents,

large crystallinity of the polymer together with high roughness results in the drastic reduction in electron mobility and increase in charge recombination and trapping. On the contrary, at very low donor contents, a smooth and featureless surface results due to poor polymer crystallinity. In the optimized 1:1 and 0.88:1 w/w blend ratios (Figures 8.78 and C, respectively), the size of the domains is slightly reduced, resulting in smoother and more textured surfaces (RMS ~ 16 and 13 nm, Figures 8.8B and C, respectively) with a higher interfacial area between the grains, as supposed by AFM images and confirmed by NIR-PL spectroscopy. Moreover, the relatively high and balanced hole and electron mobilities measured on these films suggest the formation of bicontinuous and well-organized percolation paths in the entire photoactive layer, confirming the good thin film quality at these D:A compositions, in agreement with the higher OPV responses. The obtained electron mobilities are nearly identical to the optimal values calculated for the analogous optimized PCBM based blend, highlighting the capability of the PCbTb to induce morphological changes on the donor material network, maintaining optimal charge transport, electrical and morphological properties.

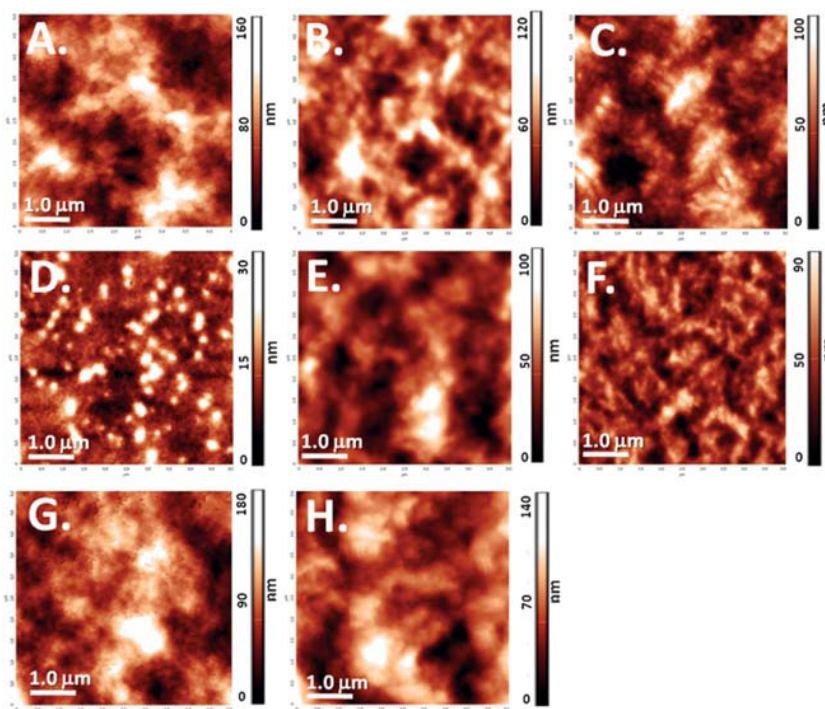


Figure 8.8: AFM images (size: 5 mm x 5 mm) of P3HT:PCBtB (or PCBM) devices, in the D:A (w/w) ratio giving the best device performances: (A) P3HT:PCBtB 1.2 : 1 (not annealed, RMS 27 nm); (B) P3HT:PCBtB 1 : 1 (not annealed, RMS 16 nm); (C) P3HT:PCBtB 0.88 : 1 (not annealed, RMS 13 nm); (D) P3HT:PCBtB 0.67 : 1 (not annealed, RMS 4 nm); (E) P3HT:PCBtB 1 : 1 (annealed at 110 °C for 10 min, RMS 18 nm); (F) P3HT:PCBtB 0.88 : 1 (annealed at 110 °C for 10 min, RMS 16 nm); (G) P3HT:PCBM 1 : 1 (not annealed, RMS 19 nm); (H) P3HT:PCBM 1 : 1 (annealed at 110 °C for 10 min, RMS 22 nm).

Thermal annealing, at 110 °C for 10 minutes, of 1:1 and 0.88:1 w/w P3HT:PCBtB films (Figure 8.8E and F, respectively), results in roughening of the film surface with more structured and confined motifs compared to the analogous as-cast films (Figures 8.8B and C). This is due to the enhanced aggregation tendency of the P3HT, which determines the formation of more defined domains with dimensions strictly dependent on the P3HT content. Nevertheless, the molecular reorganization, induced by thermal annealing, seems to generate unconnected oval or fiber-like domains, or islands (Figures 8.8E and F, respectively) that might suggest a lower D:A phase segregation, which could hinder the formation of continuous percolation pathways, limiting the charge transport processes and FF values of the active blend. This hypothesis correlates well with the drastic reduction of the resulting OPV responses.

Comparison with both as-cast and annealed P3HT:PCBM-based blend highlights that for these latter the average domain size increases up to hundreds of nanometres (Figures 8.8G and H; RMS ~ 19 and 22 nm, respectively), while smaller and more textured domains were obtained in PCBtB-based blends (Figures 8.8B and E; RMS ~ 16 and 18 nm, respectively).²⁹

8.4 Conclusions

The first continuous flow synthesis of the methanofullerene compound PCBtB was developed. A multi-step approach was developed for continuous flow generation of a reactive diazo intermediate using a supported renewable reagent, followed by direct addition to fullerene and isomerization of the crude mixture carried out by photochemical way using a low power consumption LED based light source. Such process allowed for a productivity of 6 mg of crude mixture per hour at a total flow rate of 1.5 ml h⁻¹. Upon optimization of the operating conditions, in order to improve throughput, such process will have high beneficial impact on mass production of this active fullerene compound in view of a future wide marketing of OPV devices technology.

Solution-processable BHJ OPV solar cells using PCBtB as acceptor and P3HT as donor material were fabricated, optimized, characterized and compared against P3HT:PCBM. We find that the simple design strategy of PCBtB, in particular the presence of the tert-butyl substituent, does not affect the electronic structure of the molecule, while influences the solubility and the molecular hindrance, which produce evident changes in terms of domain

size and phase segregation between the heterojunction components. Investigation of charge carrier mobility demonstrates that pristine or blended as-cast PCBTB-based devices exhibit great electron and hole mobilities, nearly identical to the reference PCBM-based film. As-cast P3HT:PCBTB-based solar cells afford PCEs of 3.1%, which are greater than the analogous as-cast P3HT:PCBM based devices. This study indicates the potential of PCBTB as a novel solution for use in combination with new donor polymers, e.g., having higher aggregation tendency. Furthermore, it could be useful to optimize the phase segregation and the interpenetrating networks by reducing the domain size and/or disrupting possible large aggregates or clusters, without the need of ‘‘processing additives’’ or additional treatments.

8.5 Experimental

[60]Fullerene, (99.5% from Bucky, USA), PEDOT:PSS (poly(3,4-ethylenedioxythiophene):poly(4-styrenesulfonate), Clevios P VP A1 4083, H.C. Starck), P3HT (poly(3-hexylthiophene), Rieke Metals), PCBM ([6,6]-phenyl-C61-butyric acid methyl ester, American Dye Source) and various anhydrous solvents (Sigma-Aldrich) were purchased from commercial sources and used without further purification. All other reagents were used as purchased from Sigma-Aldrich. All the solvents were distilled prior to use according to literature procedures. tert-Butyl-4-benzoylbutyrate **2** was prepared as previously reported.²²

8.5.1 Characterization of Compounds

¹H (250.1 MHz) and ¹³C (62.9 MHz) NMR spectra were recorded on a Bruker AC-F 250 spectrometer. IR spectra were recorded on a Nicolet 5700 spectrophotometer. Viscous compounds were analysed within KBr windows; powders were measured making KBr pellets. HPLC analyses of fullerene derivatives were carried out on a Shimadzu LC-10AT instrument, equipped with a Shimadzu SPD-10A detector at 340 nm, using a Cosmosil Buckyprep (Nacalai Tesque, 4.6 x 250 mm, eluent: toluene/n-hexane 7:3, 1 mL min⁻¹). Semipreparative separations were carried out on the same HPLC station with a SiO₂ Phenomenex Luna column(250 x 10 mm, 5 mm, eluent: toluene/n-hexane 8:2, flow rate: 2 mL min⁻¹). ESI-MS spectra were recorded on a LC-MSD-Trap-SL (Agilent Technologies, Palo Alto, USA). Samples were dissolved in methanol (~10⁻⁵ M) and injected in a stream

of the same solvent at 50 mL min⁻¹ (nitrogen nebulizing gas pressure = 20 psi; flow = 5 l min⁻¹; T = 325° C). APPI-MS spectrum of derivative **98** was recorded on the same instrument (nitrogen nebulizing gas pressure = 30 psi; flow = 4 l min⁻¹; T = 325° C; vaporizer T = 350° C). The sample, dissolved in cyclohexane (~10⁻⁵ M), was directly infused in the APPI source through a syringe pump (100 mL min⁻¹).

The redox behavior of PCBtB was studied by cyclic voltammetry, carried out in *ortho*-dichlorobenzene (ODCB)/acetonitrile (1:4) solution in the presence of Bu₄NPF₆ as supporting electrolyte on a glassy carbon electrode.

8.5.2 Synthesis of PCBtB (**88**) in Flow

The light source for the photochemical microreactor (MR-2) was an array of 75 commercial white LED (45 V, 30 mA). Two flow streams driven by syringe pumps (NE-300, New Era Pump Systems Inc.) bearing separate 5 mL syringes (GasTight, Hamilton); stream 1 containing a solution of [60]fullerene (23.3 mM) in *ortho*-dichlorobenzene (ODCB) and stream 2 containing the diazoester **101** in ODCB (57.5 mM). On the basis of previous oxidation experiments, it is assumed a quantitative conversion of hydrazone **100** into diazoester **101** after passing a solution of **100** in ODCB through a flow tube (Omnifit, 10 mm x 10 mm) packed with excess NiO₂ at room temperature. In particular, the tube was packed with 1.5 g of technical-grade NiO₂ and 3.0 g of glass microspheres that were used as filling material. The yield reported in the text for PCBtB **98** refers to a [60]fullerene flow rate equal to 1.0 mL h⁻¹ and diazoester **101** flow rate = 0.5 mL h⁻¹.

8.5.3 Device Fabrication and Measurements

The photovoltaic cells consisted of a polymer blend P3HT with PCBtB (or PCBM) thin film, sandwiched in-between a transparent anode (Indium Tin-Oxide, ITO, R_s 10 U/M) and a metal cathode (LiF/Al). Before device fabrication, the glass substrates coated with ITO were accurately cleaned, dried with N₂ stream from a blow gun and placed in an oxygen plasma chamber for 10 min. A thin layer (~30 nm) of PEDOT:PSS was then spin-coated on the anode to modify the ITO surface, followed by baking at 150° C for 15 min. The P3HT:PCBtB (constant concentration of PCBtB: 17 mg mL⁻¹) and P3HT:PCBM (18:18 mg mL⁻¹) solutions were prepared in dry ODCB, which is a good solvent also for PCBtB. Note that the concentration of PCBtB was kept constant at the optimal value of 17 mg mL⁻¹ (in ODCB), since higher concentrations determine inhomogeneities and/or visible aggregates during the deposition process. The D:A (w/w) ratios were controlled only by

varying the P3HT amount, thus obtaining mixture solutions with slightly different total concentrations. The mixture solutions were sonicated, and then spin-coated inside the glove box (<0.1 ppm of O₂ and H₂O), on top of the ITO/PEDOT:PSS surface. The wet active layers were then slowly dried in covered glass Petri dishes to undergo the solvent annealing process (or slow growth). Before cathode deposition, the thin films were thermally annealed by varying the temperature and the time of the process (Table 8.1). To complete the device fabrication, LiF/Al cathodes (~0.6 nm/~100 nm) were next deposited sequentially without breaking vacuum (~10⁻⁶ Torr) using a thermal evaporator directly connected to the glove box. The current–voltage (I–V) characteristics of completed OPV devices were recorded by a Keithley 236 source-measure unit under simulated AM1.5G illumination of 100 mW cm⁻² (Abet Technologies Sun 2000 Solar Simulator). The light intensity was determined by a standard silicon photodiode fitted with a KG5 color glass filter to bring spectral mismatch to unity. The active area of the device was exactly 6 mm². During testing, the individual devices were accurately isolated, by a calibrated mask, to avoid an excess photocurrent generated from the parasitic device regions outside the overlapped electrode area. All solar cells were tested, inside the glove box with oxygen and moisture free environment.

8.5.4 Thin-film characterization

All thin-film characterizations were performed in air. Thin film optical absorption spectra were recorded on a JASCO V-550 spectrophotometer. Luminescence spectra in the NIR range between 0.75 and 1.4 eV were measured by using a modified FT interferometer (Bruker RFT 100) equipped with a liquid nitrogen cooled Ge detector, the same set-up was used for measuring Raman scattering exciting at 1.16 eV (1064 nm) with cw Nd–Yag laser. Measurements were performed by exciting with 488 nm Ar⁺ laser lines. The thickness of the various films was measured by a profilometer (KLA Tencor, P-6). All active films were characterized on glass/ITO/PEDOT:PSS substrates and subsequently corrected for the background signal, in order to reproduce the effective condition and the real nanomorphology of the active layer. Atomic Force Microscopy (AFM) images were taken with a Solver Pro (NT-934 MDT) scanning probe microscope in tapping mode. The AFM images were recorded directly on the tested devices.

References

- ¹ H. O. Pierson, *Handbook of carbon, graphite, diamond, and fullerenes*, **1993**, Noyes Publications.
- ² H. W. Kroto, J. R. Heath, S. C. O'Brien, R. F. Curl, R. E. Smalley, *Nature*, **1985**, 318, 162.
- ³ A. Hirsch, *The Chemistry of the Fullerenes*, **2002**, Wiley-VCH.
- ⁴ <http://www.solarbuzz.com/Marketbuzz2010-intro.htm>, accessed July 27, 2010.
- ⁵ *Acc. Chem. Res.*, **2009**, 42, 1689, Special issue on: Organic Photovoltaics.
- ⁶ *J. Mater. Chem.*, **2009**, 19, 5276, Themed issue: Solar Cells
- ⁷ A. C. Arias, J. D. MacKenzie, I. McCulloch, J. Rivnay and A. Salleo, *Chem. Rev.*, **2010**, 110, 3–24
- ⁸ R. Tipnis, J. Bernkopf, S. Jia, J. Krieg, S. Li, M. Storch and D. Laird, *Sol. Energy Mater. Sol. Cells*, **2009**, 93, 442–446.
- ⁹ <http://www.osa-direct.com/osad-news/mitsubishi-chemical-announces-an-organic-photovoltaic-cell-with-85-conversion-efficiency.html>, March 7, 2011.
- ¹⁰ C. J. Brabec, V. Dyakonov, J. Parisi, N. S. Sariciftci, *Organic Photovoltaics*, **2003**, Springer.
- ¹¹ R. Po, M. Maggini and N. Camaioni, *J. Phys. Chem. C*, **2010**, 114, 695–706.
- ¹² M. Muccini, R. Danieli, R. Zamboni, C. Taliani, H. Mohn, W. Muller and H. U. ter Meer, *Chem. Phys. Lett.*, **1995**, 245, 107–112.
- ¹³ H. Hoppe and N. S. Sariciftci, *J. Mater. Res.*, **2004**, 19, 1924–1945.
- ¹⁴ M. D. Perez, C. Borek, S. R. Forrest and M. E. Thompson, *J. Am. Chem. Soc.*, **2009**, 131, 9281–9286
- ¹⁵ P. A. Troshin, H. Hoppe, J. Renz, M. Egginger, J. Y. Mayorova, A. E. Goryachev, A. S. Peregudov, R. N. Lyubovskaya, G. Gobsch, N. S. Sariciftci and V. F. Razumov, *Adv. Funct. Mater.*, **2009**, 19, 779–788.
- ¹⁶ L.-M. Chen, Z. Hong, G. Li and Y. Yang, *Adv. Mater.*, **2009**, 21, 1434–1449.
- ¹⁷ G. Li, V. Shrotriya, J. Huang, Y. Yao, T. Moriarty, K. Emery and Y. Yang, *Nat. Mater.*, **2005**, 4, 864–868
- ¹⁸ M. Seri, A. Marrocchi, D. Bagnis, R. Ponce, A. Taticchi, T. J. Marks and A. Facchetti, *Adv. Mater.*, **2011**, 23, 3827–3831.
- ¹⁹ J. A. Mikroyannidis, A. N. Kabanakis, S. S. Sharma and G. D. Sharma, *Adv. Funct. Mater.*, **2011**, 21, 746–755.
- ²⁰ Y. He, H.-Y. Chen, J. Hou and Y. Li, *J. Am. Chem. Soc.*, **2010**, 132, 1377–1382.

-
- ²¹ J. C. Hummelen, B. W. Knight, F. Lepeq, F. Wudl, J. Yao and C. L. Wilkins, *J. Org. Chem.*, **1995**, 60, 532–538.
- ²² R. Gonzalez, J. C. Hummelen and F. Wudl, *J. Org. Chem.*, **1995**, 60, 2618–2620.
- ²³ R. B. Ross, C. M. Cardona, D. M. Guldi, S. G. Sankaranarayanan, M. O. Reese, N. Kopidakis, J. Peet, B. Walker, G. C. Bazan, E. Van Keuren, B. C. Holloway and M. Drees, *Nat. Mater.*, **2009**, 8, 208–212.
- ²⁴ Helga Seyler, Wallace W. H. Wong, David J. Jones, and Andrew B. Holmes, *J. Org. Chem.*, **2011**, 76, 3551–3556.
- ²⁵ K. Nakagawa, R. Konaka and T. Nakata, *J. Org. Chem.*, **1961**, 27, 1597.
- ²⁶ E. Rossi, T. Carofiglio, A. Venturi, A. Ndobe, M. Muccini and M. Maggini, *Energy Environ. Sci.*, **2011**, 4, 725–727.
- ²⁷ J. Liu, Y. Shi and Y. Yang, *Adv. Funct. Mater.*, **2001**, 11, 420–424.
- ²⁸ A. L. Ayzner, D. D. Wanger, C. J. Tassone, S. H. Tolbert and B. J. Schwartz, *J. Phys. Chem. C*, **2008**, 112, 18711–18716.
- ²⁹ M. Seri, E. Rossi, T. Carofiglio, S. Antonello, G. Ruani, M. Maggini and M. Muccini, *J. Mater. Chem.*, **2011**, 21, 18308–18316.



Chapter 9: Flow Processing of Carbon Nanotubes

9.1 Fundamentals of Carbon Nanotubes

Following the enthusiastic wave of interest for carbon allotropes that risen after the discovery of buckyballs fullerene family (see Chapter 8), a new breakthrough emerged soon. In 1991, Dr. S. Iijima at NEC Fundamental Research Laboratory of Japan showed high-resolution transmission electron microscope (HRTEM) images of a needle-like carbonaceous substance with an hollow core, that was identified in the insoluble residue of arc-discharge burned graphite rod. Such structures were 4-30 nm in diameter and up to 1 micron in length, and were thus denominated carbon nanotubes (CNTs) for their peculiar aspect.¹ Effectively, CNTs have been produced and observed much earlier, in particular by Oberlin, Endo, and Koyama in 1976,² and probably even before, and the paternity of the discovery is controversial still today; however, Iijima surely had the merit of bringing nanotubes in the awareness of the whole scientific community.³

9.1.1 Nanotubes Structure and Production

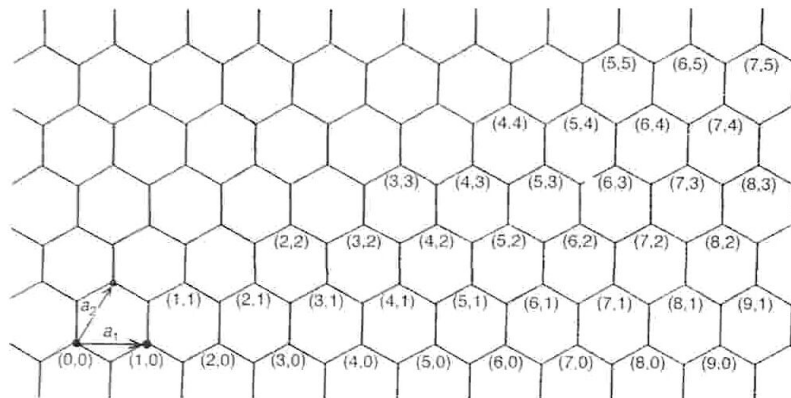


Figure 9.1: example of possible rolling modes for a 2D graphene sheet. Bracketed indexes represent (n,m) values associated to the CNT obtained by superimposition of the correspondently labelled carbon atom with atom (0,0).

Nanotubes can be imagined as hollow tubes made of 2D graphene sheets, that are layer of one-atom thickness, rolled up and eventually capped at the extremes with spherical fullerene-like structures. These sheets can be rolled in discrete modes, following specific

chiral angles, which denote the orientation of the nanotubes hexagons with respect to the nanotube axis.

The rolling vector is expressed as the sum of two vectorial components $m\vec{a}^1 + n\vec{a}^2$, where \vec{a}^1 and \vec{a}^2 are unit vectors in the two dimensional hexagonal lattice and m and n are integers. Figure 9.1 shows some of usual rolling vectors: when $m = 0$ or $n = 0$ chiral angle is zero and the resulting structure is defined as zig-zag. Instead, when m and n are equal chiral angle is 30° and nanotube possesses armchair structure; in other cases nanotube is said to be chiral. Examples of each structure type are reported in Figure 9.2. Noteworthy, at each structure correspond a definite tube diameter: the combination of rolling angle and radius concurs in determination of tube properties, as described below.

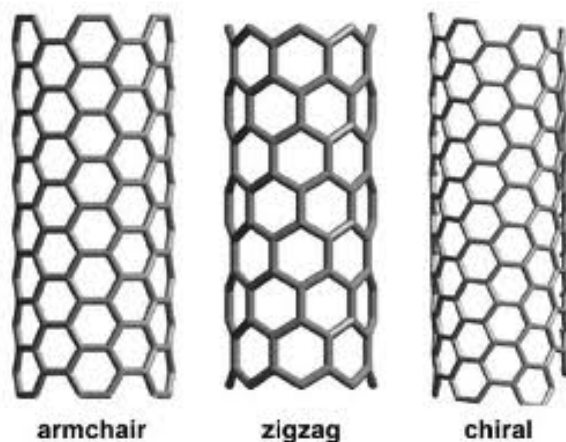


Figure 9.2: examples of SWCNTs rolling types.

CNTs are generally classified as single-walled (SWCNTs) and multi-walled (MWCNTs) carbon nanotubes, depending on the number of layers that made up tube wall. In particular, MWCNTs can be figured out to have a *Russian Doll* like structure.

Pristine nanotubes usually form superstructures as ropes or bundles by mean of intermolecular van der Waals interactions, in particular π -stacking. Such behavior is usually considered to be responsible in part for the lack of reactivity on CNTs towards chemical functionalization.

Production of carbon nanotubes may involve several methods. The most known is the classical electrical arc-discharge on graphite rods, that is also employed in fullerenes production: upon addition of transition metal catalysts the grown of tubular structures results to be enhanced respect to nucleation of spherical caged fullerene structures. Other methods involving graphite vaporization embodies plasma or laser ablation of graphite or other carbonaceous materials. Alternatively, Chemical Vapour Deposition (CVD) methods

have been employed, involving decomposition of hydrocarbons or organo-metallic compounds over transition metals catalysis. Controlling the heating method, substrate activation and other deposition parameters, permits a wide control of the nanotubes properties.⁴

9.1.2 Nanotubes Properties and Applications

The electronic and mechanic characteristics of CNTs provide the basis for several applications. The sp^2 bonds backbone and the low percentage of structural defects give them remarkably mechanical properties, in terms of elasticity, bending ability and tensile strength far higher respect to classical materials. For such reasons, together with the extreme lightweight, nanotubes have potential infinite applications in aerospace and automotive field, as fillers and reinforcements for fibers and plastic matrices.

Electronic properties are also important: CNTs with $n = m$ possess metallic and hence highly conductive character, whereas other tube types are semiconductors with variable band-gap. This, coupled with the quantistic effects deriving from the electrons confinement, since they can propagate only along tube axis, opens up a wide range of applications such as electrodes, nanowires, field effect transistors (FETs) and others.⁵

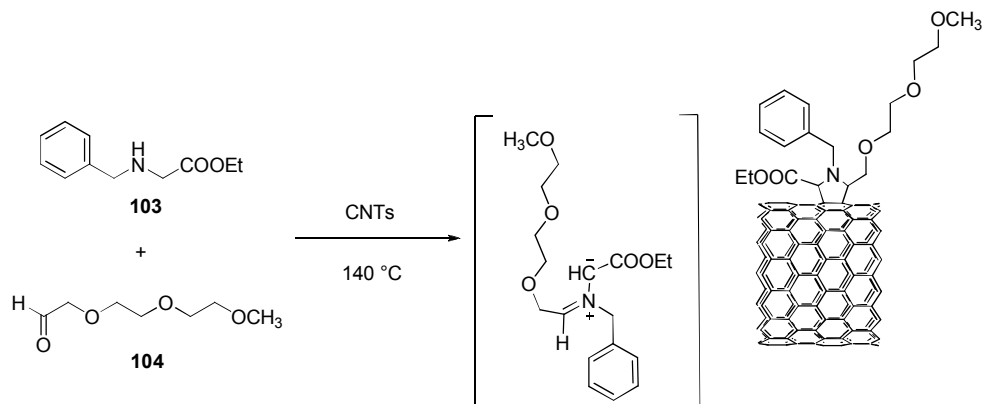
Furthermore, CNTs have unique pore and surface structures and exhibit unique adsorption/desorption behaviors, such as high hydrogen adsorption capability, that proposed them as possible storage materials. Again, the discovery that CNTs can penetrate into cells has stimulated their biomedical exploration as novel delivery systems able to transport and release bioactive molecules to specific active sites.⁶ This ability has also opened up questions about possible toxicity effects of CNTs towards human cells, and similarly their fiber-like shape and aggregation tendency that closely resembles asbestos can pose a serious risk for human health.⁷ Anyway, still much remains to know about this particular material, and research in this field is needed.

9.1.3 Enhancing Nanotubes Processability

Carbon nanotubes (CNTs) have been extensively studied in the past decades to understand and explain their structure, reactivity and properties. In order to enhance dispersibility and solubility in common solvents, and combine CNTs intrinsic properties with those of other molecular structures, functionalisation chemistry of CNTs has put forth a number of interesting derivatives that widen the potential of this carbon allotrope in nanomedicine and materials science.⁸

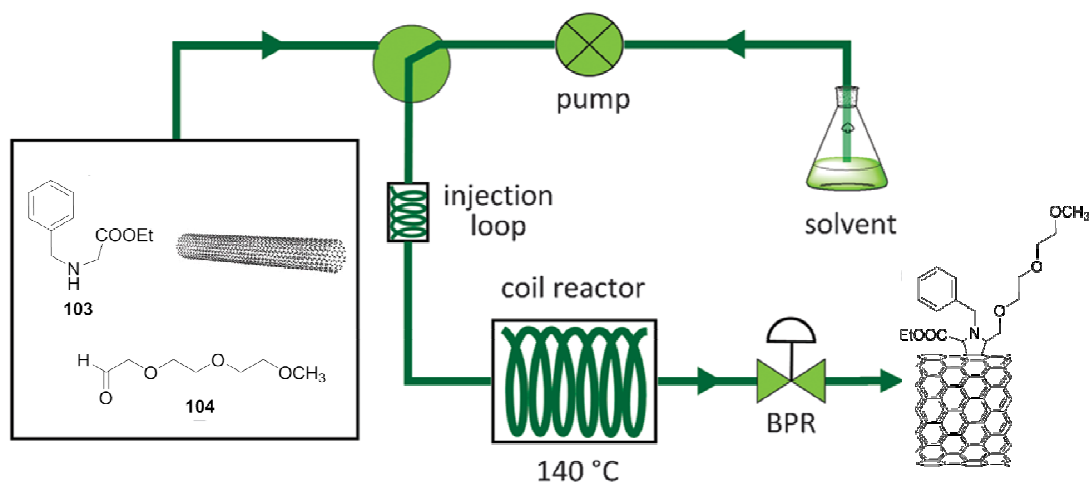
Usually, small scale production of covalently-functionalised CNTs is carried out, owing to the long reaction time and the amount of solvent required for disentangling and dispersing the CNT starting material. To mitigate this problem, a solvent-free technique, combined with microwave irradiation, has been proposed as a fast and potentially scalable protocol to produce functionalised CNTs.⁹ To this end, flow chemistry could contribute as well, since continuous processes are intrinsically easier to scale up than their flask counterparts, while offering a safer processing and the opportunity to rapid reaction screening and optimization using a relatively small amount of reagents. Continuous processing for carbon nanotubes solubilization would thus help the widespread application of CNTs in technological devices by supplying proper materials at higher rates. With such an objective, we began our effort to develop a continuous flow processing method by using microstructured flow-reactors.

9.2 Results and Discussion



Scheme 9.1: synthesis of functionalised SWCNTs .

Among numerous approaches reported for the covalent functionalisation of CNTs, we chose the 1,3-dipolar cycloaddition of azomethine ylides as a proof of concept because it is an easy and robust one-pot reaction that has been widely used to modify carbon nanostructures. Scheme 9.1 shows the cycloaddition to CNTs of the azomethine ylide that forms when N-benzyl glycine ethylester **103** reacts with 2-(2-(2-methoxyethoxy)ethoxy)acetaldehyde **104**. The resulting pyrrolidine ring integrates representative residues that can be regarded as general models for more elaborate solubilizing and aromatic moieties. Encouraged by the reported dispersibility of CNTs in



Scheme 9.2: continuous-flow synthesis of functionalised SWCNTs, simplified flow scheme.

N-methyl-2-pyrrolidone (NMP) and N-cyclohexyl-2-pyrrolidone (NCP), we considered these solvents as an alternative to N,N-dimethylformamide (DMF) for both flask and continuous-flow functionalisations. Single walled carbon nanotubes (SWCNTs) were first considered for the conventional flask synthesis: a dispersion of SWCNTs in the selected solvent, containing glycine derivative **103** and aldehyde **104**, was heated to 140 °C for 3 days. Fresh ylide precursors were added every 24 hours to compensate thermal degradation, as suggested by the literature protocol.¹⁰ Scheme 9.2 shows the simplified reactor configuration that was employed to carry out the flow experiments. Suspensions of solid materials are not suitable to be pumped through traditional HPLC type pumps, as they will cause blockage of pumping pistons. In order to overcome such problem, we equipped the flow reactor with an additional sample loop, made of a PTFE tubing coil (outer diameter = 2 mm) with a total volume of 11 mL. A stock dispersion of SWCNTs and reagents, in the selected solvent, was injected in the sample loop, than a switching valve was used to inject a plug of the dispersion in a stream of carrier solvent (DMF) that provides pumping to the main flow line. The reaction stream passed through a 400 cm segment of polytetrafluoroethylene (PTFE) tubing (inner diameter = 800 mm) submerged into an oil bath set to 140 °C. The total reactor volume was 2 mL. The first experiment for the optimization procedure was chosen at 9.7 mg (0.81 mequiv. of carbon) of SWCNTs, 70 mg (0.36 mmol) of compound **103**, 59 mg (0.36 mmol) of aldehyde **104** in DMF (10 mL) and a residence time of 30 min that was established by setting the flow rate to 4.0 mL h⁻¹. The reaction mixture was collected at the outlet and used for further runs or workup. In order to overcome thermal degradation, we chose to recycle the first reaction mixture for further two runs by adding fresh aldehyde and amino acid at each cycle without exceeding

the boundary on the total equivalents of **103** and **104** that were used for the flask synthesis. This protocol has given functionalised CNTs with solubility comparable to CNTs processed under batch conditions. The entire flow synthesis, for treating about 10 mg of SWCNTs in 10 mL of the solvent, requires 7.5 hours. A control experiment, in which the amount of **103** and **104** was doubled in the first run, gave functionalised SWCNTs only slightly more soluble than SWCNTs treated with the amount of **103** and **104** as indicated above.

The flow synthesis was also applied to the functionalisation of double-walled (DWCNTs) and multi-walled carbon nanotubes (MWCNTs). Since both nanostructures disperse in NCP more efficiently than their single-walled counterparts, the ylide functionalisation proceeded smoothly without fouling, affording products with solubility in NCP of about 1 mg mL⁻¹.

9.2.1 Characterization of Functionalized CNTs

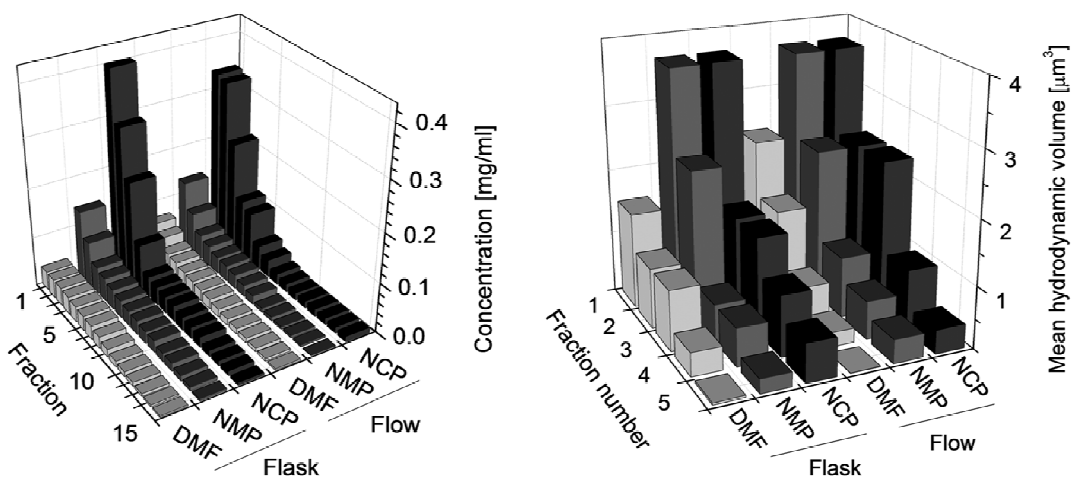


Figure 9.3: concentrations (left) and DLS mean hydrodynamic volumes (right) of SWCNTs derivatives in NMP extracts (n fractions of 2 mL each) of reaction mixtures from flask and flow experiments.

The flask vs. flow functionalisation efficiency was first established on the basis of the solubility of the modified SWCNT samples. However, since CNT materials are bundles with tubes of different lengths and diameters, it is reasonable to assume that this can lead to mixtures of CNTs with a different degree of functionalisation and, therefore, with a wide range of solubilities. Accordingly, instead of referring to a generic solubility of a CNT sample after functionalisation and solvent extraction of the crude mixture, we carried out a

sequence of extractions with NMP that better reflect the distribution of functionalised CNTs (Figure 9.3 and Experimental paragraph 9.4). Concentrations were calculated from optical absorption data, using the tabulated extinction coefficient for SWCNTs of $30.3 \pm 0.2 \text{ mL mg}^{-1} \text{ cm}^{-1}$ at 1.2 eV.¹¹ The concentration decreases within each series of extractions, since the most functionalised (soluble) material is extracted first. The dispersing ability of the solvent towards the starting nanotubes (NCP > NMP > DMF)¹² plays an important role to determine the solubility of the final product, as reflected by the data in Figure 9.3 where the higher efficiency of NCP to de-bundle CNTs leads to more soluble products. It is important to note that a nice feature of the continuous-flow CNT functionalisation is the effective shortening of the reaction time: 7.5 hours flow synthesis afford CNT samples with solubilities comparable to those of samples after a 72 hour treatment in the flask under the same conditions. In order to complement the comparison between flask and flow processing, dynamic light scattering (DLS) was used to characterize the size distribution of the functionalized CNT products. Mean hydrodynamic volumes of the first five extracted fractions for each flask or flow experiment are reported as well in Figure 9.3. Nanotubes in the early fractions are the most soluble because they are well functionalised. This translates into larger solvation spheres and thus bigger hydrodynamic radii.¹³ The above extracts were also characterized by Raman spectroscopy. Figure 9.4 reports, as representative examples, the Raman spectra of pristine and functionalised SWCNTs in the first five NMP extracts from the reaction that was carried out under continuous-flow conditions in NCP. The spectra show the increase of the D-band ($\sim 1300 \text{ cm}^{-1}$, sp^3 carbons) at the expense of the G-band ($\sim 1600 \text{ cm}^{-1}$, sp^2 carbons). Importantly, the nanotube electronic structure is conserved also in the derivatives as indicated by the G' band at 2650 cm^{-1} that is substantially unchanged in all spectra. Thermogravimetric analysis (TGA) of functionalised SWCNT material, that was isolated after solvent evaporation from the first fraction of flask or flow experiments, respectively, is shown in Figure 9.4. The weight loss between 200 and 600 °C corresponds to the degradation of the organic addends. It increases with the solubility of the material that, in turn, depends on the degree of functionalisation.

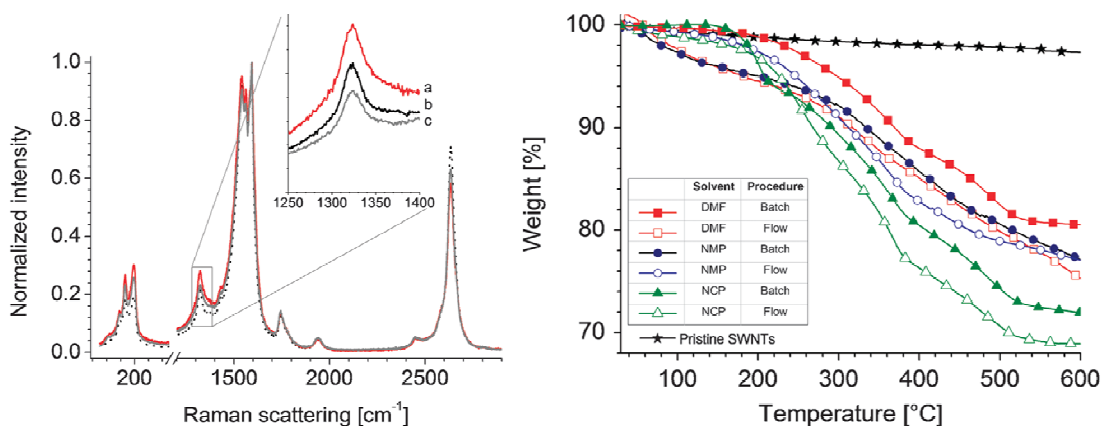


Figure 9.4: left) Raman spectra of respectively pristine nanotubes (a) and first (b) and third (c) extract fractions from continuous flow synthesis using NCP as solvent; right) TGA analysis of pristine nanotubes (black line) and SWCNT derivatives obtained by solvent evaporation of the first extract fraction for each reaction.

9.3 Conclusions

In conclusion, this study demonstrates that the organic functionalisation of carbon nanotubes can benefit from a continuous-flow processing. The use of a simple setup (pump, PTFE tubing, heating system) and NCP as a solvent, produced approximately 10 mg of functionalised SWCNT samples in 7.5 hours at 140 °C, with a solubility of about 1 mg mL⁻¹ in NCP. In order to reach a comparable productivity and solubility, the flask synthesis required 72 hours at 140 °C. Addition of parallel reactors would allow a high throughput, continuous production of functionalised CNT samples. The flow approach was effectively extended also to DWCNTs and MWCNTs. Additional advancements of this technology include the extension to other CNT covalent functionalisation approaches with potential advantages in terms of tunability and scalability.

9.4 Experimental Section

Single-walled carbon nanotubes (SWCNTs) were purchased from NanoCarlab (SWCNT purity: 70–80 wt%, diameter: 1.2-1.4 nm, length: 1-5 μm), double-walled carbon nanotubes (DWCNTs) were provided by Cheap Tubes Inc (DWCNT purity > 90 wt%, DWCNT purity > 60 wt%, outer diameter: 2-4 nm, length: 5-30 μm). Multi-walled carbon

nanotubes (MWCNTs) were purchased from Sigma Aldrich (MWCNT purity > 90 wt%, outer diameter 10–15 nm, inner diameter: 2–6 nm, length: 0.1–10 µm) were used as received. 2-(2-(2-Methoxyethoxy)ethoxy)acetaldehyde **104** was synthesized according to a literature procedure.¹⁴ Ethyl 2-(benzylamino)acetate **103** was purchased by Sigma Aldrich and used as received. All solvents were purchased from Sigma Aldrich and purified by distillation under reduced pressure. Dispersions of CNTs were achieved using the Sonicator 3000 (Misonix) with the following pulse parameters: time on = 3 sec, time off = 3 sec, power level = 5 (15-20 watt). The sonicated solutions were centrifuged with an IEC CL10 centrifuge (Thermo Electron Corporation) at 3500 rpm for 3 minutes. Absorption spectra of nanotube samples, dispersed in air-equilibrated solvent, were registered with a Varian Cary 5000 spectrophotometer, at room temperature, between 280 and 1400 nm, data interval = 0.5 nm, scan rate = 300 nm/min, SBW = 2 nm. DLS measurements of nanotube samples dispersed in air-equilibrated NMP were performed with a Zetasizer Nano S (Malvern Instruments) at 20 °C setting 20 runs of 10 seconds for each measurement. Raman spectra of carbon nanotubes, drop-casted on pre-cleaned glass micro slides (Corning Inc.) and annealed at 100°C, were recorded with an Invia Renishaw Raman microspectrometer (50× objective) using the 633 nm laser line of an He–Ne laser at room temperature with a low laser power. Thermogravimetric analyses (TGA) of CNT samples, precipitated by adding cyclohexane and dried at 80 °C at 0.2 mbar overnight, were carried out with a TA SDT 2960 TGA under nitrogen from 100 °C to 1000 °C with a heating rate of 20 °C/min.

Functionalisation of SWCNTs in flask

A dispersion of SWCNTs in the selected solvent, containing glycine derivative **92** and aldehyde **93**, was heated to 140 °C for 72 h in a 25 mL flask under vigorous stirring. Fresh ylide precursors were added every 24 h to compensate thermal degradation. Then the mixture was centrifuged (3500 rpm for 3 min), the supernatant discarded and the black solid residue washed with toluene (5 x 7 mL). The functionalised carbon material was dried under vacuum (0.2 mbar) at 80 °C for 4 h and weighted. Aliquots of soluble carbonaceous material were extracted from the crude SWCNT sample by means of sonication/centrifugation cycles as described above.

Continuous-flow functionalisation of CNTs

The flow reactions were carried out in a PTFE (polytetrafluoroethylene) tubing (O.D. = 1.58 mm, I.D. = 0.8 mm, total volume = 2 mL, Supelco, Item no. 58696-U) coiled and immersed into an oil bath, set to 140 °C, for 400 cm of effective length. A Rheodyne valve was used to inject a stock dispersion of CNTs and reagents **103** and **104**, in the selected solvent, to the main flow line through a sample loop (I.D. = 2.0 mm, volume = 10 mL, length = 80 cm). The main flow was set to 4 mL/h by a HPLC pump (Model KP-12-01S by Flom, Japan). The reactor outlet was connected to a mechanical back-pressure regulator (S series Metering Valve, Swagelok) set to 25 psi. The reagents, before loading, were kept under vigorous magnetic stirring.

The 2.0 mL total volume of the reactor coil corresponds to a residence time of 30 min with a flow rate of 4.0 mL/h. The first reaction mixture was recycled for further two runs by adding fresh aldehyde and aminoacid at each cycle for a total residence time of 90 minutes and an overall processing time of 7.5 hours. The final mixture was then centrifuged at 3500 rpm for 3 minutes, the supernatant was removed and the black residue washed with toluene (5 × 7 mL). The residual carbon material was dried under vacuum (0.2 mbar) at 80 °C for 4 h and weighted. Aliquots of soluble CNT material were extracted from the crude sample by means of sonication/centrifugation cycles. For the extractions, 2.0 mL of NMP were added to the CNT material, followed by 1 minute sonication (see above for sonicator parameters). The resulting dispersion was centrifuged again at 3500 rpm for 3 min, and the supernatant characterized by UV-Vis spectroscopy and DLS analysis immediately after centrifugation. Each DLS measurement was averaged over 20 runs (10 s per run). It is worth noting that the less soluble fractions gave DLS data poorly reproducible for the presence of large aggregates. Therefore, only DLS data for the first five extracts, in the solvents indicated in Figure 9.3, were considered. The distribution of particle sizes was obtained by plotting the number size distribution provided by correlograms taken with the software program by Malvern. Raman spectra were taken on samples prepared by drop casting the solutions, previously subjected to DLS measurements, on glass micro slides. In order to produce smooth CNT layers and reproducible Raman spectra, the drop-casted samples were annealed at 100 °C. CNT samples corresponding to the most soluble fractions (the first one for each reaction solvent) were precipitated from NMP by adding methanol (5 mL) and the solid was washed with methanol (2 x 5 mL). The residue was dried under vacuum (0.2 mbar) at 80 °C for 2 h and was analyzed in a thermogravimeter

instrument under nitrogen from room temperature to 1000 °C with a heating rate of 20 °C/min.

References

- ¹ S. Iijima, T. Ichihashi, *Nature*, **1993**, 363, 603–605.
- ² A. Oberlin, M. Endo, T. Koyama, *J Cryst Growth*, **1976**, 32, 335–349.
- ³ *Carbon*, **2006**, 44, 1621–1623.
- ⁴ *Carbon Nanotubes and Related Structures*, ed. D. M. Guldi and N. Martin, **2010**, Wiley-VCH.
- ⁵ A. Jorio, G. Dresselhaus and M. S. Dresselhaus, *Carbon nanotubes: advanced topics in the synthesis, structure, properties, and applications*, **2008**, Springer, Berlin.
- ⁶ A. E. Porter, M. Gass, K. Muller, J. N. Skepper, P. A. Midgley, M. Welland, *Nature Nanotechnology*, **2007**, 2, 713.
- ⁷ C. A. Poland, R. Duffin, I. Kinloch, A. Maynard, W. A. H. Wallace, A. Seaton, V. Stone, S. Brown, *Nature Nanotechnology*, **2008**, 3, 423.
- ⁸ P. Singh, S. Campidelli, S. Giordani, D. Bonifazi, A. Bianco and M. Prato, *Chem. Soc. Rev.*, **2009**, 38, 2214–2230.
- ⁹ E. Vazquez and M. Prato, *ACS Nano*, **2009**, 3, 3819–3824.
- ¹⁰ V. Georgakilas, K. Kordatos, M. Prato, D. M. Guldi, M. Holzinger and A. Hirsch, *J. Am. Chem. Soc.*, 2002, 124, 760–761.
- ¹¹ S. H. Jeong, K. K. Kim, S. J. Jeong, K. H. An, S. H. Lee and Y. H. Lee, *Synth. Met.*, **2007**, 157, 570–574.
- ¹² S. D. Bergin, Z. Sun, D. Rickard, P. V. Streich, J. P. Hamilton and J. N. Coleman, *ACS Nano*, **2009**, 3, 2340–2350.
- ¹³ G. M. Koenig, R. Ong, A. D. Cortes, J. A. Moreno-Razo, J. J. De Pablo and N. L. Abbott, *Nano Lett.*, **2009**, 9, 2794–2801.
- ¹⁴ J. Carlise, R. Kriegel, W. Rees Jr, M. Weck, *J. Org. Chem.* **2005**, 70, 5550–5560.

Chapter 10: Flow Functionalisation of Porphyrin Derivatives

10.1 Porphyrins and their Properties

Porphyrins are an important class of organic molecules widely present in biological systems, where they perform many basic biochemical functions. The name porphyrin is derived from the Greek word *porphura* meaning purple, as all porphyrins have an intense red or purple colour. All porphyrinic derivatives share the backbone made of an aromatic macrocycle made of four pyrrole molecules, linked together with four methine bridging units.¹ Functionalisation of the basic structure includes both covalent linking of functional moieties to the macrocycle and coordination of pyrrolic nitrogen atoms, in particular using metallic ions.

10.1.1 Structure, Properties and Occurrence

Porphyrin heterocyclic system comprises 22 π -electrons. $4n + 2$ are aromatic π -electrons, whereas double bonds 7-8 (Δ^7) and 17-18 (Δ^{17}) retain olefine's reactivity and can be modified by reduction, or any other typical reaction of olefines, giving the so-called chlorin compounds.

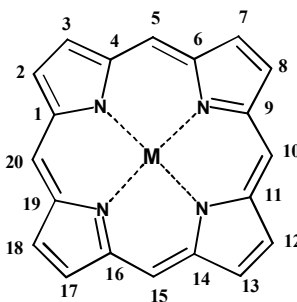


Figure 10.1: structure of the porphyrin macrocyclic backbone

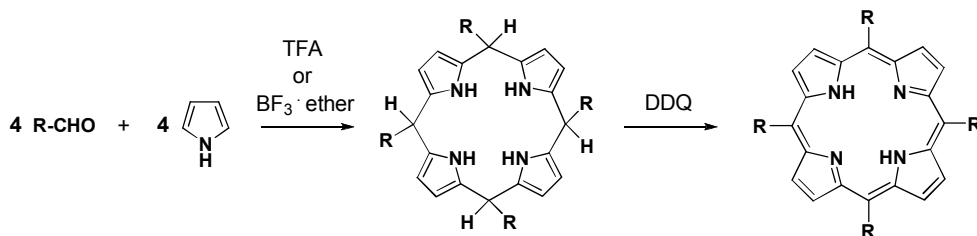
The size of the macrocycles hollow cavity allows for optimum accommodation of almost all metal ions. Porphyrinic binding complexes are called metalloporphyrins and can be found with a large variety of metals (e.g., Fe, Zn, Cu, Ni, Hg, Co, *etc.*). The metalloporphyrin ring is present in a variety of important biological systems where it plays

a key role in biochemical mechanisms: from oxygen transfer and storage (hemoglobin and myoglobin), to electron transfer (cytochrome c, cytochrome oxidase), or energy conversion (chlorophyll).

Porphyrins and related derivatives exhibit outstanding photochemical, electrochemical and catalytic properties with potential applications in opto-electronic, electrochemistry, sensing applications, photodynamic therapy (PDT) and catalysis. Accordingly, these macrocycles have been widely used for the construction of functional materials and devices. Moreover, their physical-chemical characteristics (including dipole moments, polarizability, non-linear optical response, absorption spectrum, energy transfer and catalytic behaviour) may be tuned at the molecular level by proper chemical functionalisation.

10.1.2 Synthesis and Reactivity

Chemical synthesis of the porphyrinic macrocycle is not trivial. A number of synthetic approaches have been developed, involving multi-step preparation of suitable precursor compounds as dipyrromethanes, dipyrromethenes, tripyranes and linear tetrapyrroles. Such procedures, however, are often time and labour expensive, hence strong efforts have been made to optimize the route through direct polymerization of pyrrole with suitable aldehydes. The procedure reported by Lindsey and co-workers over the period 1979-1986^{2,3} involves a two-step approach depicted in Scheme 10.1. The acid catalyzed condensation of pyrrole with a benzylic aldehyde to a porphyrinogen intermediate, followed by oxidation with a suitable reagent, usually 2,3-dichloro-5,6-dicyano-1,4-benzoquinone (DDQ), affords the final porphyrin. For the simplest derivative, meso-tetraphenylporphyrin (TPP), final yield in purified product on lab scale is almost 45-50%, and it linearly decreases in scaling up. TPP is hence a widely available porphyrin derivative and a common starting material for the preparation of functional, more complexes derivatives.



Scheme 10.1: two-step general method for synthesis of a porphyrin macrocycle.

Porphyrins undergo the characteristic reactions of aromatic compounds, in particular electrophilic substitution. In the porphyrin macrocycle two different positions can be differentiated: positions 5, 10, 15 e 20, called meso, and positions 2, 3, 7, 8, 12, 13, 17 and 18, called β -pyrrole.

Meso-functionalized porphyrinic derivatives are widely present in natural products, while the second have no counterpart in nature and were developed as functional artificial models.⁴

Functionalisation of the meso positions is synthetically more accessible, in particular by post-functionalisation of the preformed TPP molecule, a wide available starting material. However, aromatic meso substituents result to be disposed orthogonally to the porphyrin core due to steric hindrance, thus overlapping of the electronic π -systems of the macrocycle and the aromatic substitution is not possible resulting little through-bond cross-talking between the two units (Figure 10.2)⁵. On the other hand, functionalisation through the β -pyrrolic positions provides a planar system and good electronic communication between the porphyrin core and the adjacent moiety.

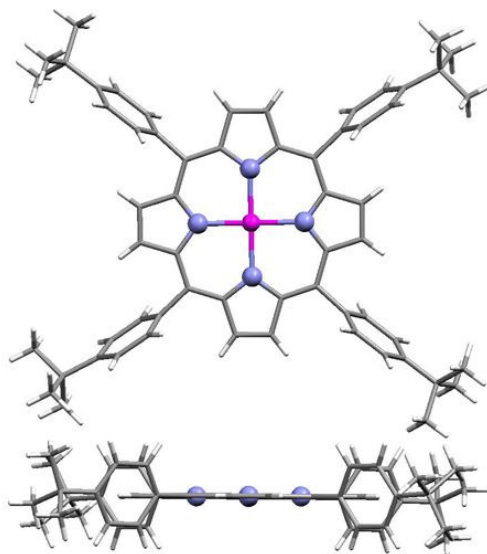


Figure 10.2: tridimensional structure of a meso-substituted porphyrin. Substituents result to be orthogonally disposed respect to macrocyclic core.⁵

This is of particular importance when porphyrin derivatives are used as photosensitizers in Gratzel-type solar cells: it has been proven that the modification of meso-tetraphenyl porphyrins by substitution at the pyrrolic β -position with functional groups with extended π -systems, leads to the best performing porphyrin based solar cells to date.⁶ A synthetic path for β -substitution in the porphyrin macrocycle usually starts from the synthesis of the

corresponding β -brominated synthon followed by metal-mediate cross-coupling carbon-carbon or carbon-heteroatom reactions for grafting to the macrocycle framework a variety of moieties.

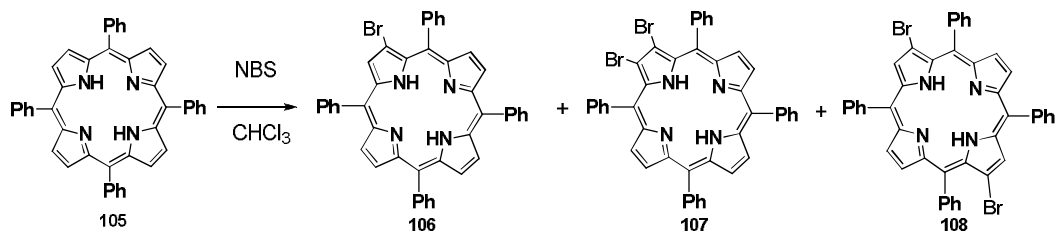
The yield limiting step is commonly the monobromination step. The original selective bromination of TPP and related porphyrins was described by Calliot in 1973.⁷ More recently, the reaction was systematically investigated by Zhang and co-workers with the aim to maximize yield and selectivity of the reaction.⁸ Reaction solvent, equivalents of NBS, temperature, the presence of additives such as pyridine and the slow addition of predissolved NBS to the TPP solution were among the main reaction parameters studied. Generally, reaction selectivity is quite poor, leading in great extents to poly-brominated products. Moreover separation of various halogenated compounds by preparative chromatography is not an easy task and often it translates into a considerable loss of the target product during its isolation. Thus, poor efficiency and productivity of this method make it unsuitable for application to a larger scale synthesis.

10.1.3 Goals

Use of continuous-flow conditions should result in a better control on bromination extent. Substantial process improvement should be achievable thanks to high throughput, fast optimization, improvement in selectivity and safer processing. In this optic, we focused to the development of a continuous-flow synthesis of the monobromo tetraphenylporphyrin (TPP-Br) using Vapourtec R4 platform for process optimization. The model reaction of choice for this research was the bromination of meso-tetraphenylporphyrin (TPP) with N-bromo succinimide (NBS) in chloroform which has been widely studied by several research groups.^{7,8}

10.2 Results and Discussion

Before carrying out the reaction under continuous flow conditions, the TPP bromination was first performed in batch following the two different established literature protocols.(Method A and B, see Experimental Section).



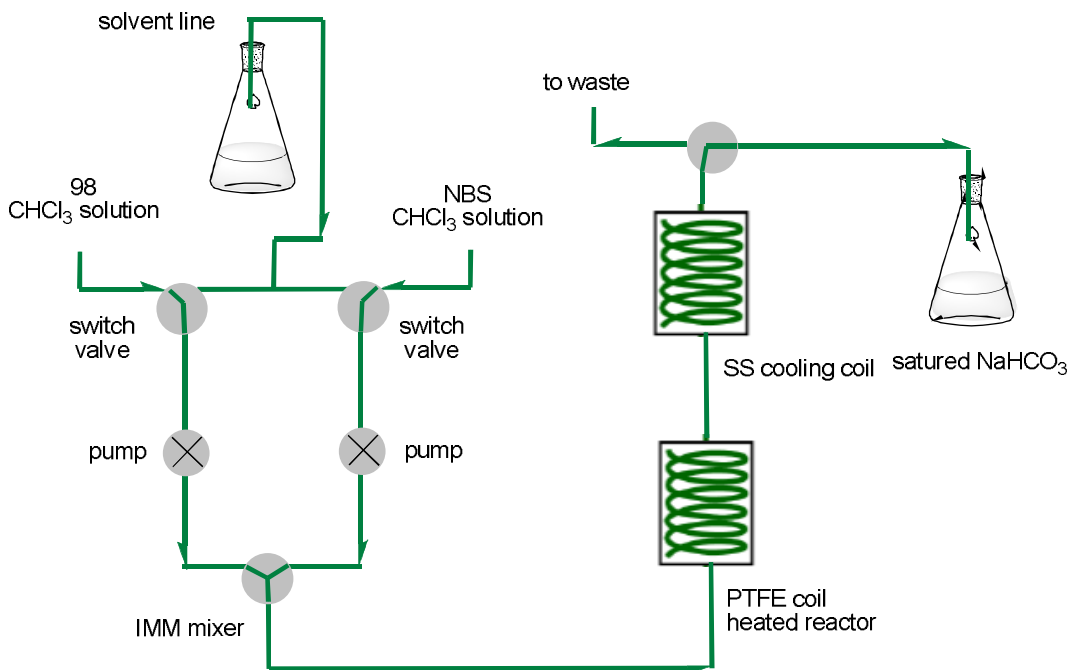
Scheme 10.2: TPP bromination reaction

Using Method A, described by Zhang,⁷ a mixture of at least 4 products was evident by TLC analysis which corresponded to a limited amount of unreacted TPP, together with the TPP-Br and two isomeric TPP-Br₂ derivatives. HPLC analysis of the reaction mixture allowed quantifying the target TPP-Br as 51%, the isomeric TPP-Br₂ as 41% and the unreacted TPP as 8%.

Method B⁸ involves slow addition of NBS and use of pyridine as an additive. In this case, TPP was almost completely consumed and a fairly good yield of 76% (determined by HPLC) in TPP-Br was obtained, whereas yield in isolated product raised as well to 30%. Products distribution was in agreement with available literature data. However, the method presents three main drawbacks: the use of the unpleasant pyridine additive, a long reaction time resulting from the slow addition of the NBS solution and the large excess of brominating agent (3 equivalents) used.

On the basis of these preliminary results, we decided to develop an alternative continuous flow synthetic protocol with the aim of reaching TPP-Br yields comparable with those observed under batch-wise conditions but with a better reaction productivity and without need for additives. Another goal was to minimize the amount of poly-halogenated compounds so to simplify purification procedures and to improve process economy through extended recovery of unreacted starting material in view of application to more expensive and elaborated porphyrins.

For continuous flow studies we made use of a commercial flow reactor supplied by Vapourtec. Since mixing efficiency is likely to be a fundamental issue for determining reaction selectivity, we managed to enhance standard mixing capability of Vapourtec platform by using a slit interdigital micromixer (see Chapter 1 and Chapter 3) supplied by Institut für Mikrotechnik Mainz (IMM, Germany). This device combines reactor feeding streams through multilamination, thus reducing diffusion path, and flow focusing for radical enhancing of reagents mixing rate. Initially we performed a process development study using the flow reactor set-up reported in Scheme 10.3 and injecting plugs of reaction



Scheme 10.3: scheme of the continuous flow equipment employed for evaluation and optimization of TPP mono-bromination reaction.

mixture in the reactor using a chloroform stream as carrier. Using this methodology a fast screening of reaction conditions was achieved with a minimal consumption of reagents, a key factor when considering relatively expensive starting materials. Reaction quenching was accomplished by cooling down the reaction stream followed by a chemical quenching/extraction step (see Experimental Sections for details) and HPLC quantification of products distribution. Experiments were performed in order to determine the influence of key parameters on reaction yield and selectivity, in particular the effect of reaction temperature, reaction time and stoichiometry were investigated. Results are summarized in Table 10.1.

First of all we studied the effect of the temperature on the outcome of the TPP bromination. It should be pointed out that, thanks to the use of a back-pressure regulator placed at the end of the reaction stream, the reaction temperature could be safely raised well above the solvent boiling point (61°C in the case of chloroform), an option not easily accessible with conventional apparatus. For these experiments the TPP/NBS molar ratio was set to one. In addition, the residence time was set at 5 minutes to assure a reasonable productivity. At room temperature (Table 10.1, entry 1) the bromination of TPP took place only in a minimum extent (8%). Raising the temperature up to 125°C resulted in the formation of TPP-Br with a 45% yield, an improvement if compared to the conventional batch methodology. The amount of dibrominated porphyrins was low (3%). On the basis of

these results, we decided to set up the temperature to 125 °C for all the following optimization experiments.

As a second operational parameter, we studied the effect of the residence time ranging from 1 to 10 minutes (Table 10.1, entries 5-6). As expected, decreasing the residence time from 5 (Table 10.1, entry 4) to 1 minute (Table 10.1, entry 5) caused a decrease in TPP-Br yield from 45% to 21%. On the other hand, increasing the residence time to 10 minutes (Table 10.1, entry 6) resulted in rising of the amount of TPP-Br to 59%. At this stage a consideration has to be made: although absolute yield under entry 6 conditions is higher than that obtained with a residence time of 5 minutes (45%), the correspondent product throughput results to be lower, due to double residence time. Choice of optimal reaction conditions should be made, considering the specific synthetic target, meaning if maximum atom economy (entry 6) or higher throughput (entry 5) is looked. Therefore we decided to keep the residence time at 5 minute and to study the effect of NBS equivalents on the yield of TPP-Br (entries 7-10). By increasing amounts of NBS the yield of TPP-Br could be raised up to 72% (entry 10) but with a concomitant formation of polybrominated porphyrins up to 14%.

Table 10.1: Selected results for continuous flow bromination of TPP

Entry	NBS (equiv.)	Residence time (min)	Temp. (°C)	TPP-Br (%) ^a	TPP (%) ^a	TPP-Br ₂ (%) ^a
1	1	5	25	8	92	nd
2	1	5	75	20	79	1
3	1	5	100	40	58	2
4	1	5	125	45	52	3
5	1	1	125	21	78	1
6	1	10	125	59	37	4
7	0.8	5	125	47	50	3
8	1.1	5	125	56	37	7
9	1.25	5	125	59	30	11
10	1.5	5	125	72	14	14
11 ^b	1	10	125	66	29	5

a: HPLC determined amounts.

B: Performed with a 10 ml PTFE tubing coil reactor.

In order to verify robustness and applicability of the flow methodology we also performed a preparative scale test. It should be pointed out that one of the advantages of the microreactor technology is that the scaling up process does not require, as often happens in the case of batchwise syntheses, re-optimization of the experimental conditions. Indeed, reactors can be built in parallel or simply kept running until the desired amount of target compound is produced. We thus employed conditions of entry 6, Table 10.1 to process a total amount of 100 mg (0.163 mmol) of TPP; output stream was sampled and analyzed by HPLC, resulting in constant mean product distribution very close to the expected one (~60% of mono-brominated porphyrin).

Finally, in view of a possible future application to an higher production scale of TPP-Br, we also managed to improve process productivity by a scale up procedure using an higher volume reactor (10 mL instead of 5mL): in fact doubling the reactor internal volume results in doubled productivity for time unit. Surprisingly, we could observe even an yield increased up to the 66% together with a very good selectivity for the mono-bromo derivative (entry 11). This was probably due to an enhancement of efficiency of the mixing device determined by the higher flow rates used.

Advantage of continuous processing over batch systems becomes clearer while calculating space-time yields for the various approaches: space time yield in fact is defined as amount of material produced per unit time and reactor volume, therefore this is the best way to compare performances of batch versus continuous apparatus. Yield values calculated on the basis of experimental results obtained are $9.2 \cdot 10^{-7} \text{ mmol mL}^{-1} \text{ min}^{-1}$ for batch method A and $6.6 \cdot 10^{-7} \text{ mmol mL}^{-1} \text{ min}^{-1}$ for method B. Surprisingly, method B has lower space-time efficiency, despite the higher yield obtained, due to larger amount of solvent needed for processing. Space time yield value for continuous approach is instead surprisingly high: $2.9 \cdot 10^{-5} \text{ mmol mL}^{-1} \text{ min}^{-1}$; an increase of two orders of magnitude over batch processing is achieved thanks to reactors smaller footprint and reaction rate enhancement allowed by working at solvent over-boiling temperature.

10.3 Conclusions

In conclusion, we have demonstrated that high degree of reaction control for TPP bromination can be obtained with continuous flow reactors. Comparison between results obtained in batch and flow mode are reported in Table 10.1. As may be noticed, batchwise processing afforded higher absolute yield values in mono-brominated porphyrin: however,

process inefficiencies in terms of long reaction times, high dilutions and use of hazardous additive (pyridine) result in difficult scale up. Moreover, starting material is completely consumed during reaction, giving a low atom economy. Continuous flow processing allows in turn for tuning of reaction conditions in order to favor both product yield and selectivity depending on desired recover of starting material. In any case, larger space-time yields respect to batch methods could be obtained. Furthermore, the flow process developed in this study has been demonstrated to be easily scalable to higher productions.

10.4 Experimental Section

All chemicals were purchased from Sigma-Aldrich and used as received, with the exception of NBS that was recrystallized from hot water prior to use.[se c'è un rif mettilo] All reactions solvents were HPLC grade, except where differently stated. Reactions were monitored by TLC (eluent: toluene/cyclohexane 1:1) on Machinery-Nagel pre-coated plates. HPLC analysis were performed using a Phenomenex Luna 5 μ on silica with an isocratic elution with a 80:20 mixture of cyclohexane/toluene with 0.1% TEA, analytes were revealed by UV-Vis detector at 420 nm.

Batch Synthesis Method A:⁷

A mixture of TPP (200 mg, 0.326 mmol) and N-bromo succinimide (1.8 eq, 102 mg, 0.573 mmol) in CHCl₃ (50 mL) was stirred at room temperature for 6 h. The solvent was evaporated and the mixture was washed with water, extracted with CHCl₃, dried (Na₂SO₄), filtered and concentrated (HPLC yields: 51% TPP-Br; 41% TPP-Br₂; 8% TPP). The residue was purified by gravity column chromatography (silica gel, toluene/cyclohexane 1:1) affording H₂- β -bromoTPP (**106**) as a red solid (41 mg, 18% yield).

¹H-NMR (300 MHz, CDCl₃): δ .8.95-8.84 (m, 5H), 8.79 (m, 2H), 8.28-8.17 (m, 6H), 8.15-8.09 (m, 2H), 7.86- 7.70 (m, 12H), -2.80 (s, 2H).

¹³C-NMR (75 MHz, CDCl₃): δ 142.04, 141.71, 140.80, 138.02, 134.57, 134.52, 134.50, 134.40, 134.30, 129.59, 128.79, 128.21, 127.93, 127.81, 126.94, 126.80, 126.72, 126.69, 120.72, 120.28, 120.01, 119.56.

UV-vis, CH₂Cl₂, λ_{\max} nm (Log ϵ) 421 (5.55), 518 (4.27), 553 (3.72), 593 (3.70), 648 (3.67).

MS (ESI): 693 (M+1)⁺, 347 [(M+2)/2]⁺.

FLUOR: CH₂Cl₂, λ_{\max} nm 657, 718.

Batch Synthesis Method B:⁸

To a three neck round-bottom flask charged with TPP (1.27 g, 2.1 mmol) and CHCl₃ (300 mL) were added 12 mL of pyridine. After refluxing for 5 min, a solution of N-bromosuccinimide (3.0 eq, 1.12 g, 6.3 mmol, dissolved in 500 mL of CHCl₃) was added dropwise over a period of 3-4 h to the reaction mixture. The solution was refluxed for additional 2 h, cooled to room temperature, quenched with acetone (150 mL), and concentrated to dryness (HPLC yields: 76% TPP-Br; 21% TPP-Br₂; 3% TPP). The residue was purified via gravity column chromatography (silica gel, toluene/cyclohexane 1:1), affording H₂-β-bromoTPP (437 mg, 30% yield).

Flow Synthesis

Flow reactions were performed using a Vapourtec R4 platform supplied by Vapourtec Ltd (UK) coupled with a IMM micromixer (Meinz, Germany). Reactors employed were PTFE tube assemblies of total internal volume of 5 and 10 mL, equipped with a 100 psi cartridge based back pressure regulator. A solution of meso-TPP in CHCl₃ (8.4mM) and a solution of NBS in CHCl₃ (8.7 mM) were used as reactor feeds. A thermal quench was performed at the end of the reactor assembly using a refrigerated coil, followed by chemical quench/extraction at the collection point performed thorough dropping of reaction output in saturated aqueous bicarbonate. After phase separation organic layer was collected and diluted with chloroform, dried over magnesium sulphate and accurately filtered. Collected samples were than analyzed by HPLC after suitable dilution in the eluting phase.

Preparative run was accomplished by following the same procedure and employing conditions reported in Table 10.1, entry 6. After quenching of reactor output, organic layer was washed with water, than dried (Na₂SO₄), and the solvent removed. The residue was purified via gravity column chromatography (silica gel, toluene/cyclohexane 1:1), affording H₂-β-bromoTPP (53 mg, 47% yield).

References

- ¹ *The Porphyrins*, ed. D. Dolphin, **1978**, Academic Press.
- ² J.S. Lindsey, H.C. Hsu, I. C. Schreiman, *Tetrahedron Lett.* **1986**, 27, 4969.
- ³ J.S. Lindsey, I. C. Schreiman, H.C. Hsu, P. C. Kearney, A.M. Marguerettaz, *J. Org. Chem.* **1987**, 52, 827.
- ⁴ L.R. Milgron, *The Colours of Life*, **1997**, Oxford University Press.
- ⁵ R. Słota, M. A. Broda, G. Dyrda, K. Ejsmont and G. Mele, *Molecules*, **2011**, 16, 9957-9971.
- ⁶ W. M. Campbell, K. W. Jolley, P. Wagner, K. Wagner, P. J. Walsh, K. C. Gordon, L. Schmidt-Mende, M. K. Nazeeruddin, Q. Wang, M. Grätzel and D. L. Officer, *J. Phys. Chem. C*, **2007**, 111, 11760.
- ⁷ H. J. Callot *Tetrahedron Lett.* **1973**, 14, 4987.
- ⁸ G.-Y. Gao, J. V. Ruppel, A. D. Brett, Y. Chen, X. P. Zhang, *J. Org. Chem.*, **2007**, 72, 9060-9066.



Concluding Remarks

The research carried out during the present PhD project was focused on application of continuous flow technology for the synthesis of molecular structures with potential applications in medicinal chemistry and material science. In particular, synthetic processes were designed with the aim of being easily scalable to production on industrial scale.

Glass modular reactors supplied by Corning Inc. (Avon, France) were used to develop a flow process for continuous synthesis and employment of diazomethane, an highly hazardous substance. The procedure was initially optimized at small scale, using a low volume reactor, and then readily scaled up by increasing reaction dimensions, with a minimal need for re-optimization of process parameters. Final process allowed for preparation of 19 mol/day of diazomethane in a safe and reliable way, was hence potentially applicable to industrial productions of pharmaceuticals or other fine chemicals.

Heterocyclic compounds bearing pyrimidinamine and 4-anilino-quinazoline core scaffolds were prepared by continuous flow using Vapourtec R4 platform. Such molecules have potential application as oncological drugs for the selective inhibition of tyrosine kinase enzymes, biological factors deeply involved in development of various tumor forms. Continuous flow technologies were demonstrated to be valuable tools for the confinement of production of biologically active molecules, thus increasing process safety. The optimized flow syntheses moreover allowed for efficient preparation of libraries of similar compounds in high throughput, should be hence potentially used for both screening of new drug candidates and industrial scale production. This work was largely carried out in collaboration with Fabbrica Italiana Sintetici (FIS) Spa, sited in Montecchio (Vicenza).

Finally, continuous flow reactors were applied to the chemical functionalisation of molecular nanostructures, based on fullerene, carbon nanotubes and porphyrin derivatives.

In particular, a methanofullerene derivative, PCBtB, was prepared using a continuous two step synthesis in microstructured reactors, previously fabricated by lithographic techniques using a photocurable thiolenic resin. Synthetic protocol involved *in-situ* preparation of a highly reactive diazo species on a renewable metal reagent, and a photochemical isomerization step carried out by using a low power consumption LED light source, with a definite energy saving. Moreover, PCBtB showed great potential as active material for

polymeric solar cells: good power conversion efficiencies, comparable to benchmark devices, were obtained without need for thermal annealing procedures, resulting in simplification of construction process.

A continuous flow set-up was optimized for the covalent functionalisation of carbon nanotubes. Continuous flow allowed for a ten-fold decrease in processing times respect to typical batch procedures, and afforded a material that is more soluble in organic solvents and, on consequence, easier to process for applications in energy and materials technology. This set-up was also claimed in an Italian patent request.

Finally, the continuous flow bromination of tetraphenylporphyrin was implemented on continuous flow Vapourtec R4 platform. The influence of reaction temperature, time and stoichiometry over selectivity for mono-bromination was studied, and the parameters were optimized to afford a process with highly increased space-time yield respect to batchwise synthesis. Continuous flow process is indeed suitable for application in large scale productions of mono-bromo-tetraphenylporphyrin; this latter is a valuable precursor for preparation of highly technological materials, with potential applications in electronic and sensoristic field, based on porphyrinic scaffold.

The results here reviewed have been in large part collected in a number of publications on international journals and in an Italian patent request, together with unpublished data that will be completed soon. Both published and unpublished results have been extensively presented in national and international meetings and schools.

Concluding, this thesis work has demonstrated the high flexibility of continuous flow equipment for adapting on rather different synthetic conditions and methods. In all cases examined, translating from traditional batch approach to continuous one resulted in definite improvements on synthetic efficiency, safety and economy, thus demonstrating that the widespread diffusion of miniaturized continuous processing will be the next evolution step in chemical manufacturing.

List of Publications

- 1 Rossi E, Woehl P, Maggini M, “Scalable *in-situ* diazomethane generation in continuous-flow reactors”, *Organic Process Research & Development*, **2011**, DOI: 10.1021/op200110a.
- 2 Seri M, Rossi E, Carofiglio T, Antonello S, Ruani G, Maggini M, Muccini M, “Efficient as-cast bulk-heterojunction solar cells based on a tert-butyl substituted methanofullerene acceptor”, *Journal of Materials Chemistry*, **2011**, 21, 18308 – 18316.
- 3 Carofiglio T, Maggini M, Menna E, Pace A, Rossi E, Salice P, “Metodo di sintesi di nanotubi di carbonio funzionalizzati per cicloadizione in flusso continuo ed apparato per lo stesso”, *Italian Patent Application*, **2011**, PD2011A000153.
- 4 Salice P, Maity P, Rossi E, Carofiglio T, Menna E, Maggini M, “The continuous-flow cycloaddition of azomethine ylides to carbon nanotubes”, *Chemical Communications*, **2011**, 47, 9092 – 9094.
- 5 Rossi E, Carofiglio T, Venturi A, Ndohe A, Muccini M, Maggini M, “Continuous-flow synthesis of an efficient methanofullerene acceptor for bulk-heterojunction solar cells”, *Energy & Environmental Science*, **2011**, 4, 725 – 727.
- 6 Collini E, Fortunati I, Scolaro S, Signorini R, Ferrante C, Bozio R, Fabbrini G, Maggini M, Rossi E, Silvestrini S, “A fullerene-distyrylbenzene photosensitizer for two-photon promoted singlet oxygen production”, *Physical Chemistry Chemical Physics*, **2010**, 12, 4656 – 4666.
- 7 Carofiglio T, Donnola P, Maggini M, Rossetto M, Rossi E, “Fullerene-promoted singlet-oxygen photochemical oxygenations in glass-polymer microstructured reactors”, *Advanced Synthesis & Catalysis*, **2008**, 350, 2815 – 2822.

Communications to Conferences and Seminars

August-September International Convention “The Centenary”, Padova (PD), Italy; poster presentation: “Synthesis of Oncological Drugs by Flow Techniques”.

2009

September 2010 Ischia Advanced School of Organic Chemistry (IASOC 2010), Ischia (NA), Italy; poster and oral presentation: “Micro/meso-structured Reactors for Chemical Synthesis: Applications in Materials Science and Medicinal Chemistry”.

September 2011 XXIV National Convention of the Italian Chemical Society, Lecce (LE), Italy; poster and oral presentation: “Scalable in situ diazomethane generation in continuous-flow reactors”.

October 2011 3rd Symposium on Continuous Flow Reactor Technology for Industrial Applications, Como (CO), Italy; poster presentation: “Scalable in situ diazomethane generation in continuous-flow reactors”.

Acknowledgments

First of all, I wish especially to thank the scientific supervisors of this thesis work, Prof. Michele Maggini, for important support during all the work, for the helpful suggestions and also for the large autonomy I had in my study.

A special acknowledgment is for all the collaborators that have in large part contribute to the realisation of the published papers. In particular, I wish to thank Prof. Tommaso Carofiglio, Prof. Enzo Menna, Dr. Michele Muccini (ISMN-CNR, Bologna) and Dr. Pierre Woehl (Corning Incorporated). A special thanks to Dr. Andrea Castellin (FIS SpA) for the support during all PhD thesis, and to Dr. Miriam Mba for precious support and assistance in proofs reading.

Finally, I am also grateful to Dr. Elisa Lubian for the technical and moral assistance during all my Ph.D research, and all the colleagues for supporting this work with precious advices.

Finally, I wish to thank Regione Veneto for PhD grant through FSE program. Financial Support for this work was provided by Fondazione CARIPARO through project MISCHA and the University of Padova through Progetti Strategici bando 2008—HELIOS.